Synthetic Heme Dioxygen Complexes

Michel Momenteau* and Christopher A. Reed*

Institut Curie, Section de Biologie, URA 1387 CNRS, Centre Universitaire, 91405 Orsay, France, and Department of Chemistry, University of Southern California, Los Angeles, California 90089-0744

Received October 25, 1993 (Revised Manuscript Received February 21, 1994)

Contents

I. Introduction

Essential to all mammalian life, the transport and storage of dioxygen by hemoglobin holds a particular fascination for molecular scientists. Our present understanding of how hemoglobin works has arisen from a notable interplay of studies on both the protein itself and on synthetic chemical models. The stage was set for this chemical understanding in the 1960s by the Nobel prize-winning determinations of the X-ray structures of hemoglobin and myoglobin by Perutz and by Kendrew. Work on synthetic heme dioxygen complexes began in earnest in the early 1970s and the paradigm of constructing superstructured porphyrins has, over the past 20 years, been raised to something like a new high art. The necessary and sufficient conditions for dioxygen binding to a heme group are qualitatively now well understood and model compounds have played a particularly important role in developing this understanding.

It has been more than 15 years since a comprehensive review of synthetic heme–O_2 complexes has been attempted.[1,2] Particular aspects have been covered in several reviews including the preparation of synthetic analogs,[3-11] spin state/structure relationships,[12] vibrational aspects,[13] thermodynamic properties,[4,5,8,9,14-18] and autoxidation mechanisms.[19] In this review we try to provide a comprehensive assessment of the present state of our knowledge about heme–dioxygen complexes, particularly with respect to what they tell us about hemoglobin. Despite the enormous amount of information collected on proteins and model compounds, a number of chemical questions remain to be answered. For example, our understanding is quite incomplete when we attempt to quantify the factors affecting O_2 affinity, delineate proton-dependent decomposition pathways, or precisely describe the structure of the FeO_2 moiety.

II. Nature of Dioxygen and Iron O_2 Complexes

A. Dioxygen Moieties

The electronic configuration of molecular oxygen, O_2, is unusual. It is the only stable homonuclear diatomic molecule that has a paramagnetic ground state. Simple electron-pair bonding between two oxygen atoms, while successful in predicting a double bond, fails to rationalize the triplet ground state. A molecular orbital description is necessary. The $1s^22s^22p^4$ configurations of two oxygen atoms interact and lead to a $(1\sigma_g)^2(1\sigma_u^*)^2(2\sigma_g)^2(2\sigma_u^*)^2(2p\sigma_g)^2(2p\pi_u)^4(2p\pi_g^*)^2$ molecular configuration for the $^3\Sigma_g^-$ ground state (Figure 1). The two unpaired electrons are in degenerate π^* orbitals. The first excited state of O_2 is a $^1\Delta_g$ singlet 22.5 kcal mol^{-1} above the ground state.

The reduction of O_2 by one electron gives the superoxide ion, O_2^-, and by two electrons, the peroxide

0009-2665/94/0794-0659$14.00/0

Michel Momenteau was born in Boulogne-sur-Seine, France, in 1939. He studied chemistry at the University of Paris and obtained a first doctorate with Pierre Sigwalt. He moved to the Muséum National d'Histoire Naturelle, Paris, and received his Doctorat d'Etat in Biophysic in 1971 under the supervision of Michel Rougée. After two post-doctoral stays with Françoise Labeyrie (Gif-sur-Yvette) and Jürgen Fuhrhop (Braunschweig) he joined Jean-Marc Lhoste at the Institut Curie, Section de Biologie in Orsay, where he is now a Research Director of the Centre National de la Recherche Scientifique (CNRS). His current research interests include the chemistry of porphyrins and metalloporphyrins; the synthesis, reactivity, and structural investigations of hemoprotein models; and the preparation of new tetrapyrrolic photosensitizers for antitumor and antiviral activities.

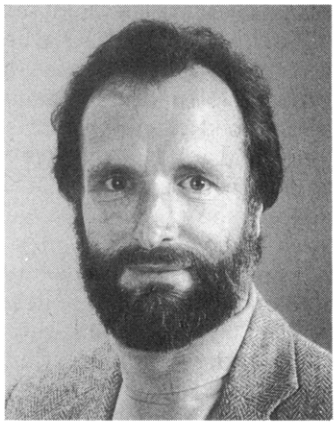

Chris Reed was born a "kiwi" in 1947. He received his education in his native land at the University of Auckland, New Zealand. His Ph.D. studies (1969–71) were on the oxidation addition and ligand reaction chemistry of iridium with Warren Roper F.R.S. His interest in bioinorganic chemistry began during postdoctoral studies with Jim Collman at Stanford University in the first days of picket-fence porphyrin. In 1973 he joined the faculty of the University of Southern California where he has been Professor since 1982. His research interests include bioinorganic chemistry, spin-coupling phenomena, fulleride chemistry, the silylium ion problem (R_3Si^+), and the search for the least coordinating anion with derivatives of $CB_{11}H_{12}^-$. He has served on the editorial board of *Inorganic Chemistry*. He has been honored with an A. P. Sloan Fellowship, a Dreyfus Teacher-Scholar Award, the USC Associates Award for Creativity in Research and Scholarship, and visiting professorships at many institutions, most recently as Foundation for Inorganic Chemistry Lecturer at the University of Sydney.

ion, O_2^{2-}. As electrons are added to the π_g^* orbital, the bond length increases to about 1.34 Å in the superoxide ion and to about 1.49 Å in the peroxide ion. This compares to 1.21 Å for molecular oxygen.[2] This reflects the expected trend in bond order: $2(O_2)$, $1.5(O_2^-)$, and $1(O_2^{2-})$.

The thermodynamics of the stepwise reduction of O_2 are very dependent on the presence of protons. Thus, while the first reduction potential of O_2 in aprotic media

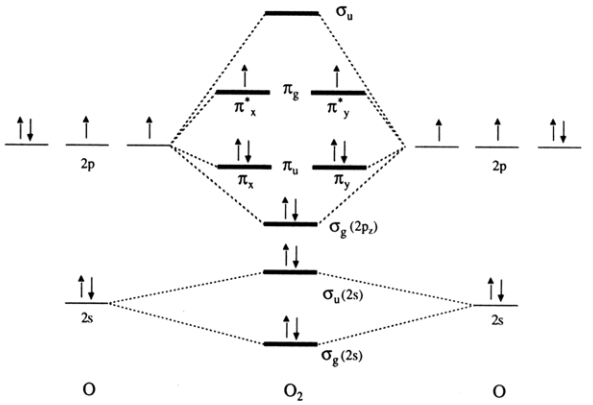

Figure 1. The molecular orbital energy-level description for O_2.

indicates that superoxide formation is highly endothermic

$$O_2 + e^- \xrightarrow{DMF} O_2^- \qquad \mathcal{E}^0 = -0.60 \text{ V (vs NHE)}$$

the presence of protons makes it exothermic[20]

$$O_2 + H^+ + e^- \xrightarrow{DMF} HO_2^- \qquad \mathcal{E}^0 = +0.12 \text{ V (vs NHE)}$$

This can be understood in terms of charge compensation and O–H bond formation overcoming the disfavored placement of the extra electron in the antibonding π_g orbital. The second one-electron reduction to peroxide is subject to the same considerations such that the formation of H_2O_2 from O_2^- is highly thermodynamically favored even in the weak acidity of neutral water.

$$O_2^- + 2H^+ + e^- \xrightarrow{pH\ 7} H_2O_2 \qquad \mathcal{E}^{0\prime} = +0.89 \text{ V (vs NHE)}$$

There is a direct conceptual parallel between protons and metal ions in that both can drive the formal reduction of O_2 via charge compensation and bond formation. As a consequence, the reversible binding of O_2 to a metal can only be achieved if competition with protons is rigorously controlled and further reduction to peroxide and oxide is thwarted. This is discussed more fully below in connection with autoxidation mechanisms of iron(II). We also note that there is a large thermodynamic driving force for the complete four-electron reduction of O_2 to water:

$$O_2 + 4H^+ + 4e^- \xrightarrow{pH\ 7} 2H_2O \qquad \mathcal{E}^{0\prime} = +0.82\text{V (vs NHE)}$$

It is the capture and storage of the free energy released by coupling this reduction to the oxidation of foodstuffs to CO_2 that is the basis of respiratory life. The "oxygen electrode" of nature's fuel cell in higher organisms is cytochrome oxidase. This enzyme catalyzes the four-electron reduction of O_2 to water and shows oxymyoglobin-like binding in the initial step.[21] Catalysis by an oxygen-binding heme center is necessary because although reduction of dioxygen in the presence of protons is thermodynamically favored, it is kinetically slow and difficult to control. The binding of O_2 to metals can be quite fast as can the stepwise reduction.[22]

B. Dioxygen Complexes

In order for transition metal complexes M^n (n = oxidation state) to react with dioxygen to form dioxygen

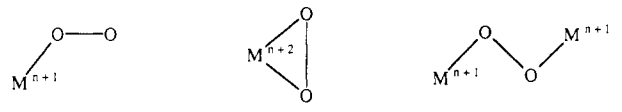

Figure 2. Structures and formal oxidation states of iron–dioxygen complexes.

complexes there must be a vacant site (or sites) for binding and an accessible higher oxidation state (or states).

The stoichiometry of dioxygen binding can be 1:1 or 1:2. Figure 2 shows the three structural types of dioxygen complexes that have been characterized. Complexes 1 are formally considered as complexes corresponding to a one-electron transfer to dioxygen, while in complexes 2 and 3 the oxidation states reflect a two-electron transfer. Two other structural types have been characterized but are presently unknown in heme iron chemistry. These are the μ^2-η^2 binding of dioxygen to binuclear copper in hemocyanin[23] and the hydroperoxide complex of the oxo–diiron center of hemerythrin.[24]

C. Oxidation State Formalism and Structure

The assignment of superoxo and peroxo oxidation state formalisms to iron–dioxygen complexes has in the past been controversial.[25,26] Partially, this arose from a lack of definitive structural information about FeO_2 moieties. It was simply not possible to decide on the most appropriate formalism (or indeed, whether to use one) until minimally, bond length, bond angle, and νO–O data became available. On the other hand, a largely unnecessary debate about whether an iron(II) dioxygen or an iron(III) superoxide formalism was the best description for the FeO_2 moiety in oxyhemoglobin arose simply from a misunderstanding of the utility of oxidation state formalisms. The confusion arose when some measure of electron transfer from iron to dioxygen was compared with that indicated by one of the formalisms. Since measured or calculated electron distributions between atoms in molecules rarely match the unit charge designations of formalisms, such oxidation state assignments are inherently easy targets for the criticism that they are unrealistic. However, if they are not taken literally, i.e. as real charges, they can be very useful for rationalizing many chemical and physical properties and for classifying particular chemical entities. This is particularly true for iron–dioxygen complexes now that most of the important structural and electronic data are available. As described more fully below, the complexation of O_2 to a hemoglobin-like iron(II) heme is best formalized as an iron(III)–superoxo complex (type 1 in Figure 2). On the other hand, the complexation of O_2 to an iron(I) heme is best formalized as an iron(III)–peroxo complex (type 2 in Figure 2). Diiron(III)–μ-peroxo complexes (type 3 in Figure 2) are also described.

Complexes of the type $[Fe(porphyrin)(O_2)]^-$ have been reported to arise from treatment of iron(I) porphyrins with molecular oxygen,[27] iron(II) porphyrins with superoxide ion,[28,29] or from one-electron reduction of a dioxygen adduct of an iron(II) porphyrin.[30] The eventual full characterization of $[Fe(TPP)(O_2)]^-$ led to the conclusion that an iron(III)–peroxo formulation was both useful and appropriate. The structure of the FeO_2 moiety was deduced from EXAFS to be consistent with a triangular geometry i.e. of the η^2-peroxo type (see Figure 2).[31] The bound dioxygen is peroxidic in nature as indicated by νO–O at 806 cm^{-1} in $[Fe(OEP)(O_2)]^-$.[28] EPR,[32] Mossbauer spectroscopy,[27,33] and magnetic susceptibility measurements[33,34] confirm the high-spin iron(III) nature of the metal center.

A monomeric dioxygen adduct of a base-free iron(II) porphyrin has yet to be isolated and fully characterized. Nakamoto[13,35] has made the intriguing observation that under matrix isolation conditions *two* different types of complexes are formed. They have ν(O–O) at 1106 and 1195 cm^{-1}. Isotopic ^{18}O shifts to 1043 and 1127 cm^{-1} respectively confirm the assignments. Structures corresponding to these frequencies must certainly include an end-on angular geometry. Balch *et al.*[36] have shown by NMR that in toluene solution at −80 °C, picket-fence porphyrin forms an oxygen adduct of probable formula $Fe(T_{piv}PP)(O_2)$. It is diamagnetic, suggesting a similarity to base-liganded, hemoglobin-like species although water as axial base cannot be rigorously ruled out.

Balch *et al.* have shown that μ-peroxodiiron(III) complexes (type 3 in Figure 2) can be stabilized and studied at low temperatures.[36,37] For example, oxygenation of toluene solutions of Fe^{II}(TPP) at dry ice temperatures leads to (TPP)FeOOFe(TPP). ^1H NMR[36,37] and Mössbauer spectroscopy[38] have been used to show that a high-spin iron(III) formulation with moderate antiferromagnetic coupling through the bridging peroxide ligand is appropriate.

In hemoglobin-type dioxygen complexes the FeO_2 moiety is now known to have an end-on angular structure, i.e., type 1 in Figure 2. Accordingly, it is formally described as an iron(III) superoxo complex. This is not to say that there is a full, one-electron transfer from iron to dioxygen, although remarkably, the ν(O–O) stretching frequencies are very close to those of the free superoxide ion.[1,2]

Historically, the first information about the nature of the FeO_2 moiety in hemoglobin came from magnetic susceptibility studies by Pauling and Coryell in 1936.[39] They observed that when high-spin deoxyhemoglobin reacts with molecular oxygen, which is also paramagnetic, the resulting oxyhemoglobin is diamagnetic. They concluded that profound changes in electronic structure accompanying O_2 coordination. The diamagnetism posed an immediate problem for understanding the structure and bonding in the FeO_2 moiety. Griffith[40] introduced the idea of involving the π^* orbitals of dioxygen and proposed a triangular structure. A linear Fe–O–O moiety has also been discussed.[41] In 1964, both Pauling[42] and Weiss[43] proposed the end-on angular structure that we now know to be correct. Pauling emphasized that there must be an even number of electrons around dioxygen and proposed iron(II) and iron(IV) resonance forms. Weiss emphasized one-electron transfer to give an iron(III)–superoxide complex and rationalized the diamagnetism by invoking antiferromagnetic coupling. The visible spectrum of the heme in oxyhemoglobin was interpreted as iron(III)-like.[44] The landmark experiment which resolved the uncertainties posed by these different proposals was the determination of the X-ray crystal structure of a "picket fence" porphyrin model for

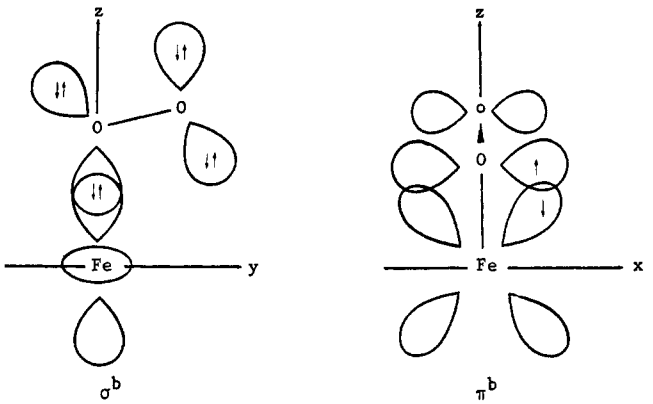

Figure 3. Simple bonding model for angular superoxo-type Fe–O_2 complexes.

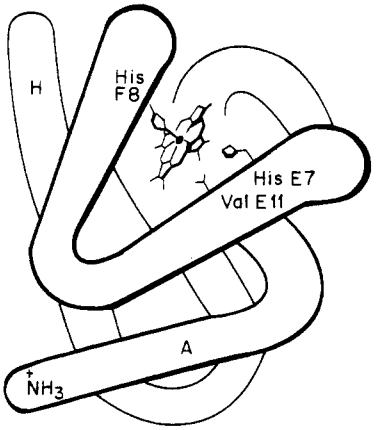

Figure 4. Schematic representation of the folding of the polypeptide around the heme group in deoxymyoglobin.

oxyhemoglobin. In 1973, Collman *et al.*[45] showed that the FeO_2 moiety adopted the angular end-on geometry favored by Pauling and by Weiss. The Fe–O bond was found to be quite short (1.75 Å) consistent with the idea that some π bonding was augmenting the σ-donor bonding. In 1978, the angular geometry was first demonstrated in a protein when low-temperature methods allowed the X-ray structure of oxymyoglobin to be determined.[46] A qualitative bonding model that adequately rationalizes the bent structure and the diamagnetism within the framework of the iron(III)–superoxo formalism has been presented by Reed[25] and qualitative molecular orbital energy level diagrams have been presented by Basolo *et al.*[2] Figure 3 shows the essential elements of the bonding. One lone pair from an sp^2-rehybridized superoxide ion acts as a σ donor into an empty σ orbital of predominant d_{z^2} character on the low-spin iron(III) atom. This rationalizes the angular structure. The σ bond is augmented by π bonding between the half-filled d_{xz} orbital on iron and the half-filled π^* orbital on the superoxide ion. This rationalizes the short Fe–O bond length and the diamagnetism. The π bond is a two-electron molecular orbital that is delocalized over the three atoms of the FeO_2 moiety. It has bonding character with respect to the Fe–O bond and antibonding character with respect to the O–O bond. It differs from the antiferromagnetic coupling proposed by Weiss in that a low-lying paramagnetic state has not been identified and the contribution of the π bond to the Fe–O bond energy may be considerably more than the few hundred wavenumbers of magnetic coupling.

During the 1970s, and even to this day, a large number of physical probes as well as several different calculational approaches have been applied to oxyhemoglobin and its model compounds in order to probe the appropriateness of the formalism. This has sometimes been a futile exercise and no attempt is made to review the literature comprehensively. Several reviews on the calculational approaches to understanding the electronic structure of the FeO_2 moiety appeared in the arly 1980s[47-50] and rather little has appeared since.[51,52] Importantly, the sense of the polarity of the bond i.e. $Fe^{\delta+}$–$O_2^{\delta-}$ has never really been questioned. A consensus seems to have developed that the iron(III)–superoxo formalism for oxyhemoglobin is the most appropriate one but that it has the limitations inherent in any unit-electron formalism. Most of the physical studies have corroborated earlier intuition and deductions of bond polarity, diamagnetism and angular structure. Perhaps the only serious challenge came from a remeasurement of the magnetic susceptibility of oxyhemoglobin with the suggestion of a low-lying paramagnetic state.[53,54] Pauling,[55] however, suggested that the results must arise from experimental artifact, which turned out to be the case.[56] The most important physical probes of the nature of the FeO_2 moiety involve electronic, vibrational, and nuclear (Mössbauer, NMR) spectroscopies, and these are discussed in section VII.

III. Natural Oxygen Carriers (Hemoglobin, Myoglobin)

In oxygen-carrying hemoproteins (myoglobin and hemoglobin) the active site consists of an iron(II) protoporphyrin IX (the heme) encapsulated in a water-resistant pocket and bound to the protein through a single coordinate bond between the imidazole group of the "proximal" histidine residue (F8) and the iron atom (Figure 4). Numerous residues from the protein hold the heme in position by hydrophobic interactions. Hemoglobin, which transports oxygen in the blood, is a tetrameric molecule with an $\alpha_2\beta_2$ subunit structure. Myoglobin, which stores oxygen in muscles, is monomeric. In the native deoxy form, the ferrous ion of the heme is in a five-coordinate state. It reversibly binds molecular oxygen in the sixth, vacant coordination site. A variety of other small ligands (CO, NO, alkyl isocyanides) also bind to the sixth coordination site of the iron. Around it, distal amino acid residues control the immediate environment. They can induce polar, hydrophobic, or steric interactions which help regulate the affinities of the bound ligands. Trying to understand the chemical basis of these distal influences on ligand binding affinities has been a major preoccupation of recent studies.

In hemoglobin, the interactions between the subunits are known under the general term of allosteric properties and are of great physiological importance. They determine the cooperative binding of O_2. In the deoxy form, the iron atom of each heme is in the high-spin ($S = 2$) five-coordinate Fe(II) state and lies about 0.5 Å out of the heme plane in the direction of the proximal histidine.[57] The proximal Fe–N (imidazole) bond vector has an approximately 10° tilt off the heme normal.

The binding of O_2 modifies both the structure and electronic configuration of the heme. The oxygenated heme adopts a low-spin six-coordinate state with the iron atom more nearly centered in the porphyrin plane.

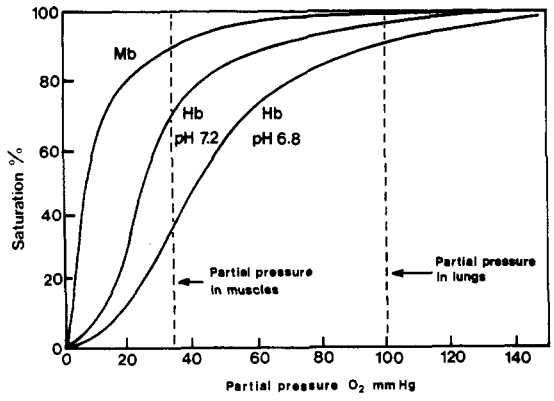

Figure 5. Oxygenation curves for myoglobin (Mb) and hemoglobin (Hb).

Furthermore, the Fe–N (imidazole) off-axis tilt is reduced along with a lateral shift of the protein F helix. The O_2 molecule is bound in a bent geometry.[46,58] Recent X-ray studies of HbO_2[59] and neutron diffraction studies of MbO_2[60] have provided strong evidence for H-bonding between the imidazole N–H of the distal histidine (HisE7) and bound O_2. The distal histidine cannot form a direct coordinate bond with iron in the deoxy form of hemoproteins because it is too far away. An important observation made from structural studies on carbon monoxide derivatives is that close nonbonded contacts between the bound CO and amino acid residues in the vicinity of the distal site (His E7 and Val E11) seem to result in a bent and/or tilted geometry for this ligand.[61]

The binding of dioxygen to Mb or to isolated α or β monomeric subunits of Hb shows the behavior expected for 1:1 association between dioxygen and protein:

$$Mb + O_2 \rightarrow MbO_2$$

The value of $P_{1/2}{}^{O_2}$ (the partial oxygen pressure which leads to 50% saturation) is in the range 0.4–0.7 Torr.

The equilibrium uptake of O_2 by tetrameric hemoglobin is more complex. Typical plots of equilibrium O_2 uptake data for hemoglobin and myoglobin are shown in Figure 5. In contrast to the hyperbolic curve obtained with the data for myoglobin, the data obtained for hemoglobin show sigmoidal behavior. The sigmoidal shape of this curve reflects that there is a cooperative effect of oxygen binding resulting from interactions between the subunits and the conformational changes of each of them during the oxygenation–deoxygenation process. The physiological importance of the difference between Mb and Hb lies in the need for hemoglobin to saturate with O_2 readily at the arterial pressure in the lungs but to release O_2 to myoglobin at lower venous pressures in the tissues. Thus, cooperativity is an O_2 unloading mechanism at lower partial pressures of oxygen, and the chemical basis of this affinity lowering has been a major target of investigation.

Hill plots (Figure 6) allow the affinity constants to be determined.

$$K_{O_2} = \frac{[Hb(O_2)_n]}{[Hb][O_2]^n}$$

If

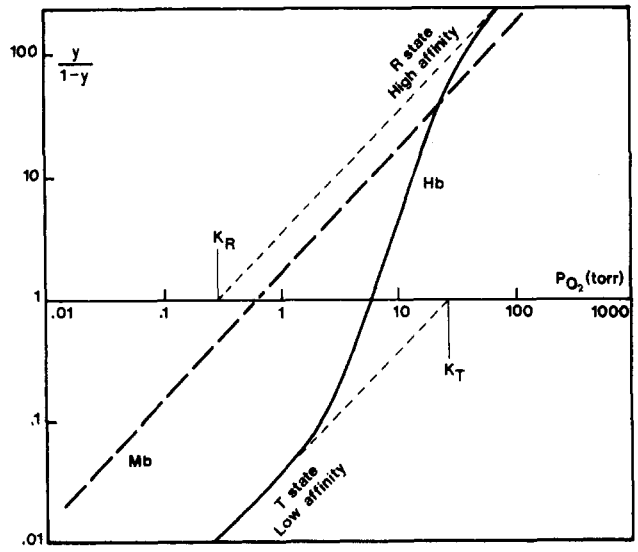

Figure 6. Hill plot for O_2 binding to myoglobin (Mb) and hemoglobin (Hb).

$$y = \frac{[Hb(O_2)_n]}{[Hb] + [Hb(O_2)_n]}$$

then

$$\ln\left(\frac{y}{1-y}\right) = \ln K_{O_2} + n \ln P_{O_2}$$

where y is the fraction of sites occupied by dioxygen and n is the Hill coefficient.

The Hill plot for Hb shows an inflexion indicative of an interaction between the subunits. At intermediate pressures of O_2, the exponent n is observed to be around 3 rather than 1 as for myoglobin. This value indicates a positive cooperativity. Extrapolations of the linear portions (n = 1) at both high and the low O_2 partial pressures give the affinity constants for the deoxygenated T form (K_T) and for the fully oxygenated R form (K_R).

From the crystallographic data of hemoproteins in both liganded and deoxy forms and from molecular models, Perutz[62,63] proposed a stereochemical mechanism for a cooperative interaction on the basis of the earlier two-state allosteric model of Monod, Wyman, and Changeux.[64] In this concept, two structures of each subunit are possible: (a) a low O_2 affinity structure (T or tense state) and (b) a high O_2 affinity structure (R or relaxed state). These two states differ both in the tertiary structure of each subunit and in the relative orientation of the subunits in the tetramer (quaternary structure). When the first O_2 binds to a T-configuration molecule (probably to one of the α subunits) a certain amount of strain is induced into the local tertiary structure. Eventually, this strain alters the nonpolar interactions, electrostatic interactions, and hydrogen bonds between the subunits inducing an alteration of the tertiary structures of other subunits.[65–67] The degree of cooperativity given by the Hill coefficient depends upon the details of coordination process as well as the nature and the kind of interactions which change during the conformational transition. For n = 3, it corresponds to about 3.6 kcal mol^{-1} and is referred to as the energy of heme–heme interaction.

Using the structural changes of the heme predicted by Williams[68] and by Hoard,[69] Perutz proposed a "trigger" mechanism for the cooperative interaction.[62]

The out-of-plane iron atom in the deoxy form was proposed to be held in a "tense" five-coordinate state in the T conformation. The successive binding of O_2 molecules was proposed to relieve this tension as the oxygenated protein adopted a relaxed (R state) conformation. This bold proposal stimulated enormous interest in the problem of understanding the chemical basis of cooperativity. The stereochemical trigger mechanism has stood up to detailed scrutiny fairly well although notions of "tense" proximal histidine binding have given way to ideas of "tethered" or "constrained" moieties in the T state. Synthetic hemes have played a major role in developing these ideas.

Among the parameters which affect the oxygen affinity curve is the proton concentration. This is called the Bohr effect and is related to the capacity of Hb to transport carbon dioxide. The T-state conformer has a higher affinity for protons than does the R. Hence, under acid conditions the equilibrium between deoxy- and oxyhemoglobin is shifted in favor of deoxygenation. This means that the oxygen saturation curve for hemoglobin in Figure 5 is shifted toward the right with increasing acidity. Three other naturally occurring substances are known to reduce the oxygen affinity by preferentially interacting with the T state: carbon dioxide, chloride ions, and 2,3-diphosphoglycerate (DPG). Carbon dioxide exerts its effect in two ways. First, it increases the proton concentration when it dissolves in blood plasma to form bicarbonate ions ($CO_2 + H_2O \rightarrow HCO_3^- + H^+$). The protons are picked up by hemoglobin as its unloads O_2 and the bicarbonate ions are carried to the lungs as counterions. In addition, CO_2 forms carbamates with the amino group at the beginning of each hemoglobin protein chain ($-NH_2 + HCO_3^- \rightarrow -NH-CO_2^- + H_2O$). When hemoglobin is reoxygenated, these processes are reversed. The release of acid shifts the equilibrium, converting bicarbonate ions to the less soluble CO_2, which is exhaled.

IV. Synthetic Hemes for Reversible Oxygenation

A. Requirements

Ever since the finding some 50 years ago that protein-free iron(II) hemes do not reversibly oxygenate under ordinary conditions, there has been sustained interest in understanding how hemoglobin works. We now know that the necessary and sufficient conditions to mimic oxyhemoglobin in synthetic model systems are (1) formation of a five-coordinate heme precursor having a proximal base (imidazole, pyridine, etc.) and (2) thwarting pathways that lead to irreversible oxidation. This typically means the prevention of μ-peroxo dimer formation and the exclusion of acidic protons and nucleophiles from the O_2 binding site. Thus, by isolating hemes in hydrophobic environments, reversible oxygenation can usually be achieved.

In addition, it is desirable that model systems be amenable to systematic alteration. This allows a chemical probing of the factors that govern their stability. Comparisons can be made to the proximal and distal effects engendered by the protein in hemoglobin.

B. Models for Five-Coordination of Fe(II)

Addition of aromatic nitrogen base ligands (e.g. pyridine, imidazole) to four-coordinate iron(II) porphyrins in a noncoordinating solvent preferentially gives symmetrical six-coordinate complexes called hemochromes.[70] This is a major problem in the preparation of models of the active site of dioxygen-carrying hemoproteins where the globin allows only a single coordinate bond between the imidazole ring of the "proximal" histidine residue (His F8).[71]

The formation of hemochromes by addition of two ligand bases is due to a greater equilibrium constant for the addition of the second ligand (K_B^B) than for the first (K_B).

$$PFe^{II} + B \overset{K_B}{\rightleftarrows} PFe^{II}B + B \overset{K_B^B}{\rightleftarrows} PFe^{II}B_2$$

For example, in benzene at 25 °C, the binding constants of pyridine to $Fe^{II}TPP$ have been estimated at $K_B \approx 1.5 \times 10^3$ M^{-1} and $K_B^B = 1.9 \times 10^4$ M^{-1}.[72] The atypical occurrence of K_B^B being greater than K_B in successive equilibria arises from ligand field stabilization energy. The d^6 six-coordinate hemochrome is low spin and gains electronic stabilization relative to the high-spin state of five-coordination.[12] With $K_B^B > K_B$, the five-coordinated species cannot be present in any significant amount in solution. It can only be obtained if $K_B^B \ll K_B$.

Numerous approaches have been taken to limit the formation of six-coordinate iron(II) porphyrins. These include (1) steric hindrance of the axial ligand, (2) covalent attachment of the axial ligand to the heme periphery (see Figure 7), (3) steric hindrance of one of the two faces of the heme (see Figure 8), and (4) synthesis of "integrated hemes" incorporating more than one of these features (see Figure 9).

1. Sterically Hindered Ligand

When appropriately sterically hindered axial ligands are used, five-coordinate iron(II) hemes can be obtained. This was first discovered by Collman and Reed[73] with 2-methylimidazole (2-MeIm) as the axial ligand. They reasoned that the steric interaction of the 2-methyl group with the heme would not hinder five-coordination because of the ~0.5 Å out-of plane iron displacement predicted by Hoard.[69] On the other hand, six-coordination, where the iron atom is low spin and in the plane of the porphyrin, is strongly hindered. By addition of 2-MeIm to Fe(II)TPP in benzene/ethanol solution, the first monoliganded heme complex was isolated. Like deoxyhemoglobin (μ = 5.1 μ_B), the magnetic moment of 5.2 μ_B at 25 °C is close to the spin-only value for a high-spin (S = 2) ferrous ion (μ = 4.9 μ_B). The high-spin state was verified by Mossbauer measurements.[74] A second high-spin five-coordinate 2-MeIm adduct has been prepared with the Fe^{II}–picket fence porphyrin.[75]

In solution, the formation of five-coordinate high-spin complexes was demonstrated by Rougée and Brault by titration of Fe^{II}DDME and Fe^{II}TPP with 2-MeIm in toluene.[76] Affinity constants of $K_B = 1.25 \times 10^4$ M^{-1} and 2.4×10^4 M^{-1} respectively were measured at 25 °C for the two metalloporphyrins. As these values are quite similar to that of the first unhindered imidazole,[77] it was concluded that the thermodynamics of monoligation are not particularly affected by any repulsive interaction of the 2-methyl group. Even at high 2-MeIm concentrations, there is no evidence for the formation of bis(2-MeIm) adducts at room temperature.

Table 1. Comparison of Deoxyheme Stereochemistry in Myoglobin (Mb), Hemoglobin (Hb), and Model Compounds

	Fe^{II}(TPP)(2-MeIm)[a]	Fe^{II}(T_{piv}PP)(2-MeIm)[b]	Fe^{II}[$(Piv)_2C_8$](1-MeIm)[c]	Mb[d]	Hbα[d]	Hbβ[d]
Fe–Ct_N, Å	0.42	0.40	0.3	0.42	0.6	0.63
Fe–Ct_P, Å	0.55	0.53	0.34	0.55	0.6	0.63
Fe–N_P, Å	2.086	2.072	2.075	2.03	2.1	2.1
Fe–N_{Im}, Å	2.16	2.095	2.134	2.1	2.0	2.2
θ, deg	10.3	11	5	11	8	7

[a] Hoard (1975), ref 78. [b] Jameson *et al.* (1978), ref 75. [c] Momenteau *et al.* (1988), ref 81. [d] Takano (1977), ref 79.

In crystals of high-spin Fe^{II}TPP(2-MeIm)[78] and $Fe^{II}T_{piv}$PP(2-MeIm),[75] the iron atom lies 0.42 and 0.40 Å out of the mean plane of the porphyrin nitrogen atoms toward the imidazole ligand. These values compare well with estimates for the same displacement in deoxy Hb.[79,80] The length of the Fe–N_{Im} bond in these high-spin complexes, about 2.1 Å, is larger than that found in low-spin bis(imidazole) complexes. This may be attributed to the eclipsing conformation of imidazole with respect to the porphinato nitrogen atoms and the $(d_{z^2})^1$ occupation of the high-spin state. There is an off-axis tilt of the Fe–N_{Im} bond (angle θ, 9.6 Å and 11°, respectively) for the two compounds with respect to the normal of the heme. The two systems having 2-MeIm as axial ligand are characterized by a doming of the porphyrin ring which is typical of most five-coordinate metalloporphyrins. It is more predominant in TPP than in T_{piv}PP derivatives. This doming is responsible for the greater N_p···Ct and Fe–N_p (2.086 Å) distances in the unprotected porphyrin relative to those with superstructure. It is noted that the crystal structure shows a Fe–N_p distance of 2.086 Å, substantially larger than the presumed optimal core size of 2.01 Å.

Table 1 compares structural data for the two 2-MeIm model compounds with deoxyhemoproteins. The congruence is seen to be quite high, suggesting that 2-methylimidazole ligation is a good model for T-state deoxyhemoglobin. The off-normal tilt (angle θ) that is engendered by the 2-methyl group mimics the lateral pull of the proximal histidine (F8) relative to the heme in the deoxyhemoproteins. It is less, but not absent, in an unhindered 1-MeIm complex (column 3, Table 1) prepared from a one-face-hindered heme.[81] This is discussed in more detail below.

2. Covalent Attachment of the Axial Ligand

This approach was originally reported by having various peptide fragments attached to a suitable porphyrin in order to reproduce the local environment of heme peptides obtained by cytochrome *c* degradation.[82,83] Sano,[84,85] Theodoropoulos,[86] and Momenteau[87] have all described compounds bearing histidine-containing peptides covalently bound to the vinyl side chains of protoheme via thioether linkages.

Another widely used route has been the preparation of "chelated" hemes in which imidazole or pyridine ligands are covalently linked to one of the propionic acid side chains of the porphyrin ring through ester or amide linkages. These approaches are illustrated in Figure 7. From this concept a series of derivatives was synthesized using pyrro-,[88] proto-,[89] meso-,[90,91] and deuteroheme.[92] More recently, Momenteau *et al.*[93,94] have synthesized a series of chelated heme compounds in which the base is attached to the β-pyrrole position of a tetraphenylporphyrin ring. Another, older family of chelated compounds, where the chain carrying the ligand is attached to the ortho position of a meso phenyl ring of TPP, have been reported by Collman,[95] Reed,[96] Walker,[97] Ibers[98] and Chang.[99] Attachment via two linkages has been achieved by Traylor *et al.*[100] (see first structure in Figure 7).

Scheme 1

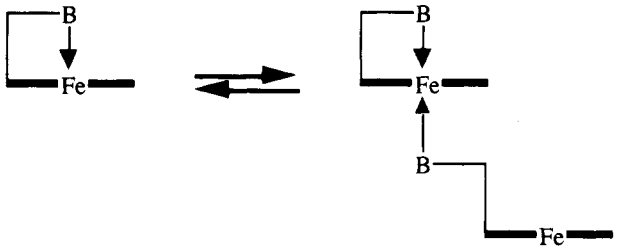

As these compounds have a built-in 1:1 base to porphyrin stoichiometry the formation of five-coordinate hemes via intramolecular binding is enhanced. Their characterization has typically been made only in solution by absorption spectroscopy. In contrast to four-coordinate hemes, these systems exhibit only one Soret band, indicating five-coordinate axial base chelation. Nevertheless, in the "chelated-histidine" system of Momenteau *et al.*,[92] evidence has been presented for a dimerization at low temperature. From spectroscopic analysis, it was argued that the expected five-coordinate complex is in equilibrium with a mixed four-coordinate/six-coordinate dimer as shown in Scheme 1. The driving force for this dimerization is related to the stability of low-spin six-coordination discussed earlier but solvation energy differences upon aggregation must also play a role. The very low dimerization constant measured at 25 °C ($<10^{-2}$ M^{-1}) makes it possible to conclude that histidine is firmly bound to iron(II) in the monomeric form and that the dimerization process is favored only by low temperature and high concentration. A similar dimerization has been confirmed by Collman and co-workers for a "tailed" picket fence complex using ^1H NMR spectroscopy and magnetic circular dichroism.[95,101]

We note that perturbations affecting the imidazole coordination can be easily introduced by modifying the linkage connecting the base to the macrocycle ring. Thus, Traylor and co-workers[102] have shown that strain introduced by the chain length or the position of attachment can have a dramatic effect on the ligand binding properties of these compounds.

3. Single-Face-Hindered Hemes

Sterically hindered porphyrins have been prepared to create a cavity on one of the two faces of the heme. This can prohibit ligation on the protected face, whereas coordination on the free face remains open. This approach has been used by many research groups to produce a wide variety of architecturally different model

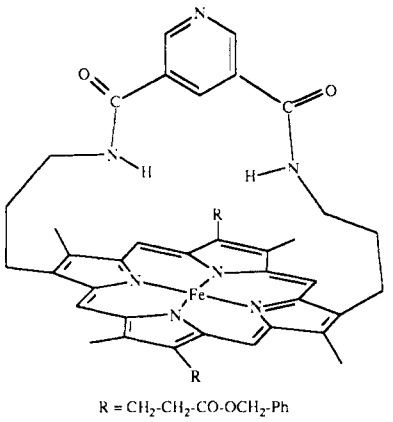

Fe-PyridineCyclophaneP (Traylor, Ref 100)

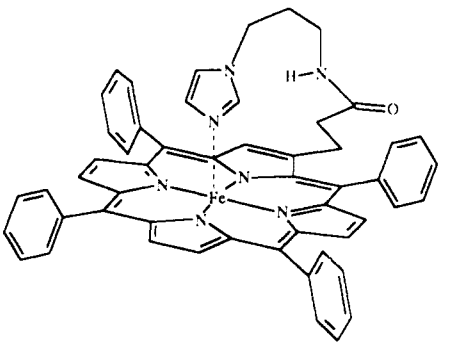

Fe-TPP-[NH(CH2)3Im] (Momenteau, Ref 93)

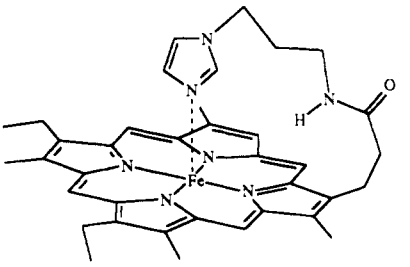

Fe-PyrroP-[O(CH2)3Im] (Traylor, Ref 88)

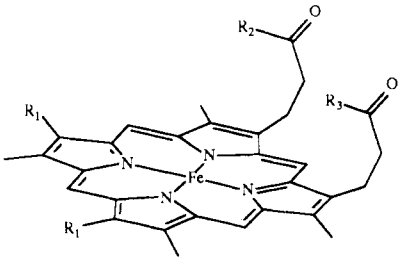

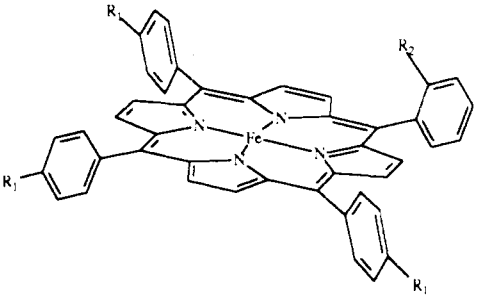

R1 = -CH=CH2 R2 = R3 =

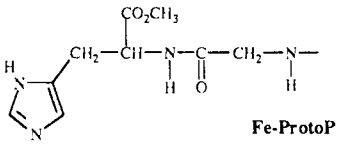

Fe-ProtoP

(Van der Heijden, Ref 89)

R1 = -CH2-CH3

R3 = -OH

R2 =

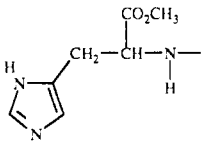

Fe-MesoP

(Hager, Ref 90,91)

R1 = -H

R3 = -OCH3

R2 =

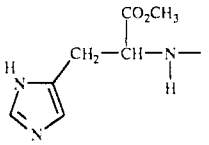

Fe-DeuteroP

(Momenteau, Ref 92)

R1 = -H R2 =

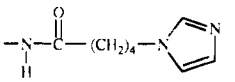

(Reed, Ref 96)

R1 = -H R2 =

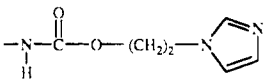

(Walker, Ref 97)

R1 = -CH3 R2 =

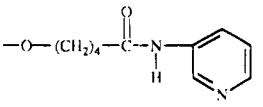

R1 = -CH3 R2 =

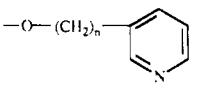

n = 2, 3

(Ibers, Ref 98)

Fe-TPP derivatives

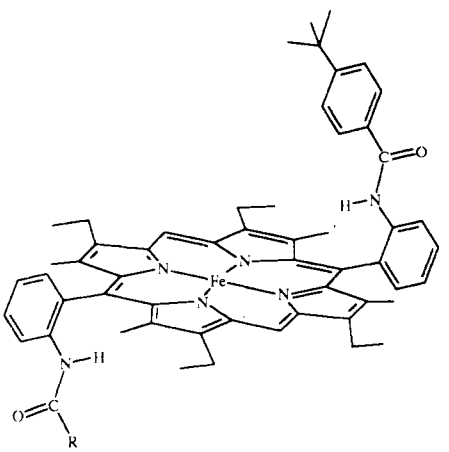

R =

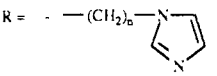

n = 2, 3

R =

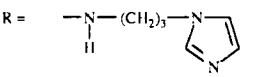

R =

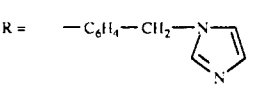

Fe-DPP derivatives (Chang, Ref 99)

Figure 7. Structures of hemes with covalently attached axial ligands.

porphyrins, e.g. picket fence,[103-106] pocket,[107] cyclophane,[108-111] cofacial,[112,113] bridged,[114] crowned,[115] capped,[116-118] strapped,[119-125] cross-strapped,[126] hybrid,[127] picnic basket,[128] jellyfish,[129,130] and reverse picket-fence ($T_{tBut}PP$).[131] The structures are represented in Figure 8. With some of these single-face-hindered hemes, the main problem of coordination control can be solved even in the presence of an unhindered ligand. The formation of five-coordinate complexes largely depends on the size of the host cavity. With compounds having a large and tightly constrained steric hindrance near one of the axial ligand binding sites, hemochrome formation is not observed because the sixth ligand affinity constant is drastically lowered. This has been demonstrated with certain capped,[132] pocket[107] and hybrid[127] porphyrins. For example, in a benzene or toluene solution containing an excess of 1-MeIm, both FeC_2Cap and $Fe(Piv)_2C8$ are five-coordinate. Increasing the length of the methylene chain in the cap or in the handle respectively gives compounds with looser superstructures which can form six-coordinate complexes, although the relation $K_B > K_B^B$ is usually maintained.

It is important to note that many of the superstructures of the single-face-hindered porphyrins cited above (and illustrated in Figure 8) are not capable of inhibiting hemochrome formation. Indeed, some of the superstructures may actually enhance axial ligand binding on the "sterically hindered" side of the heme relative to the open side. For example, it is a common misconception that the four pivalamide substituents of picket-fence porphyrin prevent six-coordination with bases such as 1-MeIm. This interpretation has unfortunately found its way into textbooks.[133] The value of these types of superstructures is, as discussed below, to provide a protected, preferential site for the binding of dioxygen which, because it can displace an axial base in a six-coordinate species, may leave the false impression that the base was excluded.

Large differences in the affinity constants for the formation of five-coordinated compounds are observed. The affinity constants for the first base on an unprotected face seems to depend on the nature of the porphyrin. This can be seen in the low values measured during the titration of capped porphyrins[132] with 1-MeIm when compared to those of other systems. X-ray crystallographic data on the free base[134] and on the iron(III)–chloro complex[135] of this compound show a large doming of the porphyrin ring induced by the cap and this is suggested to cause the unusual ligation behavior seen in this system. A related "cis" effect has been used to explain the difference in affinity constants between compounds which differ in the chemical nature of groups linking the superstructures to the macrocycle ring.[127]

Single-face-hindered, five-coordinate complexes have been characterized by a number of methods including UV–visible spectroscopy,[107] resonance Raman,[136,137] and ^1H NMR.[107] Only one, $Fe^{II}(Piv)_2C8(1\text{-MeIm})$, has been crystallized and characterized with an unhindered base.[81] Mossbauer data at 4.2 K demonstrate the high-spin state of this complex in agreement with the magnetic susceptibility (μ = 5.4 μ_B). In the crystal structure, the five-coordinate iron atom is displaced 0.31 Å from the mean plane of the four nitrogen atoms and 0.34 Å from the best least-squares plane of the 24-atom porphyrin core. These values are smaller than those observed in other iron(II) five-coordinate complexes having a 2-methyl-hindered axial imidazole ligand (see Table 1). The smaller out-of-plane distances result in a slight decrease of the average iron–nitrogen bond length compared to those previously observed for Fe^{II}(2-MeIm) porphyrin complexes. Furthermore, the off-normal tilting of the imidazole (ϕ = 5°) is smaller. These data show that in five-coordinate complexes, an out-of-plane displacement of the iron atom and some imidazole tilting are general features. X-ray structures reveal that some subtle stereochemical effects are introduced by the face-hindering superstructure and the nature of the axial ligand. Thus, the value for the dihedral angle formed by the coordinate plane containing opposite nitrogen atoms and the axial ligand plane is 34.1°. This angle is much larger than those observed in other five-coordinate imidazole complexes where the average value is 10.4°.

Iron(II) complexes with 2-MeIm may be considered as good analogs of the active site of deoxyhemoglobin in the T state.[138] They also model deoxymyoglobin for which there is also a protein-induced off-axis tilt of the proximal histidine. The similarity of proteins and models has been confirmed by EXAFS (extended X-ray absorption fine structure) of deoxyhemoglobin and $Fe^{II}T_{piv}PP$(2-MeIm) in solution.[139] The close congruence of the T-state proteins and the 2-MeIm models means that the proteins have active-site structures which fairly closely approach the intrinsic unconstrained coordination geometry of high-spin iron(II) imidazole-liganded hemes. Thus, there is little or no evidence of tension in the iron to proximal histidine linkage other than a few degrees of off-axis tilt. Rather, the proximal histidine is now viewed as tethered by the T conformation of the protein. On the other hand, the 1-MeIm model of $Fe(Piv_2C8)$ may be a rather good model for R-state hemoglobin. The imidazole tilt is less, as is the out-of-plane iron displacement and doming of the porphyrin. These changes are in the direction of those that must occur upon oxygen binding. As will be discussed below, if the imidazole is prevented from moving along this trajectory, the oxygen affinity is lowered.

4. "*Integrated*" *Compounds*

Perhaps the most effective approach to obtain deoxyhemoglobin models is the design of both-face-hindered porphyrins in which the nitrogenous base (pyridine or imidazole) is inserted into one of the straps. In these types of compounds, double attachment of the base should ensure a high degree of iron five-coordination by generation of a high local concentration of ligand near the metal center and eliminate the need of having excess free ligand in solution. In addition, the double face hindering should inhibit the intermolecular associations observed with chelated or tailed hemes (see Scheme 1 in section IV.B.2).

The preparation of these complexes has been reported independently by Battersby[140-142] and by Momenteau,[143-147] and more recently by Orth,[148] Baldwin,[149] and Rose.[150,151] A number of these structures are illustrated in Figure 9. Electronic absorption[144,145] and ^1H NMR[144,145,152] data for these compounds are characteristic of high-spin, five-coordinate ferrous porphyrins.

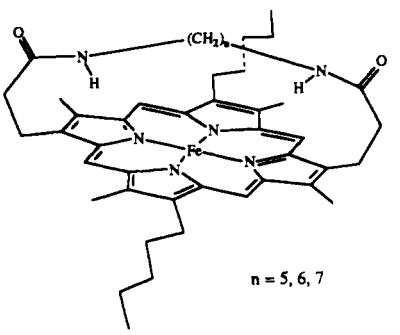

Fe-SP-(n+8) (Battersby, Ref 114)

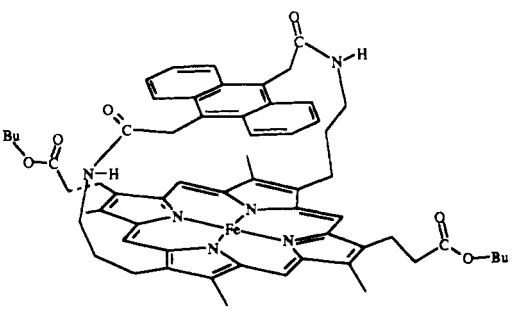

Fe-AnthraceneCyclophaneP (Traylor, Ref 109)

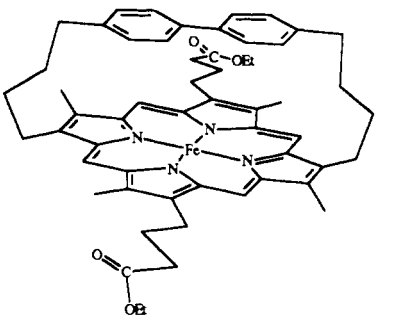

Fe-CyclophaneP (Traylor, Ref 108)

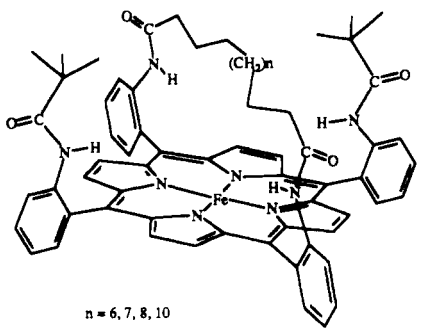

Fe-Piv$_3$C$_{(n+2)}$PP (Momenteau, Ref 127)

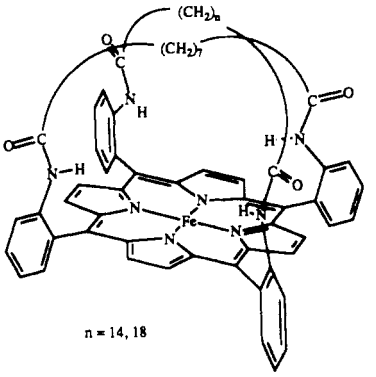

Fe-Cross-StrappedP (Uemori, Ref 126)

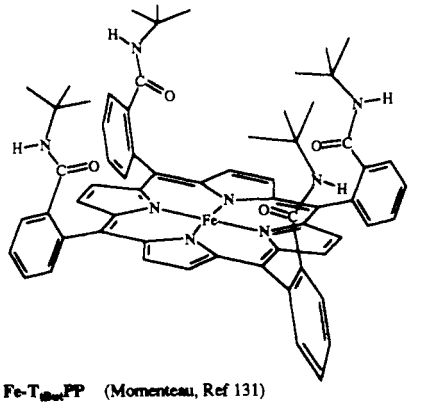

Fe-T$_{tBut}$PP (Momenteau, Ref 131)

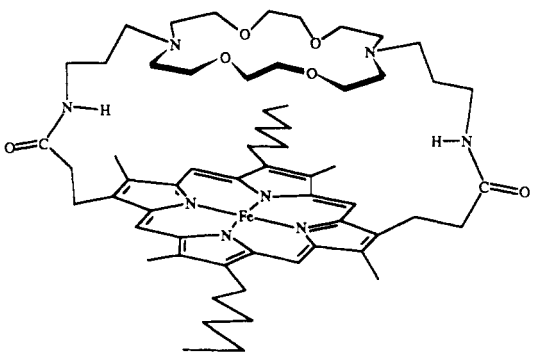

Fe-CrownedP (Chang, Ref 115)

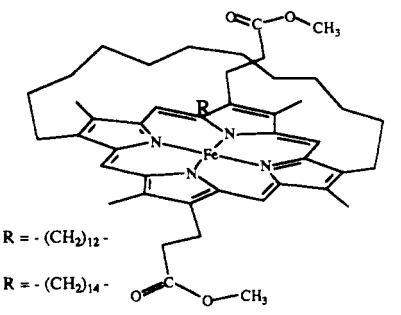

Fe-PLCn (Momenteau, Ref 125)

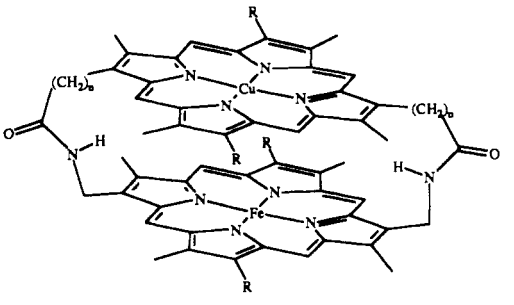

Fe-Cu-Cofacial P (Chang, Ref 113)

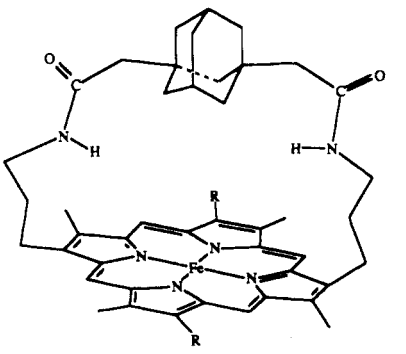

Fe-AdamanthaneCyclophaneP (Traylor, Ref 111)

Figure 8. Structures of single-face-hindered hemes.

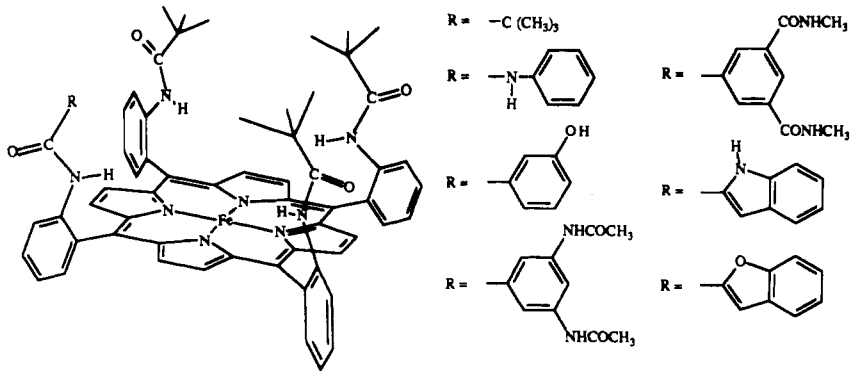

Fe-'Picket Fence'P and derivatives
(Collman, Ref 103 ; Reed, Ref 106)

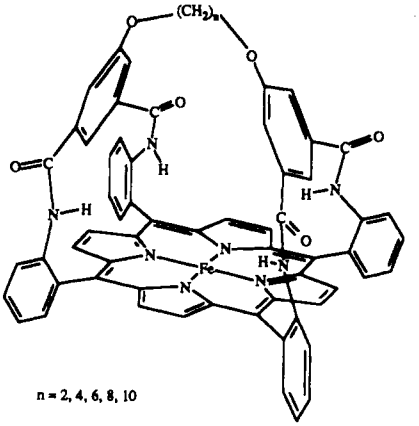

Fe-Picnic-Basket P (Collman, Ref 128)

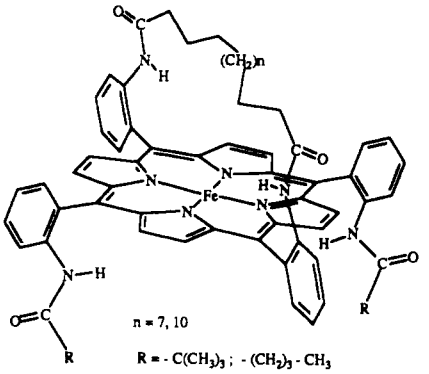

Fe-JellyfishP (Uemori, Ref 129,130)

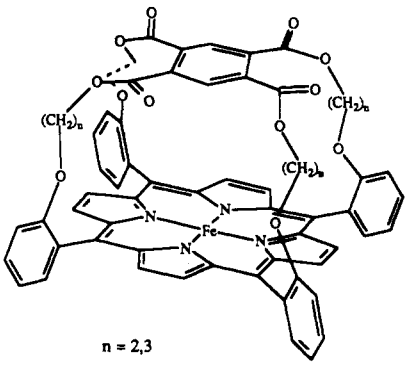

Fe-CnCappedP (Baldwin, Ref 116-118)

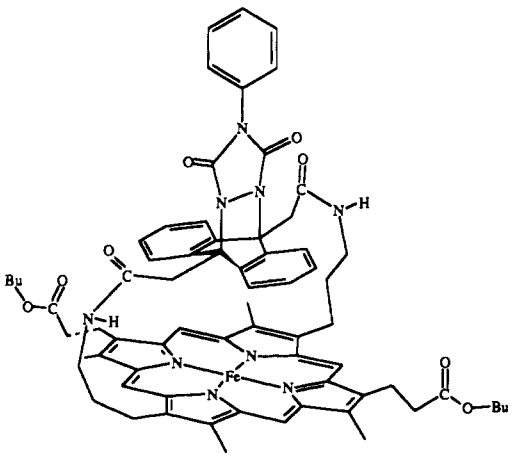

Fe-PagodaCyclophaneP (Traylor, Ref 109)

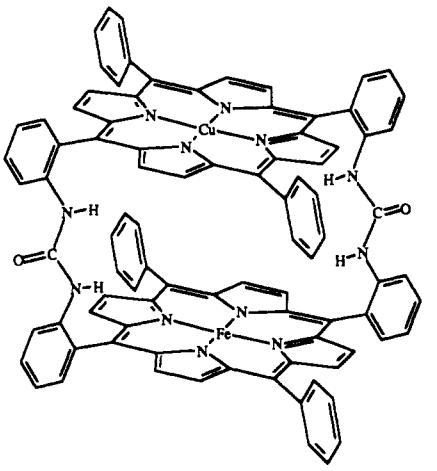

Fe-Cu-Face to face P (Collman, Ref 112)

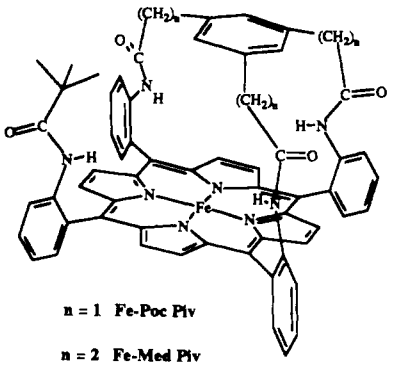

(Collman, Ref 107)

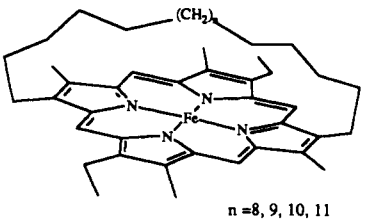

Fe-nStrappedP (Dolphin, Ref 124)

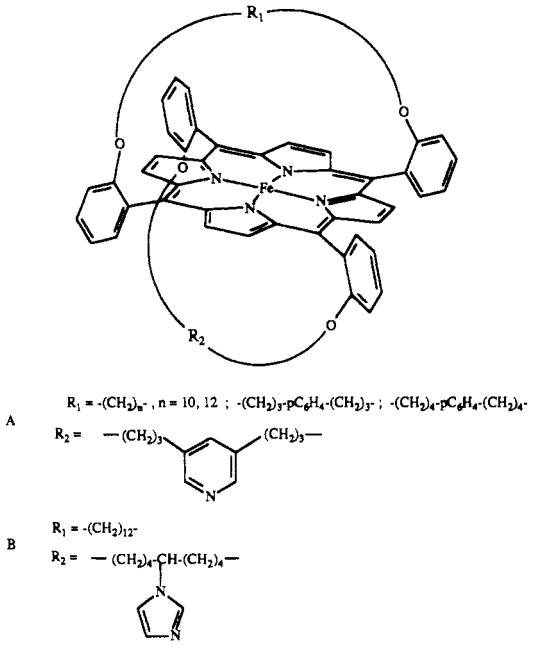

Fe-Hanging Base eBHP (Momenteau, Ref 144)

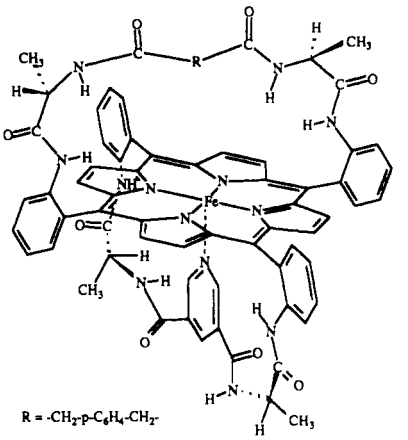

Fe-Hanging Base Chiral aBHP (Rose, Ref 150,151)

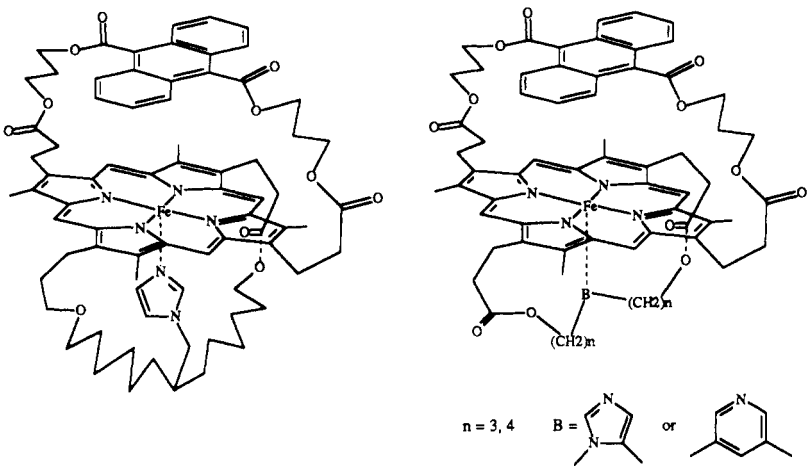

Fe-Hanging Base Doubly Bridged P (Battersby, Ref 140,141)

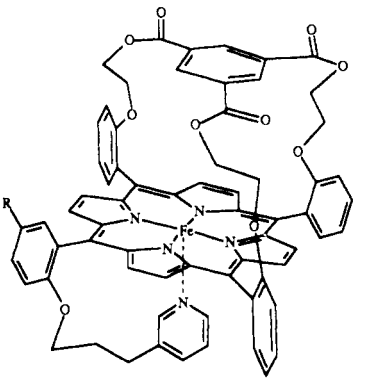

Fe-PocP[O(CH$_2$)$_3$Py (Orth, Ref 148)

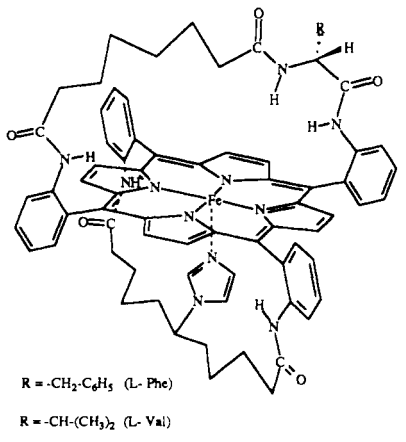

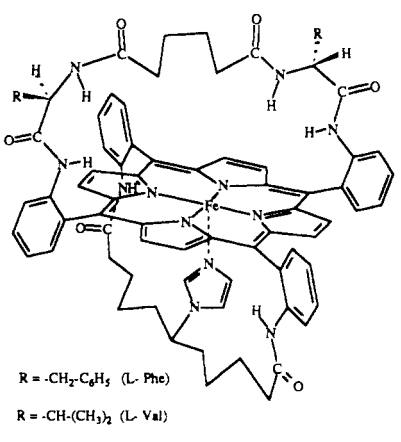

Fe-Hanging Base Chiral aBHP (Momenteau, Ref 146)

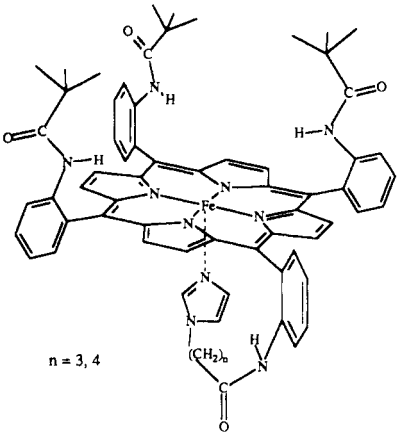

Fe-(Plv)$_3$(nCIm)PP (Collman, Ref 95)

Figure 9. Structures of "integrated" hemes with both covalently attached axial ligands and fact-hindered superstructure.

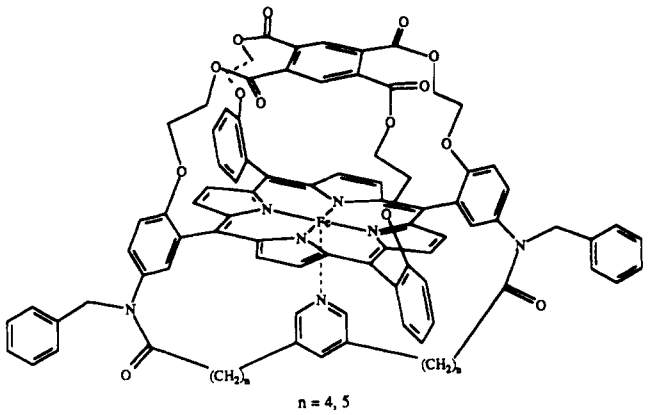

Fe-Hanging Base Capped-Strapped P (Baldwin, Ref 149)

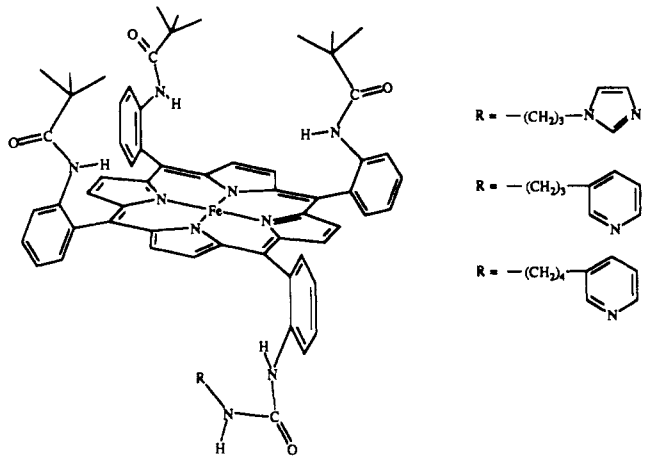

Fe-(PFnCUB) (Collman, Ref 193)

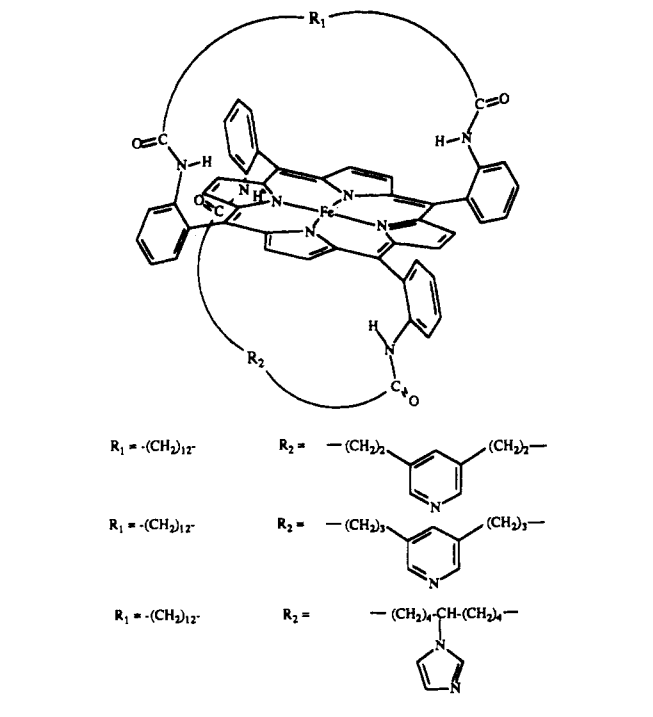

Fe-Hanging Base aBHP (Momenteau, Ref 145)

C. Inhibition of Autoxidation

It is a fact that unhindered ferrous hemes are oxidized rapidly and irreversibly in the presence of dioxygen, even in aprotic solvents. At least two general mechanisms have been identified depending on the conditions: the well-accepted μ-peroxo mechanism and the less understood, proton-catalyzed superoxide mechanism.

Cohen, Caughey, and coworkers[154-156] observed that the rate-determining step of the autoxidation of deuterohemochrome in nonaqueous solvents with pyridine as axial ligand is second order in iron(II) and first order in dioxygen. These results suggested the formation of a μ-peroxo–Fe^{III} dimer intermediate. Other studies have led to the same conclusion.[157-159] Characterization of a dioxygen-bridged diiron complex has been presented by Balch *et al.*[36,37] By using tetraphenylporphyrin and related complexes in toluene at −80 °C, a peroxo-bridged intermediate was detected by visible spectroscopy and proton NMR studies. Upon warming, this complex is unstable and is converted to a μ-oxo dimer via an iron(IV) species.[160] The mechanism of oxidation at low base concentration is summarized by the following equations:

$$(B)PFe^{II} + O_2 \rightarrow (B)PFe(O_2)$$

$$(B)PFe(O_2) + (B)PFe^{II} \rightarrow PFe^{III}—O_2—PFe^{III} + 2B$$

$$PFe^{III}—O_2—PFe^{III} + 2B \rightarrow 2\,(B)PFe^{IV}=O$$

$$(B)PFe^{IV}=O + (B)PFe^{II} \rightarrow PFe^{III}—O—PFe^{III} + 2B$$

The irreversible autoxidation of iron(II) upon exposure to dioxygen considerably limits the use of simple ferrous porphyrins as models for the active site of hemoproteins. In hemoproteins, it is clear that these reactions cannot occur because the polypeptide chain surrounding the heme prevents the close approach of two hemes. However, oxygenated hemoglobin and myoglobin under biologically active conditions are not completely stable. About 3% of hemoglobin in the body exists in the ferric form.

A number of mechanisms have been proposed to account for this autoxidation, all of which involve electron transfer from iron(II) to O_2 to form a superoxide species which undergoes further irreversible reaction. Catalysis by acid and a first-order dependence of $[H^+]$ in the rate law suggests a protonation in the rate-determining step. However, it has proved to be very difficult to determine whether the electron transfer is inner sphere or outer sphere or where the site of protonation is. In a 1982 reassessment of possible mechanisms, Caughey *et al.*[161] favored an outer-sphere electron-transfer mechanism but could not rule out displacement of O_2^- (or HO_2) from iron by a nucleophile. The displacement mechanism is favored by Shikama[19] who, among others,[162] has identified superoxide spectroscopically. More recently, Olson and co-workers[163] have favored a direct dissociation of HO_2 from protonated oxymyoglobin at low oxygen pressures. At high oxygen pressures they invoke the outer-sphere electron transfer mechanism with water as the nucleophile that stabilizes iron(III).

The common theme of these three mechanisms is the protic capture of superoxide. This is consistent

with observations on a large number of mutant hemoglobins[164] and myoglobins.[163] Mutations which disrupt the tight binding of the heme into its hydrophobic crevice typically give rise to easily oxidized subunits. It is assumed that water can more readily approach the FeO_2 distal region and catalyze the formation of a superoxide species either as a nucleophile to iron or as a source of protons and solvation. Mutations which place acidic functionality in the distal region are frequently so susceptible to autoxidation that they cannot function as oxygen carriers. An example is Hb Zürich where the β chains have a His(E7) → Arg mutation.

The proton-catalyzed superoxide pathway for the autoxidation of synthetic hemes is perhaps even more difficult to study than the proteins because of the complexity of acid–base equilibria introduced by the axial ligand. Distinguishing inner from outer sphere electron transfer is difficult because of the lability of high-spin iron(II) toward ligand association and dissociation. Using substitutionally inert ruthenium complexes, Taube and co-workers[165] have established the viability of an outer-sphere electron-transfer mechanism and illuminated the manner in which a thermodynamically disfavored one-electron transfer can be driven by protons and a further one-electron process. The essential elements of this mechanism are the capture of superoxide ion by a proton and the subsequent decomposition of HO_2. This occurs via a further one-electron transfer in the case of ruthenium but, in the general case, may also occur via disproportionation:

$$M^{II} + O_2 \rightarrow M^{III} + O_2^-$$

$$O_2^- + H^+ \rightarrow HO_2$$

$$HO_2 + M^{II} \rightarrow M^{III} + HO_2^-$$

$$HO_2 + O_2^- \xrightarrow{\text{disprop}} O_2 + HO_2^-$$

Early evidence from non-heme iron(II) has been discussed by Hammond and Wu,[158] and more recently, Busch *et al.*[166,167] have implicated the outer-sphere electron-transfer mechanism in the autoxidation of iron(II) cyclidene complexes. By studying the autoxidation of hemochromes under high axial base concentration (pyridine), Castro[168] has provided evidence for an outer-sphere electron-transfer mechanism. The rate of autoxidation is faster than the rate of axial base dissociation. It is apparent that six-coordinate iron(II) porphyrins may behave in a manner similar to the better studied, substitutionally inert complexes like those of ruthenium(II) ammines. With five-coordinate high-spin hemes, however, the details of the autoxidation mechanism remain unclear. Due to the lability of the axial base(s) it has not yet been possible to distinguish between inner- and outer-sphere formation of HO_2. In addition, it is experimentally difficult to obtain a pH profile of the reaction adequate to identify the key protonation step(s) or the subsequent two-electron chemistry.

Nevertheless, the importance of water as a source of protons and the identification of peroxide as the two-electron product is seen qualitatively in the relative stability of basket-handle porphyrins. Momenteau *et al.*[169] have shown that the stability of the oxygenated species of iron(II) basket-handle porphyrins is largely dependent on the concentration of water in the organic solvents. The steric encumbrance of both faces in these compounds (see Figure 10) inhibits oxidation via μ-peroxo dimer formation and increases the half-life of the oxygen adducts in comparison to open or single-face-hindered hemes. A hydrophobic environment is formed by the bridging chains.[170] The ultimate oxidation products in toluene or methylene chloride solution exhibit optical and ESR spectra characteristic of monomeric $Fe^{III}(OH)$ derivatives (hematins).[171] The oxygen reduction products in water-saturated methylene chloride were probed using ^{17}O NMR spectroscopy.[172] During the oxidation process some resonances of ^{17}O-enriched species were detected at low frequencies. A resonance at 11.1 ppm was assigned to $H_2{}^{17}O$ and is shifted upfield due to the presence of paramagnetic iron(III) species. Two resonances at 168.5 and 173.3 ppm were both assigned to $H_2{}^{17}O_2$. The former absorption is probably due to $H_2{}^{17}O_2$ in microscopic water droplets, present in the wet organic solvent, while the latter is truly dissolved. From these data the following water-driven (i.e. proton-driven) reaction scheme was proposed:

$$PFe^{II} + {}^*O_2 \rightarrow PFe({}^*O_2)$$

$$PFe({}^*O_2) + H_2O \rightarrow PFe^{III}(OH) + H{}^*O_2$$

$$2H{}^*O_2 \rightarrow H_2{}^*O_2 + {}^*O_2$$

For the reasons stated above, it remains uncertain whether the initial electron transfer is inner or outer sphere but the isotope data are consistent with disproportionation of HO_2 to give hydrogen peroxide.

D. Reversible Oxygenation of Iron(II) Porphyrins

Reversible oxygen binding to iron(II) porphyrins and the production of stable dioxygen adducts requires thwarting the autoxidation pathways discussed above. At room temperature, the oxygenation of base-free hemes (four-coordinate species) has not been demonstrated. As mentioned earlier, several groups have provided evidence for $FeP(O_2)$ species at low temperature,[13,35,36,173] although the rigorous absence of water as an axial ligand has frequently not been proved. It is with an axial base present that a larger number of oxyhemoglobin models have been prepared. Three basic approaches have been used to control oxygen coordination in hemes. All exploit ways to prevent μ-peroxo formation in a hydrophobic environment.

1. Immobilization into Polymers

Synthetic polymers are comparable to the hydrophobic protein matrix in hemoproteins where a principal role of the protein is to separate heme units and prevent bimolecular oxidation in the presence of dioxygen. Wang[174] was the first to demonstrate the reversible O_2 (and carbon monoxide) binding when iron(II) protoporphyrin(IX) dimethyl ester and 1-(2-phenylethyl)-imidazole were embedded in a polystyrene film. A similar system in which neither the porphyrin nor the axial ligand is covalently attached to the polymer was used more recently by Chang and Traylor.[175] They utilized an imidazole-chelated heme. Reversible oxy-

genation was observed spectrophotometrically suggesting that the heme molecules are not sufficiently mobile to form μ-peroxo complexes.

In order to obtain systems in which no free axial base was required, polymers containing a covalently attached base have been developed. Collman and Reed[73] reported the preparation of cross-linked polystyrene containing an imidazole ligand. Treatment of this resin with $Fe^{II}TPP$ in benzene gave six-coordinated hemes. In the presence of O_2, μ-oxo dimer formation was observed, suggesting that in solution the polymer matrix was not rigid enough to prevent interaction between two hemes. A modified silica gel containing imidazole groups covalently linked on the surface was reported to react with $Fe^{II}TPP$ generating active sites which are apparently five coordinate.[176,177] The resulting system is capable of chemisorption of molecular oxygen weakly at room temperature, strongly at −78 °C and irreversibly at −127 °C. No autoxidation to μ-oxo dimer was observed suggesting that the more rigid support might be effective in preventing oxidation. Other types of polymers have been reported by Tsuchida [quaternized poly(4-vinylpyridine)][178] and Fuhrhop (styrene-1-vinylimidazole copolymers).[179] In each case, the binding of dioxygen to an iron(II) porphyrin was not observed. This suggests that dioxygen is not able to replace the ligand attached to the polymeric chain due to the formation of six-coordinated hemes.

Careful studies were reported by Tsuchida[180] on the reaction of O_2 with aqueous solutions of poly-L-lysine/heme. Reversible oxygenation is evident in spectroscopic and magnetic susceptibility data. Furthermore, sigmoidal behavior of O_2 binding was characterized by a Hill coefficient of 2.1 in a pH 12 phosphate buffer at 30 °C.[181] The origin of the cooperativity could be the result of a change in the polypeptide helical structure upon formation of the polymer–heme complex. Association of "picket-fence" type porphyrins with water-soluble copolymers of polyethylene and styrene *N*-vinylimidazole containing hydrophobic moieties gives a material which binds dioxygen in aqueous solution at room temperature.[182] It is unlikely, however, that water is in the immediate vicinity of the FeO_2 binding site.

Another approach consists of covalently linking hemes to polymeric chains. In this field, Bayer and Holzbach[183] described the synthesis of a water soluble compound in which polyethylene glycol bis(glycine ester) was linked to iron(II) protoporphyrin(IX) whose propionic acid side chains were substituted by two histidine residues via acetamide functionality. As a model of the oxygen-transporting functions in red blood cells, Tsuchida[184] has found that a phospholipid picket-fence type porphyrinatoiron(II) complex of mono(1-dodecyl-2-methylimidazole) embedded in liposomes binds molecular oxygen reversibly under physiological conditions. The half-life is said to be about 12 h.

2. Low Temperature

Oxygen adducts of most iron(II) porphyrin complexes are stable at low temperature because bimolecular reaction to form μ-peroxo derivatives is dramatically slowed. Chang and Traylor[185] studied the reversible oxygenation in dichloromethane solution at −45 °C of chelated mesoheme and pyrroheme in which imidazole is linked to a pyrrolic position (see Figure 7). The spectral changes were similar to those for deuteriomyoglobin, indicating true dioxygen binding. The association constant $P_{1/2}^{O_2}$ was estimated to be 0.2 Torr. At higher temperatures the complexes were irreversibly oxidized. A similar pyridine system in methylene chloride at −45 °C showed no oxygenation and was oxidized rapidly. This led to the conclusion that pyridine does not support oxygenation. Such a conclusion is difficult to accept in the light of many more recent reports that have shown reversible dioxygen binding of iron(II) porphyrins with pyridine as axial base.[186,103]

The stabilization of oxygenated complexes of flat hemes and chelated hemes at low temperature was reported in a flurry of papers published in 1974.[187-191] These papers presented spectral evidence that hemes with pyridine, alkyl imidazoles, simple amine-type ligands, and dimethylformamide as axial ligands are capable of binding O_2 at temperatures below −45 °C with minimal oxidation. From the spectral changes during manometric titration with O_2, some affinity constants were estimated. Imidazole appears to be the best ligand and the O_2 affinities are larger in solvents of high dielectric constant. These features are discussed in more detail in section V.

3. Superstructured Heme Models

This approach uses covalently modified synthetic compounds. Each of these superstructured porphyrins is sterically encumbered on at least one side of the heme. This frequently directs the binding of a nitrogenous base to the other side. Such an approach has been developed by many groups to produce an array of different porphyrins modeling the active site of oxygen-carring hemoproteins. The bulky substituent covering one side of the heme slows irreversible autoxidation via the μ-peroxo pathway. An appropriate axial ligand concentration also favors reversible oxygenation rather than irreversible oxidation.

An attempted synthesis of a single-face-hindered porphyrin, iron cyclophane P in Figure 8, was described by Traylor.[108] However, this porphyrin was prepared in only very poor yield and no physicochemical studies were reported with the iron complex. The earliest successful work in this field was reported by Collman *et al.*[45,103,192] with the elegant "picket-fence" porphyrin (Figure 8). This compound has four pivalamido groups which form a protected binding cavity for O_2. It provides satisfactory steric protection and stabilizes reversible O_2 binding at room temperature, as long as a large excess of axial ligand (e.g. 1-MeIm) is present. A later version has three pivalamido pickets and a tailed base.[193] Following the report of picket-fence porphyrin, a great number of heme models has been described. They differ in the nature of the steric hindrance: capped,[116-118] cyclophane,[108,111,194] crowned,[115] pocket,[107,195] picnic basket,[128] cofacial,[112,113,196,197,225,226] and hybrid.[127] Representative structures are shown in Figure 8 to illustrate the variety of ways used to achieve a single-face-hindered porphyrin. Most of the oxygen binding studies have been carried out in an organic solvent in the presence of various axial ligands including 1-alkylimidazole, 1,2-dimethylimidazole, 2,5-dicyclohexylimidazole, and pyridine, always in excess. Under such conditions, they show varying degrees of reversible O_2 binding at room temperature. However, in nonpolar organic solvents, the lifetimes of the oxygen adducts

depend on the nature and the concentration of the exogenous base. For example, at low concentrations of imidazole, undesired μ-oxo dimer formation still takes place presumably via the unprotected side of the heme.

Steric encumbrance on *both* faces of the porphyrin ring prevents the bimolecular oxidation pathway but often still allows ligand binding. This strategy has been proposed by several groups: there are bis-pocket porphyrins of Amundsen,[198] Cense,[199] Suslick,[200] double-sided porphyrins of Tsuchida,[201,202] basket-handle porphyrins of Momenteau,[144-146,169,160,203] Rose,[204] Walker,[205] Mansuy,[206] and Chandrashekar,[207] and jellyfish porphyrins of Uemori.[129,130] These are illustrated in Figure 10. The degree of steric hindrance is indicated by the rates of autoxidation of the iron(II) species. Thus, in the presence or absence of a nitrogenous base, giving six- and four-coordinate complexes, respectively, iron(II) complexes of these porphyrins exhibit very good redox stability toward oxidation when exposed to 1 atm of dioxygen at room temperature. For example, in the absence of 1-MeIm, Momenteau *et al.*[169] reported that Fe(II) basket-handle porphyrins in the cross-trans-linked configuration (see Figure 10) have a half-life ($t_{1/2}$) for oxidation to hematin derivatives of 1.5–10.5 min, depending upon the nature of the handle. In toluene at 25 °C under O_2 (1 atm), the half-lives for oxidation of six-coordinate iron(II) complexes are 11–25 min.

In order to optimally solve the problem of attaining five-coordination with both-face-hindered porphyrins, pyridine or imidazole has been inserted into one of the straps. The preparation of these "integrated" compounds marks an important advance and a further refinement in the design of dioxygen carrier models. This is because incorporation of a N-donor ligand into the handle simulates the "proximal" base of hemoproteins and steric hindrance on the other face creates a protected "distal" cavity for dioxygen ligation. These kinds of compounds have been developed by Baldwin,[149] Battersby,[140-142] Momenteau,[143-147] and Rose[150-151] and are discussed in the following paragraphs.

The original one-face-capped porphyrin approach developed by Baldwin has been extended to modified capped compounds in which a pyridine strap is covalently bound to opposite meso groups over the porphyrin face opposite the cap (Figure 9). The two variants made in this manner differ by the number of the methylene groups which link the pyridine to the macrocycle (C_5 and C_4).[149] Their corresponding iron(II) complexes exhibit reversible binding in dry toluene solution at room temperature and show good stability to autoxidation. The C_5-strapped complex has a $t_{1/2}$ of several days while that of the C_4 strapped complex is several months.

Battersby and Hamilton[141] prepared compounds from coproporphyrin incorporating pyridine as axial ligand (Figure 9). Iron(II) derivatives in rigorously dried methylene chloride reversibly bind dioxygen. The resulting oxygenated species show visible spectra closely similar to those of oxyhemoproteins and had half-lives of up to 105 min at room temperature. In DMF, a more stable oxygenated species was formed having a $t_{1/2}$ of 2 h. Replacing pyridine by imidazole considerably increased the capacity of compounds to reversibly oxygen binding. The $t_{1/2}$ for the oxygenated adduct was 1 day at room temperature in DMF solution.

Momenteau *et al.*[144-147] have prepared two different series of integrated compounds, called hanging-base basket-handle porphyrins, which differ both by the mode of linkage of the handle to the macrocycle, ether and amide, and by the nature of the hanging axial base, pyridine or imidazole (Figure 9). These compounds showed reversible binding of dioxygen to give relatively stable oxygenated species. Compounds in the amide series incorporating a pendant imidazole appeared better models that those in the ether series. Their lifetime was about 1 day in dry toluene under 1 atm of O_2. Their stability was considerably diminished in wet organic solvents.[169]

More recently, Momenteau *et al.* have reported the synthesis of the first hanging-base basket-handle porphyrins in which one or two amino acid residues (L-phenylalanine or L-valine) are inserted into one of the handles, with a proximal imidazole on the second.[146] The inclusion of two amino acids in the handle imparts more rigidity in the distal cavity, providing better central steric hindrance. As well, it increases the polarity of the cavity relative to the simplest amide basket-handle porphyrins. Unusual spectrophotometric behavior and magnetic properties of the deoxy compounds are observed and can be explained by the unexpected incorporation of a water molecule in the sixth coordination site of the iron(II) atom, stabilized in the distal cavity by hydrogen bonding between water protons and the carbonyl group of the peptide bonds.[208] The presence of water does not allow good coordination of O_2 due to the resistance of the water complexes to displacement by O_2. Furthermore, significant irreversible oxidation takes place in solution, presumably because the water catalyzes the superoxide pathway of autoxidation.

V. Thermodynamic Measurement of O_2 Binding

Of great chemical interest is the problem of understanding the factors responsible for the great difference in O_2 affinity among the hemoproteins. For example, the $P_{1/2}{}^{O_2}$ at room temperature varies from 0.002 Torr for the nematode *Ascaris*[209] to ~1 Torr for mammalian myoglobin[210] (see beginning of Table 2). This large range demonstrates the important role of the surrounding protein in controlling the coordination chemistry at the iron atom. These influences can be partitioned into "proximal" effects and "distal" effects according to whether the axial base or the environment surrounding the FeO_2 moiety is being considered. Both steric and electronic effects have been investigated in model compounds. A "cis" effect, i.e. an effect arising from electronic or steric perturbation of the porphyrin, may also be a factor.

A. Experimental Approach

Several methods have been used for determination of oxygenation equilibria and kinetic constants: spectrophotometry, potentiometry, and flash photolysis. The choice of method depends on the magnitude of the equilibrium constants, the type of solvent employed, and the general stability of the oxygenated adducts. Few equilibrium constants have been determined by manometric measurements of dioxygen uptake in solution at room temperature because of limitations in the half life of the O_2 adducts. Generally, the kinetic

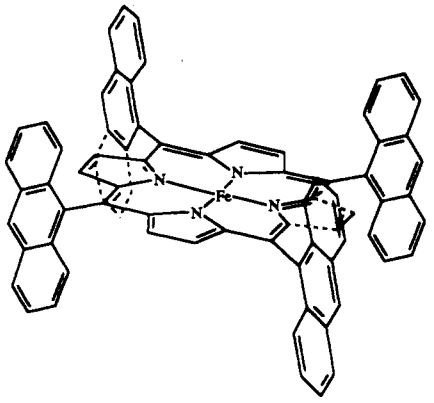

Fe-TAP (Cense, Ref 199)

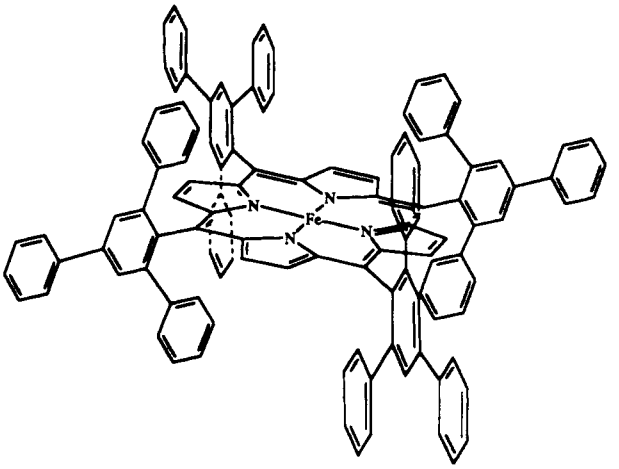

Fe-'Bis pocket'P (Suslick, Ref 200)

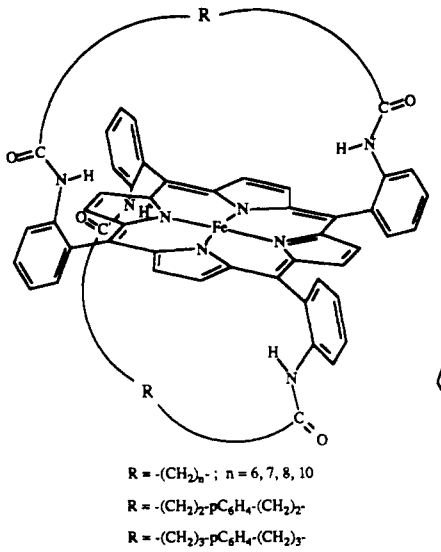

Fe-aBHP (Momenteau, Ref 145)

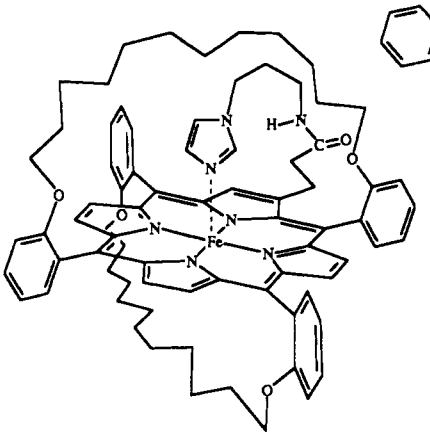

Fe-eBHP-[NH(CH2)3Im] (Momenteau, Ref 94)

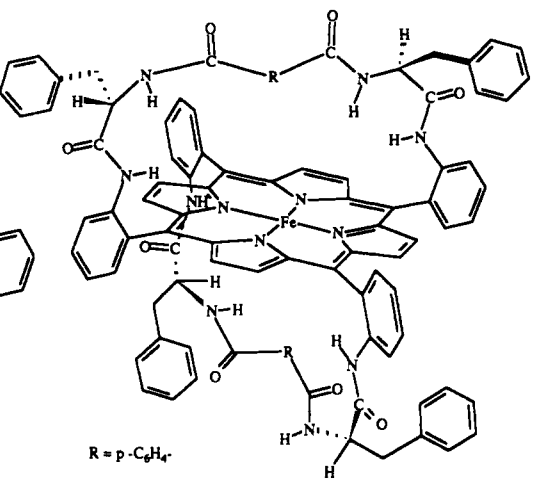

Fe-Chiral aBHP (Mansuy, Ref 206)

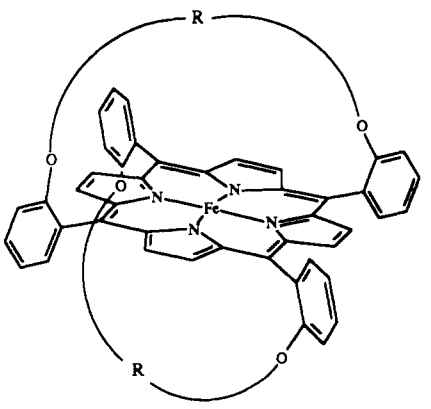

Fe-eBHP (Momenteau, Ref 170,203)

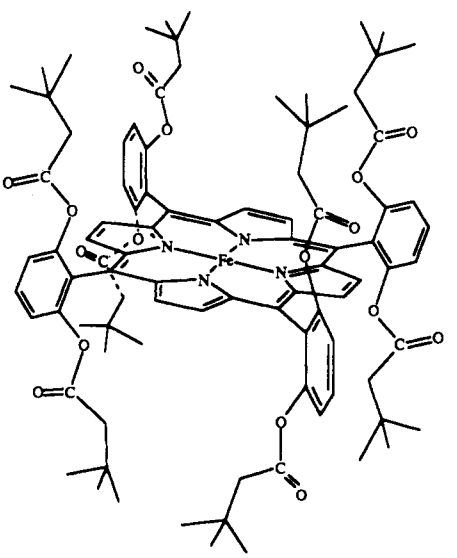

Fe-'Double-sided'P (Tsuchida, Ref 201)

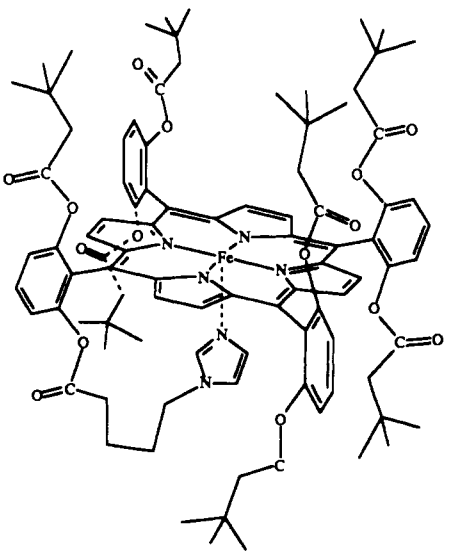

Fe-(PivO)7[O(CH2)4Im]PP (Tsuchida, Ref 202)

Figure 10. Structures of both-faces-hindered hemes.

Table 2. Equilibrium and Kinetic Data for Natural and Synthetic Dioxygen Complexes

compounds	k^+, M^{-1} s^{-1}	k^-, s^{-1}	K_{O_2}, M^{-1}	$P_{1/2}^{O_2}$, torr[a]	conditions	ref(s)
Mb (sperm whale)	$(10–20) \times 10^6$	10–30		0.29	H_2O, pH 7, 25 °C	404,210,405
				0.70	H_2O, pH 8.5, 25 °C	405
Hb (human R)				0.17	H_2O, pH 7, 25 °C	65,210,404,407
Hb (human T)				26	H_2O, pH 7, 25 °C	65,210,406–408
Hb α chain (human)	3.36×10^7	28	12×10^5	0.63	0.1 M phosph, pH 7, 5, 25 °C	409,410
Hb β chain (human)	2.24×10^7	16	14×10^5	0.25	0.1 M phosph, pH 7, 5, 25 °C	
Mb (sperm whale) (E7 His)	14×10^6	12	1.2×10^6		0.1 M phosph, pH 7, 20 °C	268
Mb (sperm whale) (E7 Gly)	140×10^6	1600	0.087×10^6		0.1 M phosph, pH 7, 20 °C	268
Hbα (E7 His) (human)	29×10^6	101	2.9×10^6		0.1 M phosph, pH 7, 20 °C	268
Hbα (E7 Gly) (human)	220×10^6	620	0.4×10^6		0.1 M phosph, pH 7, 20 °C	268
Hbβ (E7 His) (human)	100×10^6	21	5.0×10^6		0.1 M phosph, pH 7, 20 °C	268
Hbβ (E7 Gly) (human)	100×10^6	37	3.0×10^6		0.1 M phosph, pH 7, 20 °C	268
Mb (E7 Val)	250×10^6	23000	11×10^3		0.1 M phosph, pH 7, 20 °C	268
Mb (E7 Phe)	74×10^6	10000	7×10^3		0.1 M phosph, pH 7, 20 °C	268
Mb (E7 Arg)	79×10^6	890	90×10^3		0.1 M phosph, pH 7, 20 °C	266
Mb (E7 Met)	75×10^6	1700	43×10^3		0.1 M phosph, pH 7, 20 °C	266
Mb(B10 Ala)	14×10^6	18	0.8×10^6		H_2O, pH 7, 20 °C	271
Mb(B10 Val)	8.8×10^6	8.3	1.1×10^6		H_2O, pH 7, 20 °C	271
Mb(B10 Phe)	21×10^6	1.4	15 × 106		H_2O, pH 7, 20 °C	271
Hb Ascaris	1.5×10^6	0.004	3.75×10^8	0.002	0.1 M phosph, pH 7, 20 °C	209
Hb Aplysia	1.5×10^7	70	2.2×10^5	2.5	0.1 M phosph, pH 7, 20 °C	411
Leg Hb	1.5×10^8	11	1.35×10^7	0.046	0.1 M phosph, pH 7, 20 °C	411
Fe-T_{pOH}PP (1,2 Me_2Im)				5.3	toluene, −45 °C, [B] = 1.0 M	241
Fe-T_{pOCH_3}PP (1,2 Me_2Im)				0.41	DMF, −45 °C, [B] = 1.0 M	241
Fe-ProtoP(Im)	5.5×10^7	310	1.8×10^5	3.06	H_2O, pH 7.3, 22 °C, [B] = 0.01 M	412
Fe-Capped(1-MeIm)				280	toluene, 26 °C	242
Fe-C_2Capped(1-MeIm)				23	toluene, 25 °C, [B] = 1.0 M	241,246
Fe-C_2Capped(1-MeIm)				4.5	toluene, 0 °C, [B] = 1.0 M	241,246
Fe-C_2Capped(1-MeIm)				0.78	toluene, −23 °C, [B] = 1.0 M	241,246
Fe-C_2Capped(1-MeIm)				0.10	toluene, −45 °C, [B] = 1.0 M	241,246
Fe-C_2Capped(1-MeIm)				6.5	toluene, 0 °C, [B] = 1.0 M	241
				0.82	CH_2Cl_2, −23 °C, [B] = 1.0 M	241
Fe-C_2Capped(1-MeIm)				5.0	THF, 0 °C, [B] = 1.0 M	241
				0.35	THF, −23 °C, [B] = 1.0 M	241
Fe-C_2Capped(1-MeIm)				3.3	DMF, 0 °C, [B] = 1.0 M	241
				0.23	DMF, −23 °C, [B] = 1.0 M	241
Fe-C_2Capped(1,2-Me_2Im)				4000	toluene, 25 °C, [B] = 1.0 M	241,246
				930	toluene, 0 °C, [B] = 1.0 M	241,246
				162	toluene, −23 °C, [B] = 1.0 M	241,246
				27	toluene, −45 °C, [B] = 1.0 M	241,246
Fe-C_3Capped(1-MeIm)				120–181	toluene, 0 °C, [B] = 1.0 M	241,246
Fe-C_3Capped(1,5-DCIm)				54.2	toluene, 0 °C, [B] = 0.1 M	241
Fe-C_3Capped(1,2-Me_2Im)				880	toluene, −63 °C, [B] = 1.0 M	244–246
Fe-NapC_2Capped(1-MeIm)				2.3	toluene, 0 °C, [B] = 1.0 M	241
				0.28	toluene, −23 °C, [B] = 1.0 M	241
Fe-NapC_2Capped(1,2-Me_2Im)				613	toluene, 0 °C, [B] = 1.0 M	241
Fe-C_2CappedNO_2(1-MeIm)				7.1	toluene, 0 °C, [B] = 1.0 M	241
Fe-C_2CappedNO_2(1,2 Me_2Im)				413	toluene, −23 °C, [B] = 1.0 M	241
Fe-C_2Capped(pyridine)				181	toluene, 25 °C	246
				26	toluene, 0 °C	246
				4.2	toluene, −23 °C	246
				0.36	toluene, −45 °C	246
Fe-C_2Capped(3,4-lutidine)				34	toluene, 0 °C	246
Fe-C_2Capped(3-chloropyridine)				32	toluene, 0 °C	246
Fe-C_2Capped(*sec*-butylNH_2)				12	toluene, 0 °C	246
Fe-C_2Cap(*tert*-butylNH_2)				0.27	toluene, −63 °C	246
Fe-C_3Capped(*tert*-butylNH_2)				575	toluene, −63 °C	246
Fe-MesoP[$NH(CH_2)_3$Im]	3.5×10^6	22	16×10^5	0.57	$CetMe_3NBr$ (pH 7.3), 22 °C	413,414
	53×10^6	1700	3×10^4	2.8	toluene/CH_2Cl_2 90 % v/v, 22 °C	413–415
Fe-MesoP(acid)	40×10^6	33	1.2×10^6	0.46	$CetMe_2NBr$ (pH 7.3), 22 °C	413
Fe-MesoP(acid)	40×10^6	32	1.2×10^6	0.46	$CetMe_3NBr$ (pH 5.5), 22 °C	413
mesoHeme[$O(CH_2)_3$ Pyr]	17×10^6	380	4.5×10^4	12.2	$CetMe_3NBr$ (pH 7.3), 22 °C	225,413
Fe-MesoP[$O(CH_2)_2$Im]	4.9×10^7	160	0.3×10^6	1.83	$CetMe_3NBr$ (pH 7.3), 20 °C	225
Fe-MesoP[$O(CH_2)_3$Im]	2.2×10^7	23	0.9×10^6	0.61	$CetMe_3NBr$ (pH 7.3), 20 °C	225
Fe-MesoP[$O(CH_2)_4$Im]	2.9×10^7	24	1.2×10^6	0.46	$CetMe_3NBr$ (pH 7.3), 20 °C	225
Fe-ProtoP[$NH(CH_2)_3$Im]	26×10^6	47	0.55×10^6	1.0	$CetMe_3NBr$ (pH 7.3), 22 °C	413,414
Fe-ProtoP	6.2×10^7	4200	1.5×10^4	5.6	C_6H_6, 20 °C	248
Fe-MesoP[$O(CH_2)_3$Pyr]				>760	CH_2Cl_2, −45 °C	175
Fe-PyrroP[$O(CH_2)_3$Pyr]				400	toluene, −45 °C	175
Fe-PyrroP[$O(CH_2)_3$Im]				0.2	CH_2Cl, −45 °C	175
Fe-AcetylP[$NH(CH_2)_3$Im]	34×10^6	400	0.85×10^5	6.48	$CetMe_3NBr$ (pH 7.3), 20 °C	414
Fe-ProtoP[$NH(CH_2)_3$Im]	2.6×10^7	47	5.5×10^5	1	MTAB (pH 7.3), 20 °C	253
Fe-DeutP[$O(CH_2)_3$ Py]	20×10^7	7×10^4	2.5×10^3	57.4	toluene, 20 °C	217
Fe-TPP[$NH(CH_2)_3$Im]	5×10^7	2.5×10^4	1.7×10^3	84.3	toluene, 20 °C	217

Table 2. (Continued)

compounds	k^+, M^{-1} s^{-1}	k^-, s^{-1}	K_{O_2}, M^{-1}	$P_{1/2}{}^{O_2}$, torr[a]	conditions	ref(s)
Fe-TPP[O(CH_2)$_3$ Py]	10×10^7	11×10^4	1.1×10^3	130.3	toluene, 20 °C	217
Fe-(Piv)$_3$(5CIm)PP	4.3×10^8	2.9×10^3	1.48×10^5	0.58[b]	toluene, 25 °C	101,243
Fe-PocPivP(1-MeIm)	2.2×10^6	9	2.4×10^5	0.6[b]	toluene, 25 °C, [B] = 1.0 M	195,221
Fe-PocPivP(1,2-Me_2Im)	1.9×10^6	280	0.07×10^5	21[b]	toluene, 25 °C, [B] = 1.0 M	195,221
Fe-T(db)$_8$PP(1,2-Me_2Im)	4.5×10^7	7.9×10^4	5.7×10^2	230[b]	toluene, 25 °C	201
Fe-(Piv)$_3$(5CIm)PP	1.7×10^8	130	13×10^5	0.059[b]	toluene/MeOH (1/1), 25 °C	221,243
Fe-(Piv)$_3$(4CIm)PP	4.3×10^8	2.9×10^3	1.48×10^5	0.60[b]	toluene, 25 °C	101
Fe-(PivO)$_7$]O-(CH_2)$_4$Im]PP	6.3×10^7	1.2×10^3	5.25×10^4	2.5[b]	toluene, 25 °C	202
Fe-T_{piv}PP(1-MeIm)				0.49	solid state 25 °C	287
Fe-T_{piv}PP(1-MeIm)	4.30×10^8	230	1.4×10^5	1.02	toluene, 25 °C	218
Fe-(C_2PBP)(1,5-DCIm)				0.35	toluene, 25 °C, [B] = 1.0^{-3} M	265
Fe-(C_2PBP)(1,2-Me_2Im)				25	toluene, 25 °C, [B] = 1.0^{-3} M	265
Fe-(half-C_2PBP)(1,5-DCIm)				0.28	toluene, 25 °C, [B] = 1.0^{-3} M	265
Fe-(half-C_2PBP)(1,2-Me_2Im)				14	toluene, 25 °C, [B] = 1.0^{-3} M	265
Fe-T_{tBut}PP(1-MeIm)	5.50×10^7	35×10^3 (25%)	1.57×10^3	91.3	toluene, 5 °C, [B] = 1 M	131
	1.60×10^7	11×10^3 (75%)	1.46×10^3	91.3	toluene, 5 °C, [B] = 1 M	131
Fe-T_{piv}PP(1,2-Me_2Im)	1.06×10^8	46×10^3	2.3×10^3	62.31[b]	toluene, 25 °C, [B] = 0.1 M	101,221
Fe-(Piv)$_3$(Phenyl)PP(1,2-Me_2Im)	3.8×10^7	0.1×10^4	34.5×10^3	4.15	toluene, 25 °C, [B] = 10^{-2} M	218
Fe-(Piv)$_3$(phenol)PP(1,2-Me_2Im)	18.9×10^7	0.5×10^4 (77%)	37.8×10^3	3.8	toluene, 25 °C, [B] = 5×10^{-3} M	218
		4.1×10^4 (23%)	4.6×10^3	31.2	toluene, 25 °C, [B] = 5×10^{-3} M	218
Fe-(Piv)$_3$(C_6H_3(NHCOMe)$_2$)-PP(1,2-Me_2Im)	11×10^7	3.1×10^4 (65%)	3.5×10^3	41	toluene, 25 °C, [B] = 10^{-3} M	218
		15.4×10^4 (35%)	0.7×10^3	205	toluene, 25 °C, [B] = 10^{-3} M	218
Fe-(Piv)$_3$(C_6H_3(CONHMe)$_2$)-PP(1,2-Me_2Im)	14.9×10^7	11×10^4	1.4×10^3	102.5	toluene, 25 °C, [B] = 5×10^{-3} M	218
Fe-(Piv)$_3$(indole)PP(1,2-Me_2Im)	24×10^7	2.4×10^4	10×10^3	14.3	toluene, 25 °C, [B] = 5×10^{-3} M	218
Fe-(Piv)$_3$(benzofuran)PP-(1,2-Me_2Im)	27×10^7	4.3×10^4	6.3×10^3	22.8	toluene, 25 °C, [B] = 5×10^{-3} M	218
Fe-(PF3CUIm)	2.6×10^8	3.9×10^3	6.6×10^4	1.26[b]	toluene, 25 °C	193
Fe-(PF3CUPy)	3.0×10^8	1.9×10^5	1.58×10^3	52.2[b]	toluene, 25 °C	193
Fe-(PF4CUPy)				41.6[b]	toluene, 25 °C	193
Fe-MedPoc(1-MeIm)	1.7×10^7	71	2.4×10^3	0.36[b]	toluene, 25 °C, [B] = 0.1–0.5 M	221
Fe-MedPoc(1,2-Me_2Im)	5.2×10^6	800	6.5×10^3	12.4[b]	toluene, 25 °C, [B] = 0.5 M	221
Fe-TalPoc(1,2-Me_2Im)	7.4×10^8	34.5×10^3	21×10^3	4.0	toluene, 25 °C, [B] = 0.1 M	221
Fe-(Piv)$_8$PP(1,2-Me_2Im)				870	toluene, 25 °C, [B] = 0.3 M	202
Fe-(tButAc)$_8$PP(1,2-Me_2Im)	4.5×10^7	7.9×10^4	5.7×10^2	230[b]	toluene, 25 °C, [B] = 0.3 M	202
Fe-e-BHP(C_3·Py·C_3)(C_{12})	30×10^7	40×10^3	7.5×10^3	19.3	toluene, 20 °C	169
			0.74×10^3		benzonitrile/0.1 M NBu_4ClO_4	416
Fe-eBHP(C_3·Py·C_3)(C_{10})	27×10^7	42×10^3	6.5×10^3	22.1	toluene, 20 °C	169
Fe-eBHP(C_3·Py·C_3)(C_4·Ph·C_4)	16×10^7	220×10^3	0.7×10^3	205	toluene, 20 °C	169
Fe-eBHP(C_3·Py·C_3)(C_3·Ph·C_3)	10×10^7	400×10^3	0.25×10^3	574	toluene, 20 °C	169
Fe-eBHP(C_9Im)(C_{12})	18×107	1.3×10^3	13.8×10^3	1.04	toluene, 20 °C	143, 182
			120×10^3		benzonitrile/0.1 M NBu_4 ClO_4	416
Fe-aBHP(C_3·Py·C_3)(C_{12})	36×10^7	5×10^3	70×10^3	2.05	toluene, 20 °C	169
			6×10^3		benzonitrile/0.1 M NBu_4 ClO_4	416
Fe-aBHP(C_3·Py·C_3)(C_{10})	15×10^7	2.8×10^3	54×10^3	2.66	toluene, 20 °C	169
Fe-aBHP(C_3·Py·C_3)(C_3·Ph·C_3)	12×10^7	11×10^3	11.4×10^3	12.58	toluene, 20 °C	169
Fe-aBHP(C_4·Py·C_4)(C_{12})	30×10^7	47×10^3	6.4×10^3	22.41	toluene, 20 °C	169
			0.7×10^3		benzonitrile/0.1 M NBu_4 ClO_4	416
Fe-aBHP(C_9Im)(C_{12})	31.4×10^7	0.62×10^3	500×10^3	0.29	toluene, 20 °C	169
			40×10^3		benzonitrile/0.1 M NBu_4 ClO_4	416
Fe-aBHPPhe(C_9Im)	2.2×10^7	60	3.6×10^5	0.40	toluene, 20 °C	208
Fe-aBHPVal(C_9Im)	1.8×10^7	25	7.2×10^5	0.20	toluene, 20 °C	208
Fe-(Ant-7,7-cyclophane)-(1,5-DCIm)	6.5×10^7	1×10^3	6×10^4	1.4	C_6H_6, 20 °C, [B] = 0.03–0.08 M	248
Fe(Ant-6,6-cyclophane)-(1,5-DCIm)	1×10^5	800	125	6.9×10^2	C_6H_6, 20 °C, [B] = 1.2 M	248
Fe-(Ada-6,6-cyclophane)-(1,5-DCIm)	1.5×10^5	960	156	300	toluene, 25 °C, [B] = 1 M	111
Fe-SP-14(1,5-DCIm)	3×10^5				C_6H_6, 20 °C, [B] = 1 M	113
Fe-SP-15(1,5-CDIm)	1.7×10^6	250	6.8×10^3	15[b]	C_6H_6, 20 °C, [B] = 0.2 M	113
Fe-Cu5(THPIm)	1.8×10^6	91	19.8×10^3	5.0[b]	C_6H_6, 20 °C, [B] = 0.2 M	113
Fe-PLC_{14}(1-MeIm)	1.9×10^6	1.1×10^3	1.8×10^3	113	toluene, 20 °C, [B] = 0.5–2 M	125
Fe-PLC_{14}(1,2-MeIm)	1.0×10^6	10.0×10^3	1.0×10^2	1434	toluene, 20 °C, [B] = 1–2.5 M	125
Fe-PLC_{14}(Py)	3.90×10^6	6.19×10^3	6.3×10^2	227.8	toluene, 20 °C, [B] = 1–3.5 M	125
Fe-Cu4(1-MeIm)	5.2×10^5	181	3.2×10^3	31[b]	C_6H_6, 20 °C, [B] = 0.2 M	113
Fe-Cu4(THP-Im)	5×10^5				C_6H_6, 20 °C, [B] = 1. M	113
Fe-(AzCl4α)(1,2-Me_2Im)				2.15×10^3	toluene, 20 °C, [B] = 0.07 M	250
Fe-(AzCl4α)(1,5-DCIm)				18	toluene, 20 °C, [B] = 0.07 M	250
Fe-(AzCl8α)(1,2-Me_2Im)				150	toluene, 20 °C, [B] = 0.07 M	250
Fe-Piv_2C_{12}PP(1-MeIm)	62.3×10^7	130	48×10^5	0.03	toluene, 20 °C, [B] = 0.01 M	127
Fe-Piv_2C_{12}PP(1,2-Me_2Im)	31×10^7	7500	0.52×10^5	2.8	toluene, 20 °C, [B] = 10^{-1} M	402
Fe-Piv_2C_{10}PP(1-MeIm)	3×10^7	27	1.1×10^6	0.13	toluene, 20 °C, [B] = 0.01 M	127
Fe-Piv_2C_{10}PP(1,2-Me_2Im)	1.53×10^7	540	0.83×10^5	5.1	toluene, 20 °C, [B] = 5×10^{-2} M	402
Fe-Piv_2C_9PP(1-MeIm)	2.1×10^7	5	4.3×10^6	0.033	toluene, 20 °C, [B] = 0.01 M	127

Table 2 (Continued)

compounds	k^+, M^{-1} s^{-1}	k^-, s^{-1}	K_{O_2}, M^{-1}	$P_{1/2}{}^{O_2}$, torr[a]	conditions	ref(s)
Fe-Piv_2C_9PP(1,2-Me_2Im)	1.03×10^7	67	1.48×10^5	0.97	toluene, 20 °C, [B] = 5×10^{-2} M	402
Fe-Piv_2C_8PP(1-MeIm)	0.22×10^7	2	11×10^5	0.10	toluene, 20 °C, [B] = 0.01 M	127
Fe-Piv_2C_8PP(1,2-Me_2Im)	0.054×10^7	14.7	0.37×10^5	3.9	toluene, 20 °C, [B] = 5×10^{-2} M	402
P-450_{scc} + cholesterol	530×10^4	120	4.42×10^4		water, 25 °C	401
P-450_{scc} + 22(*R*)-hydroxy-cholesterol	6.2×10^4	0.77	8.1×10^4		water, 25 °C	401
P-450_{scc} + 20,22(*R*)-dihydroxy-cholesterol	3.2×10^4	0.13	24.6×10^4		water, 25 °C	400
P-450_{cam} + camphor	81×10^6	2.65	30×10^6		0.05 M phosph, pH 7.2, 15 °C	400
Fe-$T_{piv}PP(C_6HF_4S^-)Na^+$ - 18c6	2.5×10^8	7.6×10^3	3.3×10^4		toluene, 20 °C, [B] > 10^{-3} M	400
Fe-$Piv_2C_9(C_6HF_4S^-)Na^+$ - 18c6	3×10^7	7.4×10^2	4×10^4		toluene, 20 °C, [B] > 10^{-3} M	402
Fe-$Piv_2C_9(BuS^-)K^+$ - 18c6	3.5×10^6	0.9	3.86×10^6		toluene, 20 °C, [B] > 10^{-3} M	402

[a] When kinetic data are listed, $P_{1/2}{}^{O_2}$ values are calculated from the ratio of the rate constants and the solubility of O_2. When only $P_{1/2}{}^{O_2}$ values appear, they are determined from equilibrium measurements. [b] Both equilibrium and kinetic data were measured.

relationship is preferred ($K_{O_2} = k_B{}^{+O_2}/k_B{}^{-O_2}$) where $k_B{}^{+O_2}$ is the rate constant for O_2 binding to a five-coordinate species with base B and $k_B{}^{-O_2}$ is the dissociation rate.

Kinetic measurements must be studied by special methods for measuring rapid reactions in solution. Fortunately, many six-coordinate complexes of iron(II) porphyrins, as well as biological compounds, undergo a reversible photodissociation which provides a convenient means for measuring ligand recombination rates (k^+). However, in the case of a chemical system at equilibrium, one can show that the dissociation rates (k^-) are in fact the most relevant parameters to characterize the system.

The early applications to hemoproteins laid down the general principles.[211,212] These became what is now referred to as conventional flash photolysis, and this technique was subsequently applied to the reactions of the first chelated heme models.[213,214] The use of a laser to achieve photolysis has permitted the investigation of faster reactions. The simplest method would be to determine the kinetic parameters (k^+ and k^-) from photolysis experiments by studying the recombination reaction after photodissociation. If we consider the reaction

$$\text{B–PFe}(O_2) \underset{k_B{}^{-O_2}}{\overset{k_B{}^{-O_2}}{\rightleftharpoons}} \text{B–PFe}^{II} + O_2$$

the recombination reaction is exponential when conditions of pseudo first order are satisfied, i.e., the concentration of O_2 is much higher than those of the heme and the axial base. The observed recombination rate $k_r{}^{O_2}$ is then given by the relation

$$k_r{}^{O_2} = k_B{}^{+O_2}[O_2] + k_B{}^{-O_2}$$

from which the association and dissociation rate constants can be obtained from the slope and the intercept of the linear plots of $k_r{}^{O_2}$ against $[O_2]$. However, this direct rebinding method fails for photolysis and rebinding of O_2.[215] To be applied it is necessary that the oxyhemochrome is stable and that the on rate for axial base is much greater than the on rate for oxygen. Generally, these rate constants are comparable in magnitude. Base elimination competes with oxygen elimination and so the method cannot be applied. In addition, the quantum yields are low.[216] This is not the case, however, for carbon monoxide binding.

Convenient determination of the kinetic constants for O_2 binding can be made using the flash photolysis method proposed by Gibson.[211] With pure compounds fluorescence is not a problem. This indirect but elegant solution to solve the autoxidation problem is based on the technique of phototriggered ligand replacement. It uses carbon monoxide because this protects the model system against oxidation and yet can be flashed off easily with an essentially quantitative quantum yield. The Gibson equation can be used to estimate both on and off rates for oxygen binding (R = relaxation constant):

$$\frac{1}{R} = \frac{1}{k_B{}^{-O_2}} + \frac{k_B{}^{+O_2}[O_2]}{k_B{}^{-O_2}k_B{}^{+CO}[CO]}$$

In the presence of O_2 and CO, the carbonyl hemochrome is by far the dominant species. Photodissociation leads to carbon monoxide and the five-coordinated iron(II) porphyrin. Dioxygen and carbon monoxide compete for rebinding:

$$\text{B–PFe–CO} + O_2 \xrightarrow{h\nu} \text{B–PFe} + \text{CO} + O_2 \xrightarrow{k_B{}^{+O_2}} \text{B–PFe–}O_2 + \text{CO}$$

By choosing appropriate ligand concentrations, it is generally possible to adjust the reaction rates such that O_2 recombination is faster than CO in the case of the five-coordinated species. Consequently, the oxyhemochrome is formed in an initial and rapid step (from about 100 ms to a few milliseconds, depending on conditions) as a transient species which later undergoes a slower ligand replacement reaction, restoring the initial carbonyl hemochrome in several milliseconds. As a consequence, many experiments can be performed without any significant metalloporphyrin degradation. The variation of optical absorption at a wavelength corresponding to an isosbestic point for the carbonylated hemochrome and the five-coordinate complex allows observation of the formation and the disappearance of the oxygenated adduct and hence information on the oxygen combination and dissociation rates.

The strict application of the Gibson equation cannot be applied to the study of oxyhemochromes which bind dioxygen weakly ($K_{O_2} \leq 10^3$ L mol^{-1}). Lavalette and Momenteau proposed a modification of this equation in order to generalize it.[217,218] The rate constant of the slow ligand exchange may be expressed in terms of relaxation rate constants for the recombination of dioxygen ($k_r{}^{O_2}$) and carbon monoxide ($k_r{}^{CO}$):

$$k_r{}^{O_2} - k_r{}^{CO} = k_B{}^{+O_2}[O_2] + k_B{}^{-O_2}$$

and

$$\frac{1}{R} = \frac{1}{k_B^{-O_2}} \frac{k_r^{O_2}}{k_r^{CO}}$$

The carbon monoxide recombination rate constant k_r^{CO} can be determined independently by performing a direct rebinding experiment of CO with B–Fe^{II} in the absence of dioxygen. We note that the method of phototriggered competitive rebinding has now been applied not only to oxyhemochromes, but also to the study of the binding of nitrogenous bases[215,216] and water[208,219] with five-coordinate iron(II) porphyrin complexes.

B. Equilibrium and Kinetic Data

The compilation of equilibrium and kinetic constants in Table 2 is intended to be exhaustive for synthetic heme compounds. Selected values for hemoproteins are included at the beginning of the table in order to make comparisons. All equilibrium constants are reported as the dioxygen pressure at half-oxygenation $P_{1/2}$ (in Torr) in order to facilitate direct comparisons. Thus, there is an inverse relationship between $P_{1/2}$ and O_2 affinity: the lower the $P_{1/2}$ value, the higher the stability constant. Their comparison permits the determination of the chemical and stereochemical factors which control the affinity and kinetic constants of O_2 binding. The influence of the proximal base, its nature and restraint, distal steric hindrance, or distal site polarity upon dioxygen binding can be revealed. This is of considerable importance in the quantitative assessment of structure–function relationships in the hemoproteins.

There are two caveats to keep in mind when making comparisons of data in Table 2. The first concerns the validity of $P_{1/2}$ values. In the vast majority of cases these are calculated from rate data rather than measured under equilibrium conditions. This is because most oxyhemochrome solutions have limited stability at room temperature. The ratio of the rate constants gives the equilibrium constant ($K = k^+/k^-$) and $P_{1/2}$ is calculated using the solubility of O_2 in the particular solvent (e.g. 5.3×10^{-3} M atm^{-1} in toluene at 298 K).[220] When only $P_{1/2}$ data are listed in Table 2, they derive from equilibrium measurements. When rate data are listed, the $P_{1/2}$ value is the calculated value. In only a few cases have the kinetic determinations been reconciled with equilibrium determinations. These are identified in Table 2 by footnote *b*. An exemplary study of the congruence of kinetic and equilibrium data is provided by Collman, Brauman, Gibson, and coworkers.[221] In their study of picket and pocket porphyrins good agreement was obtained between kinetic and thermodynamic oxygen affinities (±15%). Inasmuch as the rate data for oxygen binding to myoglobin reliably yield an affinity constant almost twice that derived from equilibrium measurements,[210] it is possible that a similar disparity might exist in some model compounds. The origin of this effect in proteins is not well understood but it could result from an insensitivity of the spectroscopy used in the kinetics to multiple conformers of a liganded heme or to composite ligation pathways. In this regard, the lack of rigorous first-order exponential behavior for the binding of O_2 to modified picket fence porphyrins has led to the suggestions of O_2 binding to both faces of an unsymmetrical heme.[218] This is discussed in section G. The phenomenon of a composite O_2 binding process in superstructured hemes is treated in section I.

The second concern over the numbers in Table 2 is their absolute accuracy and the precision of their measurement. The 1983 admonitions of Jameson and Ibers[18] bear repeating. "In general, precision to within 15% may be possible; accuracy to better than 50% has yet to be demonstrated". Comparisons of data in Table 2 must therefore consider measurement errors as well as system comparability (temperature, solvent, heme type, etc.). As indicated by the linear free-energy relationships discussed in section H, system comparability appears to be more important than measurement error.

C. Nature of Proximal Base

Early work demonstrated that simple ferrous porphyrins are capable of binding O_2 in the presence of a great variety of axial bases at low temperatures (<–40 °C). These bases included alkylimidazoles, pyridine, simple amine-type ligands, and some donor solvents such as DMF. The basicity of the proximal ligand is expected to be a determining factor in dioxygen complex formation. Changes in basicity should provide substantial differences in dioxygen affinities because there are major electronic changes at iron upon O_2 binding. In general, as the basicity of the axial ligand increases, the O_2 affinity increases. This can be seen by comparing the affinity of O_2 in models containing imidazole (or *N*-methylimidazole) with those containing pyridine. This increase is manifest almost entirely in lower dissociation rates with little modification of the association rates.[143,193,222,223] This electronic stabilization of the O_2 adduct is consistent with the redox sense of the Fe^{II}/O_2 bonding and with π back-bonding into the π^* orbitals of O_2.

This electronic factor can be counterbalanced by steric pull on the proximal imidazole. Collman *et al.* have analyzed the replacement of 1-methylimidazole by 1,2-dimethylimidazole on the O_2 binding.[221] The introduction of a methyl group in the 2-position lowers the O_2 affinity by a factor of 10–100. The effect is predominantly in increased off rates. This decrease in O_2 affinity is similar to that observed in going from R- to T-state hemoglobins. It results from the steric interaction of the 2-methyl substituent with the heme plane which restrains the movement of the metal toward the porphyrin plane upon oxygenation. This models the decrease in O_2 affinity of the α chains of hemoglobin where the F helix is believed to similarly restrain the imidazole from close approach to the heme.[63]

Other studies on the effect of constraints on axial base binding are also available. Traylor and coworkers[102,224] and Sharma *et al.*[225] have introduced proximal base strain in tail-base heme complexes. In aqueous micellar solvent systems the model compounds which have an imidazole base attached through relatively unstrained linkages display dissociation rate constants and $P_{1/2}^{O_2}$ lower than those measured for compounds bearing a short chain connecting the imidazole to the porphyrin ring. These investigators propose that a "tension" on the iron atom imposed by the short linkage to the imidazole causes the observed increases in dissociation rates.

Momenteau *et al.*[145,169] also presented the strain effect engendered by the proximal handle length in amide basket-handle compounds having pyridine as the axial ligand (see Fe-hanging base aBHP, Figure 9). An

increase in the number of methylene carbon atoms in the chain connecting the pyridine ring to the porphyrin periphery (from C_3 to C_4) decreases the equilibrium constant by a factor of 10, principally because of a larger dissociation rate. These authors noted that ^1H NMR spectroscopy provided useful information on this system.[145] The spectrum of the pyridine C_4 derivative shows that the pyridine ring is confined in two equivalent planes passing through the pyrrole nitrogens and it undergoes a flip–flop movement. On the other hand, the pyridine ring in the C_3 compound is able to execute a continuous vibration around its average position in a plane directed along the meso carbon atoms. Thus, the constraint imposed on the proximal base in the pyridine C_4 derivative may oppose the necessary reorganization of the proximal base accompanying the movement of the iron atom toward the porphyrin plane on ligation with O_2. Again, there are parallels to be drawn to the decreased O_2 affinity in the α chains of T-state hemoglobin relative to the R state.

The influence of the proximal base on the dioxygen affinity of five-coordinate hemes may also occur via hydrogen bonding of the exo N–H moiety of an imidazole ring. Thermodynamic considerations[226] and oxidation potentials[227-229] suggest that such hydrogen bonding should have the effect of releasing electron density to the iron atom thereby stabilizing the O_2 adduct by decreasing the dioxygen dissociation rate. Such a hypothesis has been formulated for hemoproteins.[65,138,230,231] Traylor and Popovitz-Biro[232] reported the O_2 (and CO) affinities of a cyclophane–heme with an internally hydrogen-bonded imidazole [4-(2-*N*-piperidylethyl)imidazole] (see Figure 10). Both kinetics and equilibria were changed very little in comparison to those obtained with 1,5-dicyclohexylimidazole as proximal ligand. The authors argue that either the hydrogen bonding is too weak to strongly polarize the N–H bond or the dioxygen affinity is not very sensitive to small changes in electron density. Since, hydrogen bonding of the proximal imidazole should stabilize a formal iron(III) complex, easier liberation of superoxide anion and an increasing tendency toward irreversibile oxidation might be expected. More studies are needed on this aspect of proximal base effects, perhaps by using discrete imidazolate[233] complexes.

D. Distal Steric Effects

The distal heme pocket of hemoproteins seems to be important in determining both the geometries and affinities of O_2 and CO ligands. X-ray crystal structures of oxymyoglobin and carbonylmyoglobin reveal that the dioxygen ligand is bound end on with an Fe–O–O angle of about 120° and that CO may be significantly displaced from the heme normal in a bent and/or tilted geometry.[234,235] Crystallographic analyses of model compounds indicate that O_2 has a similar geometry[44] but that the Fe–CO unit is essentially linear and normal to the mean porphyrin plane.[236-238] The structural difference between carbonylated natural compounds and heme models is clearly related to the steric bulk of the nearby distal residues in hemoproteins (His E7 and Val E11). Thus, it has been proposed that distortion of the Fe–CO unit in hemoproteins can reduce CO affinities without affecting the O_2 affinity of the inherently bent FeO_2 group. Furthermore, this structural difference between the bonding of CO and O_2 has been proposed as a natural mechanism for lowering the toxicity of CO in natural systems. Carbon monoxide binding to myoglobin and hemoglobin is destabilized while O_2 is unaffected. This proposal was first enunciated by Collman *et al.*[239] and later adopted by Perutz, Caughey, and co-workers.[240] To study the discrimination, generally expressed as a M value, the ratio of the O_2 and CO $P_{1/2}$ values, numerous heme models have been designed.

In general, the systematic decrease of the available distal cavity size in capped,[241,242] cyclophane,[111,194] pocket,[101,195,221,243] and hybrid[127] porphyrins (see Figure 8) produces a decrease in affinity for CO while leaving the O_2 affinity roughly comparable to unstrapped porphyrins. Kinetically, the major effect is a decrease in CO association rates, consistent with steric blocking in a product-like transition state.

The O_2 binding to a series of capped hemes has been studied by Basolo *et al.*[132,244-246] They found that these iron(II) porphyrins discriminate against O_2 relative to CO. Interpretation of this unexpected result has been in terms of a severe doming of the porphyrin[134] that arises when the chains connecting the macrocycle to the central capping phenyl ring are short. More recently, a capped porphyrin that binds neither CO nor O_2 has been reported.[242]

Collman *et al.*[107] have reported the preparation and characterization of a series of sterically hindered pocket porphyrins (Fe-PocPiv, Fe-MedPiv, and Fe-TalPiv at the beginning of Figure 8). They compared their CO and O_2 affinities to open-cavity picket-fence porphyrins.[221] Increased steric hindrance in the pocket porphyrins serves to lower the CO affinity by as much as 100-fold, making the M value similar to myoglobin. The O_2 affinities of the pocket and picket fence porphyrins are similar. Kinetic analysis indicates that whereas only CO *association* rates are reduced, both O_2 association and dissociation rates are reduced for O_2, thereby leaving the O_2 affinity essentially unaffected. Very recent results[265] suggest the discrimination between CO and O_2 can be improved even further in porphyrins with tight aza macrocycle superstructures.

The influence of "central" versus "peripheral" steric effects have been also studied by Lavalette *et al.*[169] using basket-handle porphyrins in the ether-linked and in the amide-linked series (Fe hanging base eBHP and aBHP in the middle of Figure 9). Compounds which include a central phenyl group in the distal handle permit a meaningful comparison with their respective analogs that only contain a loose C_{12} chain. The presence of the phenyl group decreases the affinity of O_2 by a factor of about 30 in the ether series and 6 in the amide series. This arises from a decrease of the association rate and an increase of the dissociation rate. Comparison with CO binding showed that the decrease of O_2 binding is greater than that of CO binding in the ether series. An opposite situation prevails in the amide series. These results were interpreted as being due to a distinction between central and peripheral steric effects in the amide and the ether series due to a sideways displacement of the phenyl group. Slipped caps have been discussed by several authors.[100,247,248] The greater rigidity of the amide linkage compared to the ether one[249] should reduce the amplitude of the lateral displacement of the phenyl residue. This should

preferentially lower the CO affinity by increasing its destabilization relative to dioxygen since the former prefers to bind in a linear manner. On the other hand, in the ether series a peripheral steric effect could decrease the dioxygen affinity more than CO since the terminal O atom is more peripheral than central in the bent FeO_2 moiety.

Another approach to the central steric effect on O_2 binding has been reported by Momenteau *et al.*[127] in a series of "hybrid" compounds derived from basket-handle porphyrins (Fe-Piv_2C_{n+2}PP in Figure 8). These single-face-hindered porphyrins have been designed to hold the distal handle in a central position with two flanking pivalamide pickets. They differ by the length of the handle, offering an increase of central steric hindrance to ligands when the handle length decreases. The systematic lowering of the available space for iron-bound O_2 produces a decrease of both association and dissociation rate constants as compared with basket-handle porphyrins.

A number of other model systems have been developed which demonstrate the effects of steric hindrance on O_2 binding.[113,130,250] The most important overall result is that distal steric hindrance can significantly affect ligand binding and this effect is manifest mainly in diminished ligand association rate constants. This is in agreement with the deductions of Moffat *et al.*[251]

E. Solvent Effects

Increased oxygen affinities with increased solvent polarity have been demonstrated using various systems. For example, Chang and Traylor[213] have shown that tail-base heme complexes bind O_2 with a lower dissociation rate constant in water than in nonpolar solvents. There is only a small effect on the O_2 on rate. This effect is consistent with the aqueous environment stabilizing the dioxygen–iron bond better than less polar solvents such as CH_2Cl_2. These authors drew an analogy between the polar interaction of dioxygen and water to that observed in hemoproteins where the coordinated dioxygen is stabilized by hydrogen bonding from distal histidine (see below). This is consistent with the dipolar nature of the iron–oxygen bond ($Fe^{\delta+}$–$O_2^{\delta-}$).

Even though the distal cavity in hemoproteins is essentially hydrophobic (i.e., water is excluded) this does not mean that it is apolar. Thus, many investigators have paid attention to the fact that local polarity at the binding site might play a significant role upon O_2 affinity. This was noted by Stynes and Ibers[252] in connection with O_2 binding to cobalt porphyrin complexes. In the studies of Traylor[100,213,253–255] mentioned above the binding of CO seems not to be too sensitive to solvent polarity, while the rate constant for dissociation of O_2 increases from 90 to 1700 s^{-1} in going from aqueous DMF to 90% toluene–methylene chloride. More recently, Suslick and Fox[200] investigated the effects of solvent polarity on the relative O_2 affinities of both-face-hindered nonpolar "bis-pocket" porphyrin. They observed small increases in O_2 affinity with increasing solvent polarity but the rate constants were not determined. Similar conclusions were drawn earlier by Basolo *et al.*[241] with capped porphyrins.

F. Polarity Effects

Picket-fence porphyrin (first structure in Figure 8), synthesized by Collman *et al.*, forms dioxygen complexes that are quite stable and have high affinities.[103,221] The presence of amide residues in the pickets may contribute to this stability. Using the coordinates from the crystal structures with 1-MeIm and 2-MeIm as axial bases,[45,75,256] Jameson and Drago[257] estimated the N···O distance to be ≈4 Å, much longer than those found in typical H-bonded systems. Such a distance is not in accord with significant bonding[18] and this is confirmed by ^{17}O NMR data which did not reveal significant resonance shifts.[172] They proposed that the close contacts between the methyl groups of the pivalamido pickets and the terminal oxygen atom must influence the oxygen affinity. However, the relative role of the amide dipole versus the methyl groups remains uncertain.

A definite role of the secondary amide groups in the vicinity of the iron atom is perhaps best illustrated by the lowering of the O_2 affinity when they are replaced by esters.[202] The 23-fold decrease in affinity is mainly manifest in an increased off rate, as expected for diminished stablization of the FeO_2 moiety.

G. Distal Hydrogen Bonding

More than a simple polarity effect, the most significant distal effect invoked in the stabilization of dioxygen in hemoglobin is the hydrogen-bonding interaction between coordinated dioxygen and the distal histidine (His E7). Such an interaction not only affects oxygen affinity in myoglobin and hemoglobin, it may also stabilize the oxy form against autoxidation. Pathways involving superoxide loss may be inhibited.[163] It may also be critical in directing reaction courses during oxygen activation and reduction in other hemoproteins. While initially proposed by Pauling,[42] direct evidence was first provided by Yonetani *et al.*[258] in EPR studies of cobalt-substituted oxyhemoglobin. Subsequent X-ray structure analysis[58] and neutron diffraction studies[60] on MbO_2 have provided direct evidence for hydrogen bonding of iron-bound dioxygen with distal histidine. These studies yielded an N(H)···O distance of 2.97 Å. This electrostatic intermolecular interaction, which must contribute to the stabilization of the dioxygen adduct was confirmed in oxyhemoglobin by Shaanan.[59] X-ray diffraction gave N(H)···O distances of 2.7 and 3.2–3.4 Å for the α and β subunits, respectively.

Extensive studies on the O_2 adducts of hanging-base basket-handle porphyrins[143,145] have provided the first model systems which have shown the importance of hydrogen bonding upon the stabilization of dioxygen binding to iron. Changing the attachment mode of both the proximal and distal handles from ether to amide (see middle of Figure 9) modifies O_2 affinity. Using compounds which have the same aliphatic C_{12} chains and have pyridine as a proximal ligand, Momenteau and Lavalette[259] showed that the O_2 affinity is 10 times larger in the amide compound than in the ether one. In fact, the difference is due almost entirely to a 10-fold reduction of the O_2 dissociation rate. The association rate is not significantly modified. This increase of stability in the amide-oxygenated species was attributed to the presence of the amide linkage and to the possibility of hydrogen bonding with the terminal oxygen atom of the liganded dioxygen molecule. The low-temperature (−27 °C) ^1H NMR spectrum supports this hypothesis (see Figure 11).[186,169] The

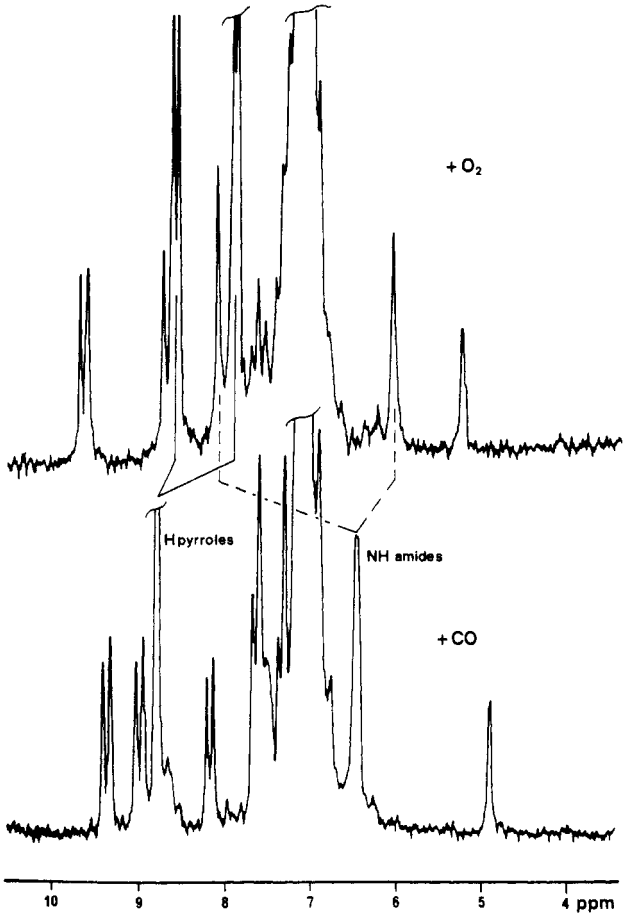

Figure 11. Proton NMR spectra (100 MHz) of CO and O_2 complexes of a-BHP(C_3-Py-C_3)(C_{12}) in [$^2H_8$] toluene at 27 °C (ref 169).

observed inequivalence of the pyrrole protons as well as the shifts of the amide protons suggests a preferred orientation of the oxygen molecule toward the NH groups. The N–(H)···O distance, ca. 3 Å, is consistent with intramolecular hydrogen bonding (see Figure 12). IR, ^{17}O NMR, and Raman spectra of the dioxygen complexes of these porphyrins corroborate the structural assignment.[127,137,172]

Modern NMR techniques allow one to assign most of the heme and distal amino acid proton resonances in the ^1H NMR spectrum of a hemoprotein[260-263] but their interpretation in terms of the effect of H bonding to dioxygen is still lacking. Studies on a series of closely related oxymyoglobin models whose differing distal effects would be reflected rationally in their differing dioxygen affinities has been reported by Reed *et al.*[218,106] These compounds are derived from picket-fence porphyrin having one of the four pivalamido pickets replaced by a variety of substituents, some with H-bonding capability (see first entry of Figure 8). Comparison of affinity and kinetic data showed that the compound bearing a phenylurea substituent binds O_2 with a 9-fold increase in affinity relative to comparable other compounds. Hydrogen bonding with the urea group close to the FeO_2 moiety, as deduced from NMR analysis, must be responsible for the stabilization of the O_2 adduct. As expected, this is mostly reflected kinetically in a decrease in the dissociation rate.

The same authors have observed some unusual behavior in the determination of the kinetic rate constants for modified picket fence porphyrins.[218] The slow exchange kinetics ($O_2 \rightarrow$ CO), observed when the competition rebinding technique was used, could be accurately described only by the sum of two exponentials. These observations imply the presence of two distinct oxygenated species dissociating at different rates (the two values of the dissociation rate constants vary by a factor of about 5). These two isomeric six- (and five-) coordinate complexes could be due to the proximal ligand (1,2-DiMeIm) binding on both faces of the porphyrin. Thus, the origin of the lowest dissociation rate was attributed to hydrogen bonding between O_2 and the modified picket (3-phenol or 3,5-diacetamide) for the isomer bearing the dioxygen molecule in the picket cavity. This oxyhemochrome would then be stabilized relative to the second isomer

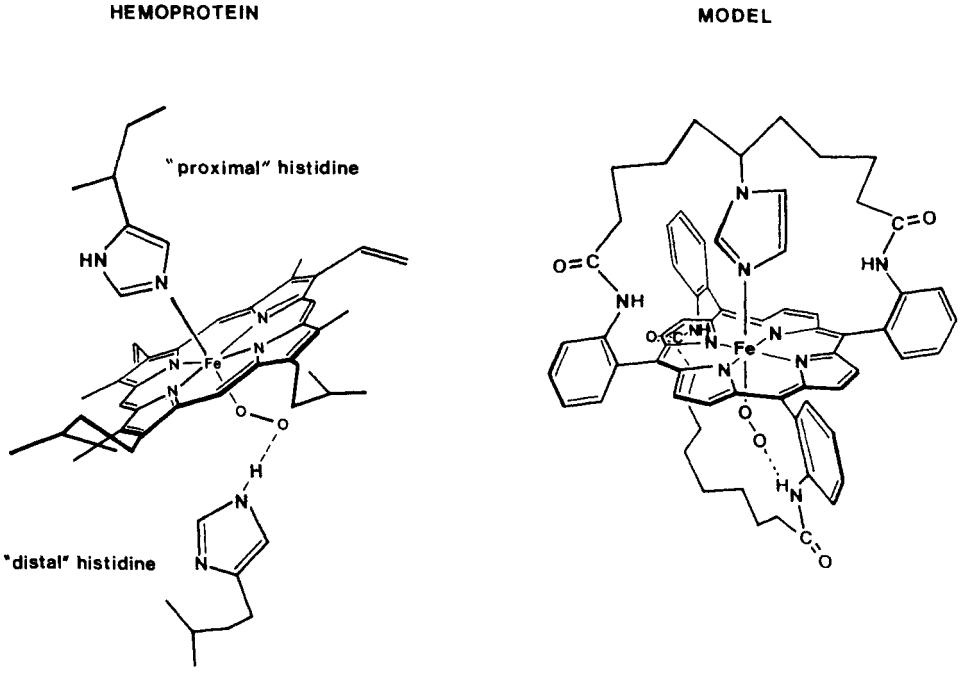

Figure 12. Representation of the hydrogen bonding between dioxygen and the distal residue in hemoglobin and amide basket-handle hemes.

having O_2 bound onto the free face of the heme where no specific stabilizing interaction is present. The discrimination of the O_2 binding between the two faces of the macrocycle is also supported by the kinetics of ligand binding with reversed-amide picket-fence porphyrins.[131] This hypothesis is the most reasonable interpretation of the kinetic and thermodynamic data, but there is yet no structural proof of the formation of two oxyhemochromes.

These examples, as well as closely related studies by Chang[264] and more recent studies by Collman[265] prove the possibility of favoring dioxygen binding and the stabilization of dioxygen adducts by introducing suitable groups in the vicinity of the iron(II) center. The relative strength of hydrogen bonds should exert control over the dioxygen affinity for hemoproteins as well as model compounds via a decrease in the dissociation rate.

In this connection, the control of O_2 affinity by the immediate environment of the heme group in hemoproteins can be probed by comparison of wild-type compounds with mutant Hb's which do not contain a distal histidine. Site-directed mutagenesis with myoglobin[266] leads to a 10-fold decrease in O_2 affinity when glycine replaces the distal histidine. The largest effect is in the off rate rather than the on rate. An effect of similar magnitude is observed in hemoglobin.[267,268]

Reed has commented on the relatively small magnitude of these effects.[106] A 10-fold change in affinity corresponds to only 1.3 kcal/mol, a low energy for an H bond. It seems likely that in both the proteins and the models the H bond is not optimally oriented for maximum effect. In oxymyoglobin[60] it is not coplanar with the Fe–O–O moiety. Rather it is positioned off to the side so that there is an oblique interaction with the two oxygen atoms. Leghemoglobin, which has a higher oxygen affinity and a more mobile distal histidine,[269,270] may bind O_2 more strongly by forming a better H bond. Accurate structural data on both proteins and models are necessary before the quantitative contribution of H bonding can be better assessed. This is because when adding or subtracting an H bond in mutants, or in models, other factors may change in ways that are difficult to predict.

More recent studies on myoglobin mutants by Olson and co-workers[271] have shown that the $C^{\delta-}$–$H^{\delta+}$ dipole of a phenylalanine residue can have an effect of comparable magnitude. A Leu → Phe change in the distal region (B10 helix) increases the O_2 affinity by a factor of about 15. The effect is mostly in a decreased off rate, consistent with stabilization of the oxy complex. This mutant also has an unusually low autoxidation rate emphasizing again that affinity and autoxidation are strongly coupled processes.

H. Linear Free-Energy Relationships

The meaningful comparison of affinity and kinetic rate constants from different heme model compounds appears very difficult due to the great variety of chemical structures which exist. In an attempt to correlate these data, the concept underlying linear free-energy relationships (LFER) can be used. In this concept, first applied to hemoglobin by Szabo,[272] it is possible to show that most heme models can be arranged in series which are objectively related from a thermodynamic point of view. If one single free-energy barrier controls the binding of ligands to the heme, the relative changes in rate and equilibrium constants following some structural perturbation can be expressed in terms of Gibb's free energy. The equilibrium constant and the rate constants are given by

$$K = e^{-(G_P - G_R)/RT}$$

$$k^+ = Xe^{-(G_T - G_R)/RT}$$

$$k^- = Xe^{-(G_T - G_P)/RT}$$

where X is some universal factor (usually taken as kT/h in Eyring's theory of absolute reaction rates) and G_R, G_P, and G_T are the free energy of reactant, product, and transition states respectively. From these equations, the following linear relationship is obtained:

$$\delta G_T = \alpha \delta Gp + (1 - \alpha)\delta Gp$$

where α may be considered as representing the fraction of the free energy change of the products already expressed in the transition state. This relation means that when several molecules are linearly correlated in the $\ln k^+$ versus $\ln K$ plot the following integral relations hold:

$$\ln k^+ = k_0 + \alpha \ln K$$

$$\ln k^- = k_0 + (\alpha - 1) \ln K$$

Thus, the change in the free energy at the transition state upon going from one molecule to another is a linear interpolation of the corresponding changes in the free energy of the products and the reactions. The α value characterizes the nature of the transition state somewhere between the two extremes: for $\alpha = 0$ the transition state behaves purely "reactant-like"; for $\alpha = 1$ the transition state behaves purely "product-like". This concept has been employed by Lavalette *et al.*[169,218] to compare a large series of basket handle porphyrins in which the structural changes are sufficiently "soft" to cause an almost continuous variation of the O_2 binding constants and rate parameters. Figure 13 shows the homogeneity of these compounds from a thermodynamic point of view. Their oxygen affinities are rather evenly distributed and the transition state behaves almost purely "reactant-like" as shown by the slope of the correlation line having an α value of 0.14. Moreover, the 1-MeIm and 1,2-DiMeIm picket-fence porphyrins, which are also derivatives of tetraphenylporphyrin, follow the same correlation.

A LFER has been constructed using selected data reviewed by Moffat *et al.*[251,273] which include R- and T-state hemoglobin, isolated α and β chains, and myoglobin. A second family of compounds is formed. Although the LFER of heme proteins in water is roughly similar to that of the tetraphenylporphyrin models in toluene, oxygen is more "reactant like" due to the lower absolute magnitude of the reaction rates in the former. From a structural point of view, the difference probably originates from the presence of central steric hindrance in the natural compounds. The structural changes brought about by the introduction of central steric hindrance in "hybrid" porphyrins compared to "basket handle" porphyrins, and in "pocket" porphyrin compared to "picket fence" analogs lead to a decrease of both the association and dissociation rate constants

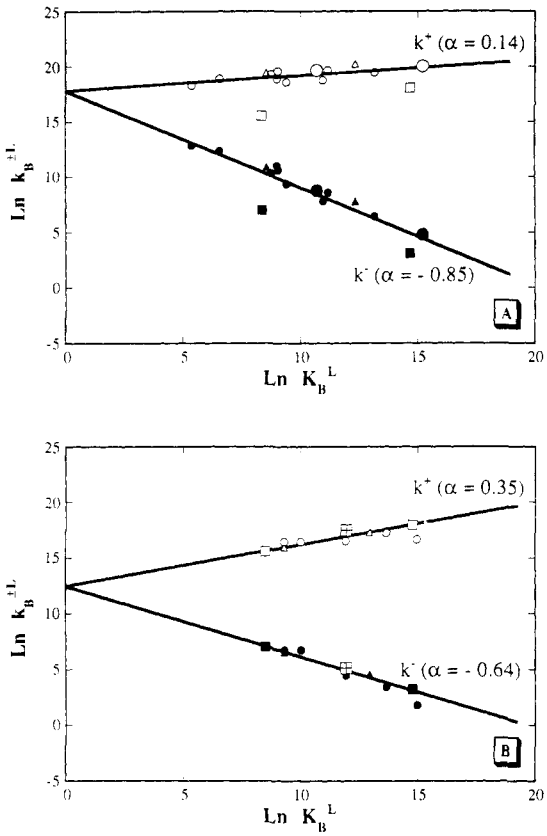

Figure 13. Linear free-energy relationships between rate and equilibrium for O_2 rebinding with heme models in toluene: (○, △, □) $k_B^{+O_2}$; (●, ▲, ■) $k_B^{-O_2}$; (A) (○, ●) BHP; (△, ▲) $T_{piv}PP$; (○, ●) Piv_2C_{12}(1-MeIm and 1,2-Me_2Im); (□, ■) myoglobin (T and R states) (ref 169); (B) (○, ●) Piv_2C_n(1-MeIm and 1,2-Me_2Im); (△, ▲) MedPivP(1-MeIm and 1,2-Me_2Im); (□) a-BHP·Phe(C_9Im); (□, ■) myoglobin (T and R states) (ref 169).

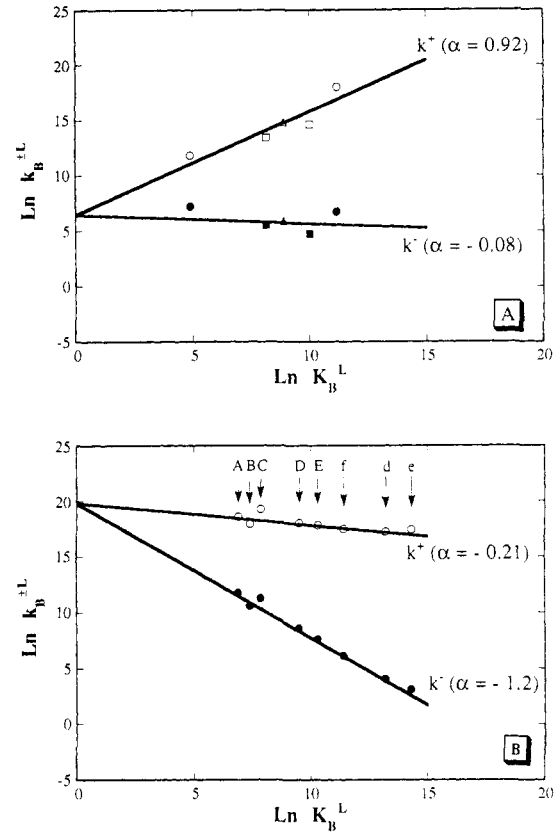

Figure 14. Linear free-energy relationships between rate and equilibrium for O_2 rebinding with (A) (○, △, □) $k_B^{-O_2}$; (●, ▲, ■) $k_B^{-O_2}$; (○, ●) cyclophane; (□, ■) cofacial; and (△, ▲) strapped hemes in toluene (ref 169); and (B) unconstrained flat hemes (○) $k_B^{+O_2}$; (●) $k_B^{-O_2}$; (A) TPP[$NH(CH_2)_3$Py], (B) TPP[$NH(CH_2)_3$Im], (C) DeutP[$O(CH_2)_3$Py], (D, d) ProtoP[$NH(CH_2)_3$Im], (E, e) MesoP[$O(CH_2)_4$Im], (f) AcetylP-[$NH(CH_2)_3$Im] (ref 169).

for O_2 binding in the same proportion (i.e. affinity-constants remain constant). This correlates better with the hemoproteins (Figure 13).

LFER correlations obtained for heme models having little or no steric hindrance are different. Flat "open" iron(II) porphyrins with a variety of fifth axial ligands and "chelated" hemes in which the distal face is free show a quite good correlation but α is negative (−0.21) (see Figure 14B). This can be rationalized by considering that the free-energy changes in the transition state are proportional but opposite to those in the products and reactants. This could be the result of electrostatic interactions between the five-coordinated reactant and the dioxygen which induce a repulsive effect in the transition state.

A contrasting situation is obtained with the LFER plot grouping the data from "cyclophane", "cofacial", and "strapped" porphyrins (see structural types in Figure 8). In this homogenous series, severe central steric effects are responsible for the drastic decrease of association rate constants of gaseous ligands but the dissociation rate constants are not affected. Here, dioxygen binding has an almost pure product-like transition state ($\alpha \approx 1$) (Figure 14A). This is consistent with a binding mechanism involving a large conformational change of the encumbered porphyrin macrocycle taking place before binding occurs and being retained in the bound state.[274]

The general observations using LFER correlations provide a convenient means for comparing families of model compounds with each other and with the hemoproteins. The factors taken into consideration are essentially structural. Other factors, such as the electronic structure of the transition state, remain unrevealed although they must be important in determining the implications of the correlations observed.

The thermodynamics of oxygenation can be interpreted as a competition between enthalpic and entropic factors

$$\Delta G^\circ = \Delta H^\circ - T\delta S^\circ$$

and the free energy ΔG° is related to the oxygenation equilibrium constant

$$\Delta G^\circ_{O_2} = -RT \ln K_{O_2}$$

ΔG° is a composite term, being the summation of all the various free-energy contributions such as electronic, solvation, and structural factors.

Collman *et al.* have investigated the thermodynamic data for oxygenation of picket-fence porphyrin model compounds.[101] Comparison of these data with those in proteins reveal differences which may reflect differences in the microenvironment surrounding the metal site. However, oxygen-binding studies on hemoproteins are necessarily performed over a rather narrow temperature range and the calculated ΔH and ΔS values are subject to large correlated errors. This makes comparisons less meaningful. The thermodynamic values of picket-fence porphyrins can be compared to those of a series of capped complexes.[246] The major differences in O_2

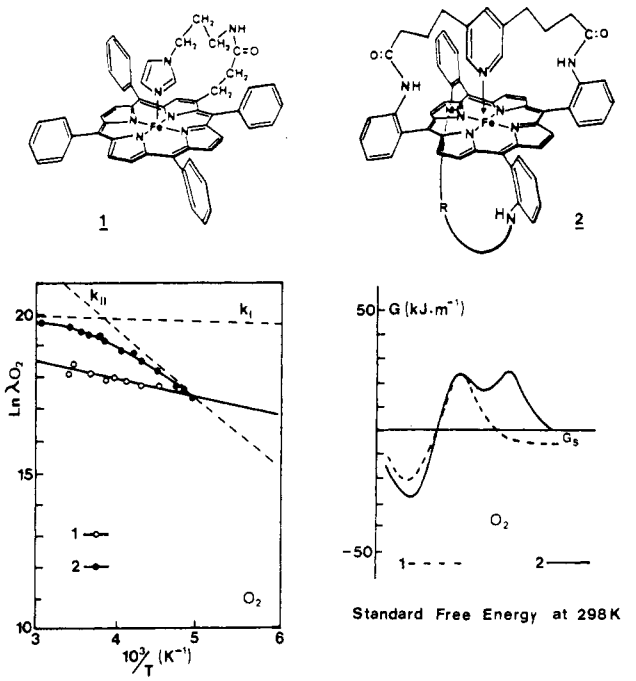

Figure 15. Temperature dependence of the second-order rate parameters for binding of O_2 to chelated heme and basket-handle porphyrin in toluene and the corresponding free-energy barriers (ref 283).

binding are manifest in the enthalpy term. With capped porphyrins, the steric hindrance of the distal face requires more energy to form the six-coordinate oxygenated complexes. The values of $\Delta H°$ are higher for the more constrained capped porphyrins. But the values of $\Delta S°$ are all much the same because the major factors contributing to this thermodynamic parameter, the loss of degrees of freedom in binding O_2 are similar for all systems. Replacing 1-MeIm by 1,2-DiMeIm produces a reduction of free energy due to a change of enthalpy terms.

I. Multistep Ligand Binding

The binding of a small ligand such as O_2 or CO to a hemoprotein can be described as the motion of the ligand over a number of successive energy barriers, characterized by temperature-independent activation enthalpies and entropies.[278,280,281] The innermost barrier corresponds to the formation of the iron–ligand bond and seems to control the overall reaction at physiological temperature.[279,282]

Recent work on superstructured model porphyrins has revealed a role of the macroenvironment which reproduces some of the dynamical characteristics found in hemoproteins. Using amide and ether basket-handle porphyrins in which intramolecular five-coordination of the iron(II) atom is assured via pyridine in the strap, Tétreau *et al.*[283,284] studied O_2 binding over a large temperature range (180–300 K). When the results are compared to those obtained with an unprotected chelated heme (see Figure 15), it is clear that O_2 binding to the superstructured heme must be a composite process. The first transition state corresponds to the bond-formation step, and the second transition state results from the orientation of solvent into the cavity formed by the distal protecting chain. The free energy of activation ΔG at 298 K for the formation of Fe–O_2 bond is remarkably similar among the encumbered compounds as well as with the unprotected chelated heme. This indicates that the "handles" located at an average distance of 6 Å from the porphyrin plane are too distant from the iron atom for interference with bond formation. This behavior also suggests that the formation of the bond does not require energy ($\Delta H \approx 0$) and that the barrier is dominated by entropy. The small difference in the entropic parameters between the two kinds of models can be explained by orientation factors and solvent effects. The losses of degrees of freedom of the small ligand must be the principal factor governing binding from within a solvent-free distal pocket.[285] Such conclusions characterize the inner barrier in hemoproteins.[286] Concerning the outer barrier, which is intimately connected with the presence of the distal chains, its free energy value suggests a relatively large participation of enthalpic and entropic components. Specific interactions between the ligand and the structural environment of the complexes must be responsible for these observation. The methylene chains, which seem to be equivalent to a matrix, induce barriers to the migration of the ligand inside the cavity surrounding the coordination site of the iron atom.

J. Cooperativity of O_2 Binding

Cooperative dioxygen binding by hemoglobin is now reasonably well understood.[63] Model compounds have been useful in two aspects. First, axial base strain in model compounds lowers the O_2 affinity, thereby lending legitimacy to the F-helix proximal constraint proposed to account for the low affinity of the α chains in the T conformation relative to the R. Second, the principle of cooperative interactions in dimeric or polymeric systems has been illustrated phenomologically.

The first report in the literature of cooperative O_2 binding to a synthetic system was given by Bayer.[183] Reversible O_2 binding to this water-soluble polyethylene oxide-bound histidinyl heme was reported with a cooperative effect closely resembling that of natural oxygen carriers. However, it has been pointed out that the isotherm, displayed as a Hill plot, was not well behaved and that the visible spectrum of the oxygen adducts did not correspond to that of known oxygenated complexes.[287]

A water-soluble poly-L-lysine heme has been described by Tsuchida *et al.*[181,288,289] This system presents the exceptional property of binding dioxygen in a cooperative manner. The sigmoidal behavior was characterized by a Hill slope of 2.1 in a pH 12 phosphate buffer at 30 °C. The origin of the cooperativity was demonstrated to be the result of the competition between O_2 and an amine residue of the poly-L-lysine that is weakly bound to the sixth site of the five-coordinate ferrous heme. As lysine NH_2 groups at the sixth coordination site are liberated upon oxygenation, the helix content of the polypeptide is modified. This apparently diminishes the stability of the remaining heme–bis(amine) complexes thereby increasing their tendency to bind O_2.

After studying the oxygenation of ferrous picket-fence porphyrin complexes with hindered imidazoles as axial ligand (2-MeIm and 1,2-DiMeIm) in organic solution, Collman *et al.* reported O_2 binding in the solid state.[313] The Hill plots which result for the solid–gas equilibria are sigmoidal in shape and give slopes corresponding

to Hill coefficients of 2.6 and 3.0, respectively. From the binding at high and low O_2 pressures, $P_{1/2}$ values can be extrapolated for the high affinity form (R) and for the low affinity form (T). The ratio is about 10, revealing a remarkable similarity to that of hemoglobin (Table 2). The mechanism of this cooperative interaction bears some relationship to that of hemoglobin. The motion of the iron atom and the hindered imidazole toward the porphyrin plane upon oxygenation is about 0.3 Å. This displacement and other concomitant changes in the molecular dimensions must induce sufficient strain to propagate conformational changes in the crystal which enhance the O_2 affinity of the remaining deoxy sites. Proximal base effects are likely to account for the change in affinity since the process is dependent on the nature of the axial ligand. It models cooperativity of hemoglobin except, of course, that in proteins the mechanism involves heme–heme interactions via the protein while that of synthetic systems must be propagated by crystal-packing forces.

Only a very limited number of examples are available that show cooperative properties in solution. Traylor *et al.*[316] exploited intermolecular dimerization of a chelated heme to design a system exhibiting a cooperative interaction. Each heme is coordinated by the side chain of the other partner because it is too short to bind internally. Cooperative activities in solution are observed for CN^- and CO but no observation for O_2 binding is described. In a different but related system,[317] the reaction of CO with a symmetric diheme exhibits two rate constants. This can be interpreted as indicating two different environments or possibly a sequential change of environment due to cooperativity. Tabushi *et al.* also reported an example of pseudo-cooperative ligand binding by a dimeric metalloporphyrin.[318-321] Carbon monoxide binding to Fe(II) "gable" porphyrins with linked imidazole ligation between the two iron atoms was investigated. However, oxygen binding was investigated with Co(II) complexes affording a chemical model of cooperative O_2 binding. The Hill coefficient was estimated to 1.5 under optimal conditions. The origin of the cooperative effect in these systems appears to be a change of complexation of imidazole ligation between the two metal atoms.

VI. Structure of Oxygenated Complexes

Despite the passage of two decades and the report of a large number of compounds that are able to form oxygenated heme adducts, picket-fence porphyrin remains the only one to give X-ray crystallographic data. Derivatives with both 1-MeIm and 2-MeIm have been reported.[45,75,256,296] Cytochrome P-450 models with thiolate axial ligands are discussed in section VIII. The structural parameters of the hemoglobin models are compared to biological systems in Table 3. Of historical importance is the fact that the first structure of oxygenated picket-fence porphyrin preceded those of oxyhemoproteins by several years. Thus, it was the bent, end-on geometry of the model compound that led to the confident expectation of a similar geometry in the proteins. The close congruence of physical properties, especially the distinctive temperature dependence of the Mössbauer quadrupole splitting,[74] left little doubt.

The structure of $Fe(T_{piv}PP)(N\text{-MeIm})(O_2)$ is illustrated in Figure 16. The terminal atom of the dioxygen ligand shows a four-way statistical disorder pointing toward the four pickets. Thus, each Fe–O–O plane is at 45° to Fe–N bonding in the equatorial porphyrin plane. This orientation may arise from a dipole–dipole alignment of the FeO_2 moiety and the amide of the picket. It may also facilitate metal $d\pi$ to $O_2(\pi^*)$ bonding. The *N*-MeIm occupies the trans position and can be considered statistically disordered between two symmetry-related sites. The iron atom lies essentially in the mean plane of the porphyrin; a slight displacement of 0.03 Å toward the O_2 molecule is observed. This contrasts with oxyhemoproteins where the iron atom is always out of the mean porphyrin plane toward the coordinated imidazole of the proximal histidine. Such a difference may be due to an eclipsed orientation of the imidazole plane relative to the pyrrole nitrogen in MbO_2 which is not present in the model compound. Among the factors which may be important to understanding the variation of the oxygen adduct stability and of structure–function relationships in hemoproteins and in model compounds is the relative orientation of bound dioxygen molecule and the proximal nitrogenous base. This factor remains unexplored for lack of sufficient structural data. A schematic view of these orientations in various oxyhemochromes is given in Figure 17. The data are taken from X-ray structure determinations, from NMR data and from the construction of molecular models.

The structure of the 2-MeIm complex $Fe(T_{piv}PP)(2\text{-MeIm})(O_2)$ has also been reported.[75,296] As with the oxygenated compound with unhindered 1-MeIm, the O_2 ligand is coordinated in the bent, end-on fashion. The iron atom is displaced 0.086 Å toward the imidazole

Table 3. Comparison of Oxyheme Stereochemistry in Myoglobin (Mb) and Model Compounds

	$Mb(O_2)$[a]	$Fe(T_{piv})PP(1\text{-MeIm})(O_2)$[b]	$Fe(T_{piv})PP(2\text{-MeIm})(O_2)$[c]
$Fe-Ct_N$, Å	0.18(3)	−0.02	0.086
$Fe-Ct_P$, Å	0.195(6)	−0.03	0.119
$Fe-N_P$, Å	1.95	1.98(1)	1.996(4)
$Fe-N_{Im}$, Å	2.1	2.07(2)	2.107(4)
Fe–O, Å	1.83(6)	1.75(2)	1.898(7)
O–O, Å	1.22(6)	1.24	1.22(2)
Fe–O–O, deg	115(5)	131	129(2)

[a] Phillips, ref 58. [b] Jameson *et al.*, ref 256. [c] Jameson *et al.*, ref 296.

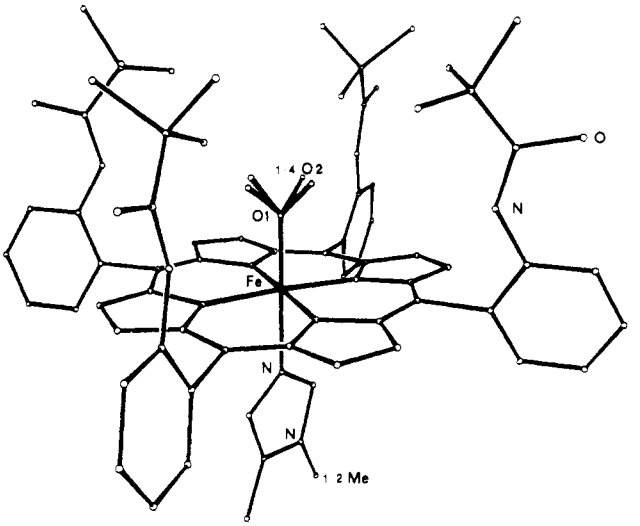

Figure 16. Structure of the O_2 adduct of the iron(II) picket-fence porphyrin (ref 45).

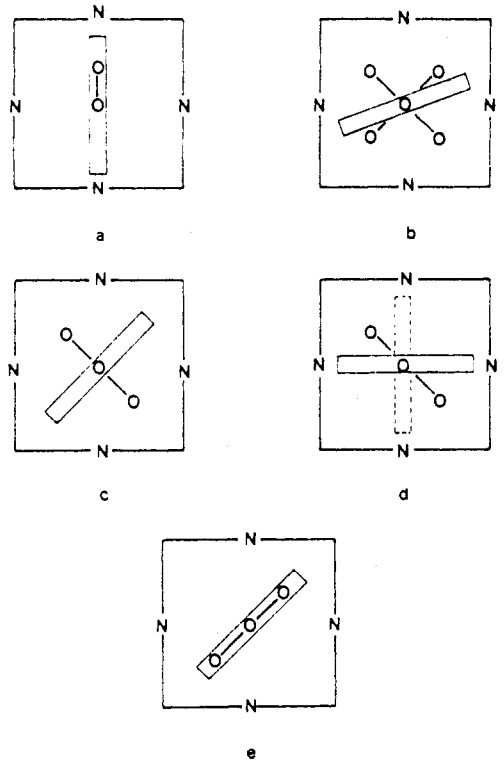

Figure 17. Schematic view of the orientation of the proximal base plane and the Fe–O–O plane in oxymyoglobin and some oxyhemochromes: (a) myoglobin, (X-rays, ref 58); (b) $T_{Piv}PP(1\text{-MeIm})$ (X-rays, ref 45); (c) a-BHP(C_3·Py·C_3)(C_{12}) (NMR, ref 186); (d) a-BHP(C_4·Py·C_4)(C_{12} (ref 169); (e) a-BHP(C_9Im)(C_{12}) (construction of molecular models).

ligand somewhat more like that in the proteins. The 2-methyl substituent on the axial base causes some lengthening of the axial bonds relative to the sterically less demanding 1-MeIm ligand but the effect is most pronounced in the Fe–O bond which is >0.1 Å longer. This correlates with the lower O_2 affinity of the 2-MeIm complex relative to 1-MeIm and models T-state versus R-state hemoglobin.

Due to disorder, there is a fair amount of uncertainty in the dimensions about the FeO_2 moiety in the model compounds. Resolution limitations and refinement uncertainties also leave something to be desired in the X-ray structures of oxyhemoproteins. Nominal distances and angles for the FeO_2 moiety in oxymyoglobin and the two models are listed in Table 3. All that can be concluded with certainty is that a bent geometry with an Fe–O–O angle of about 130° prevails, the O–O bond length is probably longer than that of free dioxygen, and the Fe–O bond length is reasonable. Whether reports of larger Fe–O–O angles in oxyhemoglobin (~155°)[59] and oxyerythrocruorin (170°)[297] should be taken at face value remains to be established. It is possible that H bonding or other distal influences could influence the Fe–O–O angle in oxyhemoproteins but the reported angular variation seems to be greater than might be expected, given the generally good congruence of physical properties between proteins and models. However, as discussed below, there are significant differences in ν(O–O) between models and proteins, indicating some structural differences. The accurate structural definition of the FeO_2 moiety remains a significant unsolved problem. Attempts have been made to obtain crystals of oxygenated picket-fence porphyrin with other axial ligands.[298] These were successful in the case of thiolates as oxy-P450 models and are discussed below.[299,300]

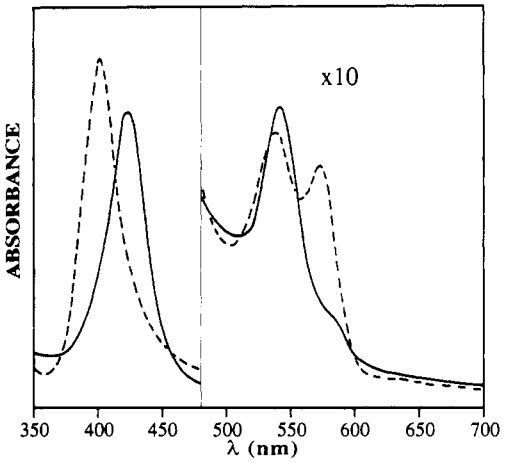

Figure 18. UV–visible spectra of dioxygen adducts of Fe^{II}-ProtoP[$NH(CH_2)_3Im$] (- - -) and $Fe^{II}TPP[NH(CH_2)_3Im]$ (—).

VII. Physical Properties

A. Electronic Spectra

Electronic spectra of metalloporphyrins are dominated by the $\pi \rightarrow \pi^*$ transition of the porphyrin macrocycle.[301,302] They can be perturbed by metal d → d and metal–ligand charge transfer type transitions. The salient features are two visible transitions (Q_o, Q_v) near 18 000 cm^{-1} (the so-called α and β bands between 500 and 600 nm and separated by ≈1250 cm^{-1}) and an intense near-UV transition near 25 000 cm^{-1} (the so-called Soret band near 400 nm). The intensity of the Soret band is usually about 10 times that of the α–β bands. The addition of the transition dipoles for the π–π^* transition is responsible for the intensity of the Soret band while their subtraction results in a low intensity for α–β bands.[303] The spectra of iron porphyrins are characterized by rather broad, overlapping bands which generally remain diffuse even at low temperature. Electronic assignments are important for interpreting spectral perturbations in terms of structural changes[304–306] and for understanding the mechanism of photolysis of six-coordinate complexes.[307]

In the case of oxyhemoproteins, the visible spectra are characterized by two peaks: α (≈575 nm) and β (≈540 nm) in the visible region and a Soret band (≈416 nm). These peaks correspond to complexes of the ubiquitous physiological protoporphyrin IX, having hydrogen atoms at the methine carbon atoms and methyl, vinyl, and propionic acid substituents at the β-pyrrole carbon atoms. Replacement of the vinyl groups of protoporphyrin IX by hydrogen atoms, 2-hydroxyethyl groups, and ethyl groups gives deuterio-, hemato- and mesoporphyrin, respectively, with only minor perturbation of the electronic spectrum. Many synthetic compounds are derived from 5,10,15,20-tetraphenylporphyrin. The presence of phenyl substituents at the methine bridges and H atoms at the β-pyrrolic carbons induces changes in the electronic spectrum. These are associated with inversion of the a_{1u}/a_{2u} HOMO and with electron-withdrawing effects. A 5–10-nm red shift usually results, and this is illustrated in Figure 18.

Several techniques have been used to characterize the electronic transitions responsible for the spectra of

oxy derivatives: polarized single-crystal absorption spectroscopy, magnetic circular dichroism,[308] and direct absorption measurements on ultrathin single crystals.[309,310] Their combined use has identified seven transitions in addition to the $\pi-\pi^*$. Five of the seven bands of oxyhemoglobin are assigned to transitions into the lowest empty molecular orbital which is delocalized over the Fe–O_2 moiety. The remaining bands are interpreted as arising from ligand field d → d transitions of the iron and charge-transfer transitions involving orbitals localized separately on the iron, the porphyrin ring, and the axial ligands. Among these transitions, a broad $x - y$ polarized band near 1000 nm is assigned to a $\pi \rightarrow O_2$ (π_g) promotion.[309,311,312]

The correlation of visible spectra of ferroheme complexes with axial ligands presents a good opportunity to carry out a systematic study of structure–spectra relationships.[313] The α/β intensity ratio and λ_{max} values correlate well with the ligand basicity of unhindered ligands: a stronger Fe–N_{axial} interaction induces a lower ratio and a red shift of absorption peaks. This behavior is more complicated with hindered ligands. An out-of-plane distortion gives red-shifted visible peaks but a blue-shifted Soret band. The α/β ratio decreases.

B. Mössbauer Spectroscopy

Excellent reviews on the application of the Mössbauer effect to hemoproteins and model compounds are available.[314] A simple Mössbauer spectrum of a heme complex is usually diagnostic of spin state and oxidation state.[315] Moreover, it is a useful criterion of compound purity and homogeneity that could be used more frequently.

The temperature dependence of the quadruple splitting of the Mössbauer spectrum of oxyhemoglobin is an unusual and distinctive feature.[316] It is reproduced in the picket-fence model.[74] Such temperature dependence is usually associated with the presence of a paramagnetic state. This, together with the spin-coupling problem engendered by the iron(III)–superoxo formalism seems to have encouraged sceptism about the diamagnetism of oxyhemoglobin. The possibility of a low-lying paramagnetic state has been considered,[317] but it does not find experimental support. Instead, Lang *et al.*[74,316] have proposed a conformational fluxionality of the Fe–O_2 moiety to account for the temperature dependence of the quadrupole splitting. One theoretical attempt to rationalize the quadrupole splitting has been published,[318] but given the difficulty of treating any quadruple splitting there is reason to be skeptical about its validity. As discussed in section VIII, the oxy form of cytochrome P-450 does not show the same temperature dependence of the quadrupole splitting although one of its models does. A deeper understanding of this phenomenon is needed.

C. Infrared and Resonance Raman Spectroscopies

Vibrational spectroscopy offers great potential for the detection of alterations in bonding associated with structural perturbations. Infrared and Raman spectra of oxyhemoproteins as well as relevant model systems have been extensively employed to get important information about the nature of the FeO_2 bonding and the structure–function relationships of hemoproteins. Available data are gathered in Table 4.

Characterization of ν(O–O) in oxymyoglobin and oxyhemoglobin was achieved with careful IR studies by Caughey *et al.*[319,320] at 1103 and 1107 cm^{-1}, respectively. The vibrational mode has also been investigated by several groups using different porphyrins. For example, ν(O–O) for picket-fence porphyrin has been observed around 1160 cm^{-1}, a value which is >50 cm^{-1} higher than those observed in the proteins. The differences could be due to differing π back-donation arising from differing orientations of the Fe–O–O plane with respect to the N–Fe–N vectors of the heme and the axial base plane. In addition, the distal effects of H bonding, dipole orientation, and steric effects lead to the expectation of considerably complex behavior of the vibrational frequencies of bound O_2. Mode coupling has been discussed by Yu *et al.*[335,336]

Given the possibility that the Fe–O stretching mode may be correlated with O_2 binding strength, it has received much attention. The Fe–O stretching mode in oxyhemoglobin was first identified by Brunner[337] at 567 cm^{-1} using resonance Raman spectroscopy, following work by Spiro.[338] The assignment was confirmed by $^{18}O_2$ substitution. The frequency shift of 25 to 30 cm^{-1} is close to the value predicted using a harmonic oscillator model. A slightly higher stretching frequency (572–577 cm^{-1}) is observed for oxymyoglobin.[319-322] A 20-cm^{-1} range is observed in hemoglobin model compounds (see Table 4). Benko and Yu[339] have questioned the assignment of this band and have suggested that it corresponds to a bending mode. However, using isotopic studies, Nakamoto *et al.*[340] argue convincingly for the Fe–O_2 stretching mode. Nakamoto has also made systematic studies of ν(O–O) and ν(Fe–O_2) resonance Raman bands of oxygen adducts in low temperature matrices.[35,13] The field has been reviewed by Spiro.[341]

Interpretations of the differences in ν(O–O) and ν(Fe–O) are not straightforward in the absence of detailed structural information. Nevertheless, some conclusions have been drawn. The low-frequency spectrum corresponding to the ν(Fe–O_2) mode is found nearly insensitive to the distal environment in a series of oxygenated Fe^{II}–amide–basket handle porphyrins.[137] The stretching frequency observed (560–563 cm^{-1}) is lower than that generally observed for other oxygenated porphyrins (e.g., ca. 570 cm^{-1} for a "picket-fence" dioxygen complex)[327] and for oxyhemoproteins. This is interpreted as corresponding to a deformation of the Fe–O–O angle promoted by intramolecular H bonding between the bound O_2 and the secondary amide group of the handle. Kitagawa *et al.*[173] generalized this interpretation by plotting the ν(O–O) frequencies against ν(Fe–O) frequencies. This plot is relatively linear for model compounds but not for proteins. The sensitivity of ν(O–O) is consistent with some distal residue influence on the Fe–O–O bond angle.[173,329]

The trans-ligand donor strength and its steric constraint are two of the major factors that determine the ν(Fe–O) frequency. Nakamoto *et al.*[330] report that a large increase in the ν(Fe–O) frequency, approximately 65 cm^{-1}, occurs upon introduction of a trans ligand (relative to none). The presence of a steric restraint to the motion of the axial base toward the porphyrin upon oxygenation has been examined using oxygen adducts

Table 4. Infrared and Resonance Raman of Oxyhemes in Myoglobin (Mb), Hemoglobin (Mb), Leghemoglobin (Lb), Cytochrome *c* Oxidase (Cyt Ox a_3), and Model Compounds

complex	ν(Fe–O)[a]	ν(O–O)[a]	conditions	ref(s)
MbO_2	572	1103 (1065)	pH 7.2, 10 °C	319–321
MbO_2	577		pH 7.2, 25 °C	322
LbO_2	576 (554)		pH 7, 25 °C	323
HbO_2	571 (540)	1107 (1065)		319,320,324,325
Cyt Ox a_3O_2	569 (540)		pH 7.4, 10 °C	326
Fe(T_{piv}PP)(1-MeIm)O_2	567 (538)		solid	327,328
Fe(T_{piv}PP)(1-MeIm)O_2	571	1159 (1075)	CH_2Cl_2	239,328
Fe(T_{piv}PP)(1-TrIm)O_2		1163 (1080)		239
Fe(T_{piv}PP)(2-MeIm)O_2	557		solid	328
Fe(T_{piv}PP)(1,2-MeIm)O_2	558 (532)			328
Fe(T_{piv}PP)(1,2-MeIm)O_2	564	1159 (1093)	CH_2Cl_2	239
Fe(PP)(1-MeIm)O_2	573		CH_2Cl_2, –120 °C	329
Fe(PA)(1-MeIm)O_2	576		CH_2Cl_2, –120 °C	329
Fe(OEP)(1-MeIm)O_2	572		CH_2Cl_2, –120 °C	329
Fe(OEP)(1-MeIm)O_2	573		DMF, –120 °C	329
Fe(TPP)(Pip)O_2	575	1157 (1093)	CH_2Cl_2, –70 °C	330,331
Fe(P-CH_2)$_3$-Im)O_2	574		CH_2Cl_2, –70 °C	332
Fe(P-CH_2)$_2$-Im)O_2	573		CH_2Cl_2, –70 °C	332
Fe(P-CH_2-Im)O_2	576 (545)		CH_2Cl_2, –70 °C	332
Fe[(Piv)$_2$-C_{12}](1-MeIm)O_2	563		toluene, 25 °C	137
Fe[(Piv)$_2$-C_{10}](1-MeIm)O_2	563		toluene, 25 °C	137
Fe[(Piv)$_2$-C_9](1-MeIm)O_2	560		toluene, 25 °C	137
Fe[(Piv)$_2$-C_8](1-MeIm)O_2	563		toluene, 25 °C	137
[Poly-lipid liposome/heme](Im)O_2		1161 (1076)	H_2O, 25 °C	333
Fe(TPP)O_2				
end-on	509 (487)	1195 (1127)	toluene, –248 °C	35,330
side-on		1106 (1043)	toluene, –248 °C	35,334
Fe(OEP)O_2				
end-on		1190	toluene, –248 °C	334
side-on		1104	toluene, –248 °C	334
O_2 gas		1156		
O_2^-		1100–1150		

[a] Frequencies (in cm^{-1}) for $^{16}O_2$ ($^{18}O_2$) adducts.

with 1-methylimidazole and 1,2-dimethylimidazole as axial ligand. Replacement of the unhindered by the hindered ligand for the oxygen adduct of picket fence porphyrin in benzene gives rise to ca. 10 cm^{-1} decrease in ν(Fe–O) in benzene or the solid state and ca. 4 cm^{-1} in methylene chloride.[328] Such results contrast with those of Hori and Kitagawa[342] who found an insensitivity of ν(Fe–O_2) to a proximal tension. Similarly, an analysis of imidazole-appended heme spectra showed an insensitivity of ν(Fe–O) to a constraint introduced into the length of the chain bearing the imidazole.[332] The electron-donating capabilities of the substituents of the porphyrin ring exert a significant effect on the O_2 binding constant.[224] However, this thermodynamic trend is not manifest in measurable changes in the iron–oxygen bond strength.[321,324,327–329] Thus, the relationship between the binding affinity and the iron–ligand stretching frequency is not necessarily straightforward. Irwin *et al.*[323] have suggested that heme ruffling, rather than changes in axial ligand bonding, leads to stabilization of an oxygen complex. This hypothesis was advanced in connection with the high affinity of leghemoglobin relative to myoglobin despite congruence of their axial ligand stretching frequencies.

D. ^{1}H and ^{17}O NMR Spectroscopy

^{1}H NMR spectroscopy of hemoproteins (including NOESY and COSY experiments) has played an important role in describing the structure and dynamics of the globin.[260] By using modern NMR techniques, assignment of heme and protein resonances is now a relatively straightforward if tedious task.[261–263] The substantial ring current of the porphyrin is useful for assigning residues close to the heme and changes in these resonances allow some suggestions to be made about the factors which affect ligand binding.[262,263] Relatively few ^{1}H NMR studies have concentrated on the oxy forms of hemoproteins because of the limited lifetime of oxygenated hemoproteins and the complications that arise from paramagnetic impurities.[260]

Oxygenated heme complexes are perhaps somewhat better targets for NMR study because even though they can be less stable than oxygenated hemoproteins at room temperature, their organic solvent solubility allows measurement at stabilizing low temperatures. In addition, with many fewer protons, ^{1}H NMR data can be collected rapidly over a considerable temperature range.

The ^{1}H NMR spectrum of an oxygenated heme complex was first reported by Collman, Brauman, La Mar, and co-workers.[95] The important finding is that the resonances are sharp and typical of a diamagnetic species (0–10-ppm range). This would seem to rule out any significant population of a low-lying paramagnetic excited state particularly since spectra remained unchanged up to 90 °C. Further attention to this criterion of diamagnetism might lay to rest recurring suggestions[53,54,343] of paramagnetism which are artifactual or remain to be substantiated.

As discussed above in section V.G. Mispelter *et al.*[169] have used ^{1}H NMR to implicate amide protons in the stabilization of oxygen adducts of basket-handle porphyrins.

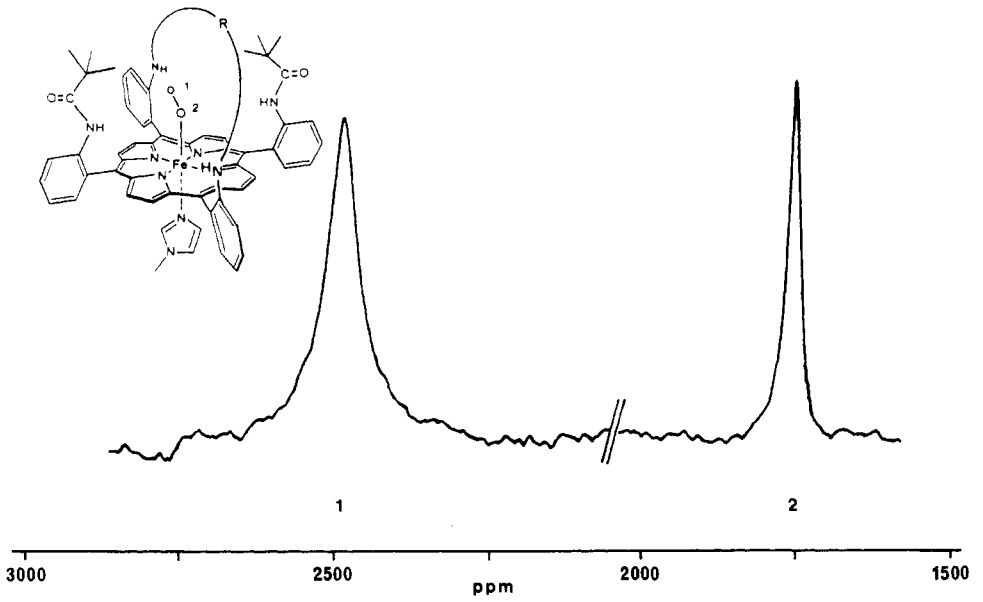

Figure 19. ^{17}O NMR spectrum of the oxygenated $FePiv_2C_8$(1-MeIm) in CH_2Cl_2 at 273 K (ref 351).

Table 5. ^{17}O Chemical Shifts and Line Widths of the Oxygen Atoms of the Fe–O_2 Moiety of Hemoprotein Models[a]

	solvent	T, °C	$\delta_{O(2)}$, ppm	$(\Delta\nu_{1/2})_{O(2)}$, Hz	$\delta_{O(1)}$, ppm	$(\Delta\nu_{1/2})_{O(1)}$, Hz	ref
Fe(a-BHP)(1-MeIm)	CH_2Cl_2	283	1762.5	2280	2486.9	6450	351
	CH_2Cl_2	273	1764.8	2640			351
Fe(e-BHP)(1-MeIm)	CH_2Cl_2	273	1754.5	990	2514.6	3750	351
Fe[$(Piv)_2(C_8)$](1-MeIm)	toluene	273	1738.0	910	2480.5	3390	351
	toluene	283	1731.4	710	2479.9	3170	351
Fe[$(Piv)_2(C_8)$](1,2-Me_2Im)	toluene	273	1760.5	2017			355
	toluene	283	1757.9	1399	2484.7	4319	355
Fe(T_{piv}PP)(1-MeIm)	CH_2Cl_2	273	1747.9	370	2518.7	2480	351
	CH_2Cl_2	283	1747.3	450	2518.2	1960	351

[a] Concentration: 2.5×10^{-2} to 1.4×10^{-2} M. Chemical shifts are reported to external 1,4-dioxane by using the sample replacement technique.

Compared to ^1H NMR spectroscopy, ^{17}O studies of oxygenated derivatives of hemoproteins and metalloproteins have received little attention. This neglect is not surprising since, of the naturally occurring oxygen isotopes, only ^{17}O possesses nuclear spin and it has $I = {}^3/_2$. Due to its electric quadrupole moment ($Q = 2.6 \times 10^{-30}$ m^2), its low natural abundance (0.037%), and the extremely low absolute sensitivity compared to that of ^1H, it is one of the more difficult nuclei to observe by NMR spectroscopy. Nevertheless, the isotropic shielding tensor and transverse and longitudinal relaxation times of ^{17}O are excellent means to probe the bonding and dynamics of oxygen-containing ligands bound to hemoproteins and model compounds. They have been applied to other metallo–oxygen complexes.[344-347]

An early attempt at observing $^{17}O_2$ resonances in oxyhemoglobin was reported by Maricic *et al.*[348] They reported a singlet at ~0 ppm and concluded that both oxygen nuclei were magnetically equivalent, thereby supporting the Griffith triangular structure. However, it was subsequently shown that the observed signal was due to $H_2{}^{17}O$ since bacteria had metabolized $^{17}O_2$ into $H_2{}^{17}O$ and the deoxyhemoglobin had oxidized to methemoglobin.[349,350]

The first successful experiment with $^{17}O_2$ was reported in 1987 by Gerothanassis and Momenteau with model compounds in organic solution using gaseous oxygen containing 30–50% oxygen-17. Figure 19 shows the ^{17}O NMR spectrum of an oxygenated "hybrid" porphyrin at 273 K. The observation of two distinct resonances at 2480.5 and 1738 ppm, which are well outside of the established ^{17}O chemical shift scale, rules out a triangular (η^2) structure and is consistent with end-on angular bonding (η^1).[352] Furthermore, it rules out a rapid flipping of the O–O group on the NMR time scale (5×10^5 s^{-1}). Data are summarized in Table 5. The values of observed chemical shifts agree with calculations of the oxygen-17 shielding constants predicted by Velenik and Lynden-Bell:[353] the nucleus of the oxygen atom O(2) near the iron atom was found to be more shielded than the nucleus of the terminal oxygen O(1). The difference of the shielding constants between the two nuclei, $\Delta\delta \approx 720$–780 ppm is constant and independent of the value of the charge q on the oxygen O(2) and the splitting ΔE of the degenerate π orbitals of the oxygen atoms on complexing.

More recently, Oldfield *et al.*[354] obtained similar results by studying oxygenated picket-fence porphyrin in the solid state. The principal components of the chemical shift tensors for both the coordinated and terminal oxygen atoms of the Fe–O_2 unit were determined and the isotropic chemical shifts occur at 1600 and 2017 ppm respectively at 298 K, somewhat shielded from the values in solution. In addition, they found that the total line width of the powder spectrum was independent of the magnetic field strength. This indicates that the chemical shift anisotropy is the dominant line-broadening interaction. These authors also studied frozen solutions of oxymyoglobin and oxyhemoglobin. These indicated general similarity with

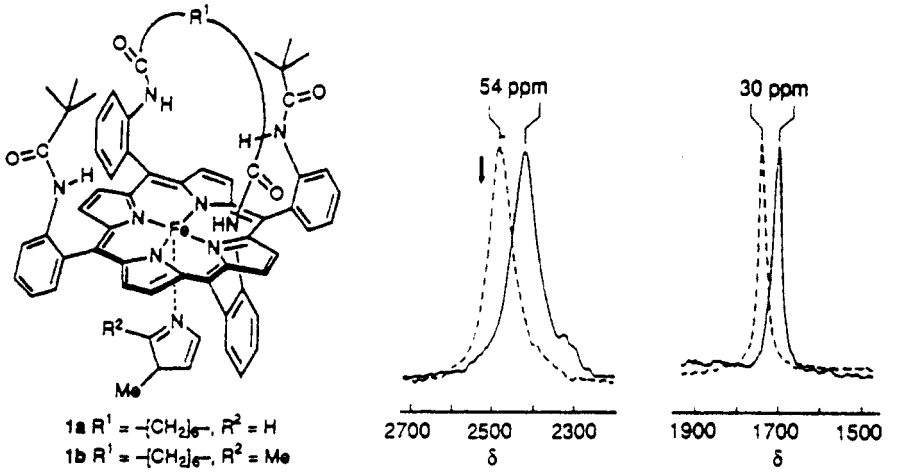

Figure 20. ^{17}O NMR spectra of the oxygenated $FePiv_2C_8$ in the presence of 1-MeIm (—) and 1,2-Me_2Im (- - -) in toluene at 283 K (ref 355).

model compounds but the achievable spectral signal-to-noise ratio does not allow detailed conclusions to be drawn.

There is currently much support for the importance of hydrogen bonding and dipole–dipole interactions in the stabilization of the oxygenated protein and model porphyrin dioxygen adducts. Such interactions secure both ends of the bound dioxygen and stabilize the oxygenated complex by lowering the off rate relative to the on rate. ^{17}O NMR spectroscopy provides a potential approach to explore hydrogen bonding and polarity effects.

Comparison of ^{17}O NMR spectra of heme models bearing secondary amide or ether anchoring chains gives a direct probe of the presence of hydrogen bonding in the former.[351] A shift of ca. 30 ppm of the resonance of the terminal oxygen atom to lower frequency is observed with *amide*-basket-handle porphyrin models (see middle of Figure 9), relative to the *ether*-basket-handle porphyrins, while the resonance of the oxygen atom coordinated to iron is shifted by ~10 ppm to higher frequency.[355] The shift of the terminal oxygen has been attributed to a hydrogen interaction with the NH of the distal handle, consistent with earlier ^1H NMR[169] and IR[127] studies. These shifts can be interpreted qualitatively by assuming that an increase in hydrogen bonding favors resonance structure II:

structure I structure II

In a variety of transition metal complexes there is a correlation between ^{17}O chemical shifts and metal–oxygen π-bond character, just as there is for carbon–oxygen and nitrogen–oxygen bonds.[356,357] Thus, it is expected that an increase in hydrogen bonding to the Fe–O_2 moiety would enhance structure II by increasing the metal–oxygen π-bond order (resulting in a high frequency shift) and decreasing the O–O π-bond order (resulting in a low shift). The value of these shifts will depend on the strength and geometry of the particular hydrogen bonds and the dielectric constant of the medium.

With oxygenated iron(II) picket-fence porphyrin with 1-MeIm as axial base in a nonpolar organic solvent the ^{17}O chemical shifts are close to those of ether-linked basket-handle porphyrin derivatives. This result confirms the absence of strong hydrogen-bonding interactions between O_2 and the secondary amide group of the pickets. However, a modification of the spectrum is observed when the dielectric constant of the medium is increased. Recent ^{17}O NMR results indicate significant and systematic shifts to higher frequency when increasing amounts of dimethylformamide are added to CH_2Cl_2.[358]

Since the discovery by Collman *et al.* that the proposed tension or strain in the histidine–iron bond in T-state Hb can be mimicked with 2-methylimidazole in a model complex,[287] numerous structural and dynamic studies have been reported on hemoproteins models with and without a hindered base. The ^{17}O NMR spectra of the T-state "hybrid" models have been recently reported in solution.[355] As with R-state models having 1-methylimidazole as axial base, the spectra exhibit two distinct resonances in accord with the end-on geometry. However, in the T-state models, the resonance of the oxygen atom coordinated to iron shifted 30–60 ppm to low field relative to that in the R-state analogs. The porphyrin and the NMR data are illustrated in Figure 20. The change in the chemical shift of the former could reflect an increase in the Fe–O length with a concomitant decrease in the Fe–O π-bond order. This is consistent with X-ray structural data on picket-fence porphyrin.[296] The shift of the terminal oxygen atom to low frequency in the T-state model relative to that in the R-state model is in the same direction. It is larger in magnitude than that observed in amide-basket porphyrins vs ether-basket porphyrins but opposite in direction. A different type of polarization of the FeO_2 bonding must be present, consistent with some role for the picket amide dipoles.

Thus, results obtained by European and American laboratories have demonstrated that ^{17}O NMR is a unique structural probe for studying oxygenated hemoprotein models in solution and in the solid state. The reason for failure in obtaining hemoprotein spectra in solution is not clear.

VIII. Cytochromes P-450

Cytochromes P-450 are monooxygenases which occur widely in liver microsomal and adrenal mitochondrial fractions of animals as well as in plants and microorganisms. They are tightly bound to membranes in mammalian systems with consequent difficulty in their

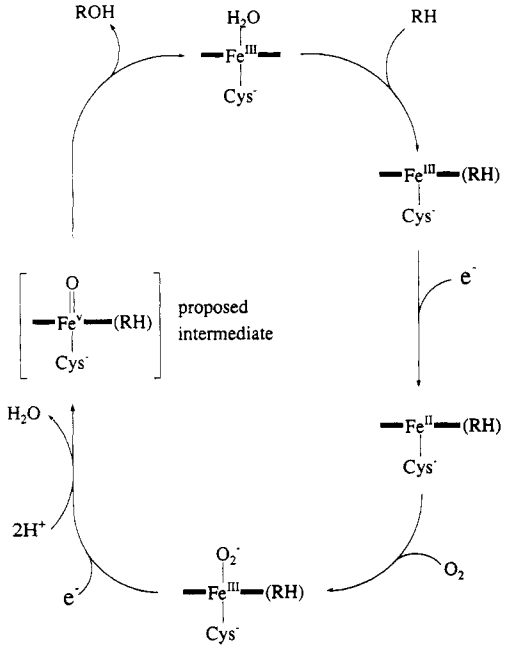

Figure 21. Catalytic cycle of cytochrome P-450.

purification. Since their discovery, intense research has been devoted to these enzymes because of the central role they play in the catalytic hydroxylation of a wide range of substrates involved in the metabolism of fatty acids, steroids, drugs, carcinogens, and other foreign compounds.[359,360]

The catalytic reaction involves the cleavage of the O–O bond of molecular oxygen. Two electrons and two protons are consumed such that one oxygen atom is eliminated as water. The other oxygen atom is introduced into the substrate such that the overall reaction is

$$RH + O_2 + 2e^- + 2H^+ \rightarrow ROH + H_2O$$

For the purposes of this review, the important observation is that oxygen reduction is preceded by oxygen adduct formation.

As in oxygen-carrying hemoproteins, the prosthetic group of cytochromes P-450 is an iron protoporphyrin IX. There is a marginally stable, oxygenated form of cytochrome P-450 that closely resembles oxyhemoglobin in its physical properties. But these two classes of hemoproteins differ in the nature of their proximal axial ligation to iron. A large body of chemical and spectroscopic data, and now X-ray crystal proof,[361,362] shows that thiolate sulfur from a cysteine residue is the axial ligand to the iron center.

The catalytic cycle of cytochromes P-450 is shown in Figure 21. It is a multistep process which includes four stable and isolable states: a low-spin ferric resting state, a high-spin ferric complex resulting from binding of substrate, a high-spin ferrous state due to a one electron reduction, and a low-spin dioxygen complex. The active oxygenating species is formed after loss of water and is believed to be an oxyferryl complex. It may be formulated as an iron(V) complex or an iron(IV) porphyrin cation radical. When the high-spin ferrous state is exposed to carbon monoxide instead of dioxygen, a low-spin ferrous carbonylated state is generated. This carbonyl adduct presents an unusual electronic absorption maximum in the Soret band region which characterizes all the cytochromes P-450 and synthetic Fe(II) thiolate complexes. It exhibits a so-called hyperporphyrin spectrum with a Soret band near 450 nm, some 30 nm lower in energy than most hemoproteins.

As with the preparation of model compounds for oxyhemoglobin, model compounds for the oxygenated state of cytochrome P-450 must meet the requirements of attaining a five-coordinate iron(II) precursor and thwarting irreversible oxidation. The problem is conceptually similar although it is made more difficult by the ready oxidation of thiolate axial ligands to disulfide:

$$2Fe^{III}P(SR) \rightarrow 2Fe^{II}P + RS\text{–}SR$$

A. Model Compounds

The simplest approach to a model compound consists of reacting flat-open hemes (TPP,[363] OEP,[364] PP IX DiMe[365–369]) with an alkyl or aryl thiolate in organic solution. These compounds bind CO reversibly and exhibit a striking spectral resemblance to those of carbonylated cytochromes P-450. However, these models present two major disadvantages. First, the poor affinity of iron(II) porphyrins for mercaptide anion imposes the necessity of using a very large concentration of ligand. Second, it is difficult to prove conclusively that they can reversibly bind dioxygen. Chang and Dolphin[369] reported that at −45 °C addition of O_2 to a protoheme–mercaptide complex in dimethylacetamide resulted in the spectral formation of a dioxygen adduct without deterioration after 1 h. However, Ruf and Wende[370] showed that the visible spectrum of the presumed oxygen adduct was the same as an iron(III)–bisthiolate complex.

Traylor[371] has used the chelated heme approach to covalently attach mercaptide to the porphyrin periphery, making it available for binding to iron without having to add excess of an external ligand. This stabilizes the iron(III) mercaptide system and allows production of a P-450-like CO complex of iron(II), but O_2 complexation gives rise to irreversible oxidation. Other chelated hemes have been synthesized[372–373] and show similar properties. Collman and Groh[374] reported the synthesis of a mercaptan-tail picket-fence porphyrin. Treatment of the arylenethiol iron(II) porphyrin with a strong base gave essentially complete coordination of the thiolate group. UV–visible and magnetic circular dichroism spectra of the carbonylated heme displayed the characteristic hyperporphyrin spectrum of P-450 in the presence of CO.

More recently, functionalized basket-handle porphyrins were designed to hold the thiolate firmly in a suitable position for coordination to iron atom by bridging it across one face of the porphyrin ring; the second handle forms a cavity allowing a controlled oxidation in the presence of O_2.[375–378] In the case of Woggon's compounds,[377] dioxygen binding to iron(II) at 10 °C in toluene solution was accompanied by an O-atom insertion into a monoactivated C–H bond of the distal handle. This autoxidation of the catalyst itself can be considered as an example of a reaction mimicking the monooxygenase activity of cytochrome P-450.

Studies of models for cytochrome P-450 have always shown that an aryl thiolate is more stable than that of an alkyl thiolate. Furthermore, the introduction of

electron-withdrawing substituents on the arene ring significantly stabilizes the aryl thiolate toward oxidation. Weiss *et al.*[299,300,379-381] have exploited this observation along with the steric protection offered by picket-fence porphyrin to provide crystalline models of each of the reaction states of P-450. They observed in the crystal structures of three thiolate derivatives of the type $[Fe(T_{piv}P)(SR)]^-$ $[Na\text{-}222]^+$ with R = C_2H_5, C_6H_5, and 2,4,5-$C_6H_2Cl_3$, that the S-donor ligand was coordinated to the ferrous ion within the cavity formed by the pivalamido pickets. However, using a bulkier, less reducing thiolate, 2,3,5,6-tetrafluorothiophenolate, they were able to get reversible dioxygen binding within the picket cavity. A remarkable stability was observed even at room temperature.[299,380] As discussed below, these compounds have been characterized by infrared,[379] resonance Raman,[380] magnetic dichroism (MCD),[382] and Mössbauer[299,380,381] spectroscopic techniques and by X-ray diffraction.[299,380]

B. Physical Properties of Dioxygen Adducts

The difference in axial ligand between hemoglobin (imidazole) and cytochrome P-450 (thiolate) is expected to give rise to distinctive and chemically significant differences in the nature of the bound dioxygen, particularly because of their *trans* relationship in the coordination sphere. The most notable of these is, of course, the unusual 450-nm Soret band of the CO complex which gives rise to the name of these cytochromes. On the other hand, the Soret peak of the oxy complex is at 418 nm,[383,384] a wavelength identical to that of oxymyoglobin. Nevertheless, MCD spectra are quite different and diagnostic of thiolate vs imidazole ligation.[382]

IR and Raman spectroscopies have been used to study the oxy forms of P-450 and its models and give insight into the electronic distribution at the heme. Arguments suggest that extra electron density is donated from the proximal thiolate ligand via the heme iron to the π^* orbitals of the bound dioxygen. The ^{16}O–^{16}O stretching vibration in the oxy-P-450 models developed by Weiss[379] is observed at 1139 cm^{-1} in the infrared spectrum. Substitution by $^{18}O_2$ shifted this absorption to 1076 cm^{-1}, in good agreement with the calculated value of 1073 cm^{-1} for a pure harmonic oscillator. This shift is comparable to imidazole-ligated oxyhemes but ca. 20 cm^{-1} lower in absolute value. Champion *et al.*[385] confirmed this assignment by examination of the resonance Raman spectrum of oxy-P-450_{cam}. This decrease for ν(O–O) in thiolate complexes relative to imidazole complexes could originate from a greater π back-bonding from iron into the π^* orbitals of oxygen, weakening the O–O bond and facilitating its cleavage.[386] Resonance Raman results concerning heme frequencies corroborate these ideas.[387] The energy of the ν_4 porphyrin band which is considered as an oxidation marker band[341] and is sensitive to spin effects[387] reflects the amount of π back-donation from dπ orbitals of iron into the π^* orbitals of the porphyrin. This band appears in the 1340–1370-cm^{-1} range for hemoproteins and model compounds. Chottard *et al.*[380] have examined a thiolate complex and have identified the ν_4 frequency at 1366 cm^{-1}. In different isozymes of P-450 they range from 1367–1372 to 1341–1347 cm^{-1}. The lowering of these frequencies compared to hemoglobin (1377 cm^{-1})[136] is in good agreement with the promotion of electron flow to dioxygen. Unfortunately, the Fe–O_2 stretching mode, observed near 565–570 cm^{-1} for other oxyhemoproteins has not been detected in oxy-P-450.

Single-crystal X-ray structural data the for oxygenated state of cytochrome P-450 are presently unavailable. EXAFS spectroscopy has been used to confirm the expected ligation state and a short Fe–S distance (2.37 Å) was noted.[388]

The crystal structure of two oxy P-450 models have been reported by Weiss *et al.*:[299,300] $[K(C222)][Fe(T_{piv}PP)(SC_6HF_4)(O_2)]$ and $[Na(C16c6)][Fe(T_{piv}PP)(SC_6HF_4)(O_2)]$. In both cases, the iron atom lies essentially at the center of the four Np mean plane. The mean value of the four Fe–Np distances is 1.994(4) Å and corresponds to the value found for a large number of low-spin S=O iron(II) porphyrins.[12] The porphyrinato core is slightly ruffled. The thiolate axial ligand lies on the unprotected face of the porphyrin, and the oxygen molecule, in a bent end-on geometry, occupies the cavity formed by the pivalamido pickets. The Fe–S bond length is 2.369(2) Å and is close to that reported for the oxygenated adduct of P-450_{cam}.[388]

The Fe–O–O bond angles of ca. 128° are in agreement with previous reports on dioxygen iron porphyrinato complexes with imidazole as axial ligand. The Fe–O bond distances, 1.837(9) and 1.850(4) Å respectively, are close to those determined by EXAFS for oxy-P-450 (1.78 Å) and close to those of imidazole-ligated models. The mean value of the two O–O bond distances (1.14(5) Å) is unacceptably short. This is the result of a rotational disorder of the O_2 molecule which differs from one structure to the other. Two nonequivalent positions are clearly found for the former complex while the O_2 molecule occupies three sites in the latter. The nature of this disorder, which may be static or dynamic in $[K(C222)][Fe(T_{piv}PP)(SC_6HF_4)(O_2)]$, is not obviously due to specific interactions with the pickets and could be the result of factors arising from the particular orientation of the trans thiolate ligand.

Mössbauer studies have been performed in order to probe the electronic structure of the iron atom.[389-391] The data on P-450 indicate that the iron is similar to that in oxyhemoglobin. The quadrupole splitting (ΔE_q = −2.15 mm/s) and isomer shift (δ = 0.31 mm/s) are similar but oxy-P-450_{cam} does not show the distinctive temperature dependence of the quadrupole splitting seen in oxymyoglobin and oxyhemoglobin.

Weiss and Trautwein[300,381,392] have reported Mössbauer measurements on polycrystalline samples of $[K(C222)][Fe(T_{piv}PP)(SC_6HF_4)(O_2)]$ and $[Na(C18c6)][Fe(T_{piv}PP)(SC_6HF_4)(O_2)]$ in the temperature range 4–300 K. The data vary according to the nature of the counterion. A definite temperature variation of the quadrupole splitting was observed for one compound but not for others. On the basis of the crystal structure showing that the terminal oxygen is disordered over three sites, it was postulated that the temperature dependence, when observed, may be a dynamic process. This is related to the postulates of rotational fluxionality advanced to explain similar behavior in oxyhemoglobin and its model compounds.[316,317,74]

C. Kinetics of O_2 Binding

While reduced ferrous P-450 can form a reversible oxygen adduct with molecular dioxygen,[384] there is limited information for O_2 binding in synthetic models.

This is because the initial binding reaction is generally followed by rapid autoxidation. The oxy enzyme is not particularly stable compared to hemoglobin but it can be stabilized and studied at low temperatures.[393,394]

On the basis of stopped-flow studies with substrate-free P-450$_{LM2}$ the first binding of dioxygen has been reported to occur in two spectroscopically distinguishable steps.[395] The first step, which occurs within the dead time of the instrument ($k > 6 \times 10^4$ min^{-1}) yields an intermediate that is converted in a slower step (k = 210 min^{-1}) to a dioxygen adduct. The rate constant for the second step is somewhat higher in the presence of a substrate. When the reaction is monitored at cryogenic temperatures rather than by stopped-flow techniques, however, only the final dioxygen complex is observed. The same behavior was observed for different cytochromes P-450 and the rate constants varied between 10^4 and 10^6 M^{-1}s^{-1}.[384,396-401] The rate constants for O_2 binding are dependent on a variety of conditions including pH and the presence of substrate. The autoxidation rate dramatically increases below pH 7. The presence of substrate stabilizes the oxygenated enzyme. The rate of association of O_2 with substrate-depleted cytochrome was at least 50 times faster than the rate of association of O_2 with substrate-bound cytochrome.[384] Changes in the chemical nature of the substrate also modify the binding rate constants.[400] This is to be expected. The substrate binding site is immediately adjacent to the O_2 binding site.[362]

Less detailed studies of the dioxygen binding reaction have been carried out with P-450 model systems. As shown by Weiss *et al.*[299,300] oxygen adducts of picket-fence iron(II) porphyrins with arenethiolates as proximal ligand are stable enough to measure both equilibrium and kinetic rate constants. Thus, El-Kasmi *et al.*[402] have recently measured oxygen affinities with such complexes by simple spectrophotometric titration methods and association rate constants by flash photolysis. Addition of a large excess of sodium 2,3,5,6-tetrafluorobenzenethiolate, cryptated by 18-crown-6, to Fe^{II}-T$_{piv}$PP and Fe^{II}-(Piv)$_2$(C$_9$)PP in toluene solution, gives only five-coordinate complexes. Values of the rate and equilibrium parameters for O_2 binding are provided at the end of Table 2. Equilibrium constants [(1–2) $\times 10^3$ M^{-1}] are greatly reduced compared to those measured when the axial ligand is an N donor (10^5–10^6 M^{-1}). This decrease is due exclusively to a large increase in the dissociation rate constants. The association rates remain almost the same for the two kinds of proximal ligand. Such results are in accord with an effect of the thiolate axial ligand which destabilizes the O_2 complex,[403] but it is not understood how such an apparently good electron donor as thiolate causes this affinity lowering. Perhaps, the fluoroarenethiolates are significantly different from alkenethiolates or alternatively, the absence of a distal H bond in P-450 may be a important factor.

IX. Conclusion

Two decades of intense study of dioxygen binding to iron(II) porphyrin complexes has led to an excellent molecular-level understanding of the phenomenon and has contributed greatly to our understanding of how oxygen-binding hemoproteins work. As a paradigm of how synthetic model compounds can contribute to an understanding of biochemistry, it is exemplary. Nevertheless, there are still areas where model complexes can be expected to further our understanding of oxygen binding to hemoproteins. These include the partitioning of the factors which contribute to the large range of observed O_2 affinities (particularly very high affinities), the origin of the temperature dependence of the Mössbauer quadrupole splitting, the accurate structural definition of the FeO_2 moiety (particularly the O–O distance and whether large obtuse Fe–O–O angles are real) and the mechanisms of activation of bound O_2 in oxygen-utilizing enzymes (cytochromes P-450, cytochrome oxidase, etc.).

X. Acknowledgments

The authors express their sincere appreciation to all collaborators and co-workers for their major contributions to this field. Much of the authors' work described in this review was supported by the Centre National de la Recherche Scientifique, the National Institutes of Health, and NATO (Collaborative Research Grant 0638/88). We particularly thank A. Marrion, B. Loock, and N. Marie for their assistance in the preparation of this manuscript.

XI. References

(1) Reed, C. A. In *Metal Ions in Biological Systems*; Sigel, H. E., Ed.; Marcel Dekker, Inc.: New York, 1978; pp 277–310.
(2) Jones, R. D.; Summerville, D. A.; Basolo, F. *Chem. Rev.* **1979**, *79*, 139–179.
(3) Collman, J. P. *Acc. Chem. Res.* **1977**, *10*, 265–272.
(4) Collman, J. P.; Halbert, T. R.; Suslick, K. S. In *Metal Ion Activation of Dioxygen*; Spiro, T. G., Ed.; John Wiley and Sons: New York, 1980; pp 1–72.
(5) Traylor, T. G. In *Bioorganic Chemistry*; Van Tamelen, E. E., Ed.; Academic Press: New York, 1978; Vol. IV, pp 437–468.
(6) Ibers, J. A.; Holm, R. H. *Science* **1980**, *209*, 223–235.
(7) Baldwin, J. E.; Perlmutter, P. *Top. Curr. Chem.* **1984**, *121*, 181–220.
(8) Suslick, K. S.; Reinert, T. J. *J. Chem. Educ.* **1985**, *62*, 974–983.
(9) Momenteau, M. *Pure Appl. Chem.* **1986**, *58*, 1493–1502.
(10) Morgan, B.; Dolphin, D. *Struct. Bonding* **1987**, *64*, 115–203.
(11) Ungashe, S. B.; Groves, J. T. In *Advances in Inorganic Biochemistry*; Eichhorn, G. L., Marzilli, L., Eds.; Elsevier: New York, 1993.
(12) Scheidt, W. R.; Reed, C. A. *Chem. Rev.* **1981**, *81*, 543–555.
(13) Nakamoto, K. *Coord. Chem. Rev.* **1990**, *100*, 363–402.
(14) Stynes, D. V. *Can. J. Spectrosc.* **1981**, *26*, 109–118.
(15) Jameson, B. G.; Robinson, W. T.; Ibers, J. A. In *Hemoglobin and Oxygen Binding*; Ho, C., Ed.; Elsevier North Holland, Inc.: Amsterdam, 1982; pp 25–35.
(16) Tsuchida, E.; Nishida, H. *Top. Curr. Chem.* **1986**, *132*, 64–99.
(17) Niederhoffer, E. C.; Timmons, J. H.; Martell, A. E. *Chem. Rev.* **1984**, *84*, 137–203.
(18) Jameson, G. B.; Ibers, J. A. *Comm. Inorg. Chem.* **1983**, *2*, 97–126.
(19) Shikama, K. *Coord. Chem. Rev.* **1988**, *83*, 73–91.
(20) Sawyer, D. T.; Valentine, J. S. *Acc. Chem. Res.* **1981**, *14*, 393–400.
(21) Malmström, B. G. *Chem. Rev.* **1990**, *90*, 1247–1260.
(22) Collman, J. P.; Denisevich, P.; Konai, Y.; Morrocco, M.; Koval, C.; Anson, F. *J. Am. Chem. Soc.* **1980**, *102*, 6027–6036.
(23) Kitajima, N.; Fujisawa, K.; Fujimoto, C.; Moro-oka, Y.; Hashimoto, S.; Kitagawa, T.; Toriumi, K.; Tatsumi, K.; Nakamura, A. *J. Am. Chem. Soc.* **1992**, *114*, 1277–1291. Kitajima, N. *Chem. Rev.* This issue.
(24) Stenkamp, R. E. *Chem. Rev.* This issue.
(25) Reed, C. A.; Cheung, S. K. *Proc. Natl. Acad. Sci. U.S.A.* **1977**, *74*, 1780–1784.
(26) Summerville, D. A.; Jones, R. D.; Hoffman, B. M.; Basolo, F. *J. Chem. Educ.* **1979**, *56*, 157–162.
(27) Reed, C. A. In *Electrochemical and Spectrochemical Studies of Biological Redox Compounds*; Kadish, K. M., Ed.; Advances in Chemistry 201; American Chemical Society: Washington, DC, 1982; pp 333–356.
(28) McCandish, E.; Miksztal, A. R.; Nappa, M.; Sprenger, A. Q.; Valentine, J. S.; Stong, J. D.; Spiro, T. G. *J. Am. Chem. Soc.* **1980**, *102*, 4268–4271.
(29) Khenkin, A. M.; Shteinman, A. A. *Kinet. Katal.* **1982**, *23*, 219–222; English translation, 185–187.
(30) Welborn, C. H.; Dolphin, D.; James, B. R. *J. Am. Chem. Soc.* **1981**, *103*, 2869–2871.
(31) Friant, P.; Goulon, J.; Fischer, J.; Ricard, L.; Schappacher, M.; Weiss, R.; Momenteau, M. *Nouv. J. Chim.* **1985**, *9*, 33–40.

(32) Valentine, J. S.; McCandish, E. In *Frontiers of Biological Energetics: Electrons to Tissues*; Dutton, P. L., Leigh, J. S., Scarpa, A., Eds.; Academic: New York, 1978; Vol. 2, pp 933–939.
(33) Burstyn, J. N.; Roe, J. A.; Miksztal, A. R.; Shaevitz, B. A.; Lang, G.; Valentine, J. S. *J. Am. Chem. Soc.* **1988**, *110*, 1382–1388.
(34) Shirazi, A.; Goff, H. M. *J. Am. Chem. Soc.* **1982**, *104*, 6318–6322.
(35) Nakamoto, K.; Watanabe, T.; Ama, T.; Urban, M. W. *J. Am. Chem. Soc.* **1982**, *104*, 3744–3745.
(36) Latos-Grazynski, L.; Cheng, R.-J.; La Mar, G. N.; Balch, A. L. *J. Am. Chem. Soc.* **1982**, *104*, 5992–6000.
(37) Chin, D. H.; Del Gaudio, J.; La Mar, G. N.; Balch, A. L. *J. Am. Chem. Soc.* **1977**, *99*, 5486–5488.
(38) Simonneaux, G.; Scholz, W. F.; Reed, C. A.; Lang, G. *Biochim. Biophys. Acta* **1982**, *714*, 1–7.
(39) Pauling, L.; Coryell, C. D. *Proc. Natl. Acad. Sci. U.S.A.* **1936**, *22*, 210–216.
(40) Griffith, J. S. *Proc. R. Soc. Ser. A.* **1956**, *235*, 23–36.
(41) Gray, H. B. *Adv. Chem. Ser.* **1971**, *100*, 365–389.
(42) Pauling, L. *Nature* **1964**, *203*, 182–183.
(43) Weiss, J. J. *Nature* **1964**, *202*, 83–84; *203*, 183.
(44) Wittenberg, J. B.; Wittenberg, B. A.; Peisach, J.; Blumberg, W. E. *Proc. Natl. Acad. Sci. U.S.A.* **1970**, *67*, 1846–1851.
(45) Collman, J. P.; Gagne, R. R.; Reed, C. A.; Robinson, W. T.; Rodley, C. A. *Proc. Natl. Acad. Sci. U.S.A.* **1974**, *71*, 1326–1329.
(46) Phillips, S. E. V. *Nature (London)* **1978**, *273*, 247–248.
(47) Dedieu, A.; Rohmer, M. M.; Veillard, A. *Adv. Quantum. Chem.* **1982**, *16*, 43–95.
(48) Gubelman, M. H.; Williams, A. F. *Struct. Bonding* **1983**, *55*, 1–27.
(49) Rohmer, M. M. In *Quantum Chemistry*; Veillard, A., Ed.; 1986; pp 377–390.
(50) Otsuka, J.; Seno, Y. In *Hemoglobin and Oxygen binding*; Ho, C., Ed.; Elsevier: Amsterdam, 1982; pp 69–73.
(51) Newton, J. E.; Hall, M. B. *Inorg. Chem.* **1984**, *23*, 4627–4632.
(52) Yamamato, S.; Kashiwagi, H. *Chem. Phys. Lett.* **1989**, *161*, 85–89.
(53) Cerdonio, M.; Congiu-Castellano, A.; Mogno, F.; Pispisa, B.; Romani, G. L.; Vitale, S. *Proc. Natl. Acad. Sci. U.S.A.* **1977**, *74*, 398–400.
(54) Cerdonio, M.; Congiu-Castellano, A.; Calabrese, L.; Morante, S.; Pispisa, B.; Vitale, S. *Proc. Natl. Acad. Sci. U.S.A.* **1978**, *75*, 4916–4919.
(55) Pauling, L. *Proc. Natl. Acad. Sci. U.S.A.* **1977**, *74*, 2612–2613.
(56) Savicki, J. P.; Lang, G.; Ikeda-Saito, M. *Proc. Natl. Acad. Sci. U.S.A.* **1984**, *81*, 5417–5419.
(57) Fermi, G. *J. Mol. Biol.* **1975**, *97*, 237–256.
(58) Phillips, S. E. V. *J. Mol. Biol.* **1980**, *142*, 531–554.
(59) Shaanan, B. *Nature* **1982**, *296*, 683–684.
(60) Phillips, S. E. V.; Shoenborn, B. P. *Nature* **1981**, *292*, 81–82.
(61) Heidner, E. J.; Ledner, R. C.; Perutz, M. F. *J. Mol. Biol.* **1976**, *104*, 707–722.
(62) Perutz, M. F. *Nature* **1970**, *228*, 726–739.
(63) Perutz, M. F.; Fermi, G.; Luisi, B.; Shaanan, B.; Liddington, R. C. *Acc. Chem. Res.* **1987**, *20*, 309–321.
(64) Monod, J.; Wyman, J.; Changeux, J. P. *J. Mol. Biol.* **1965**, *12*, 88–118.
(65) Baldwin, J. M.; Chothia, C. *J. Mol. Biol.* **1979**, *129*, 175–220.
(66) Chou, K. C. *Biophys. Chem.* **1984**, *20*, 61–66.
(67) Brzozowski, A.; Devewenda, Z.; Dodson, E.; Dodson, G.; Grabowski, M.; Liddington, R.; Skarzynski, T.; Vallely, D. *Nature* **1984**, *307*, 74–76.
(68) Williams, R. J. P. *Fed. Proc.* **1961**, *20*, 5–10.
(69) Hoard, J. L. *Science* **1971**, *174*, 1295–1302.
(70) Cohen, I. A.; Caughey, W. S. *Biochemistry* **1946**, *7*, 636.
(71) Perutz, M. F. *Br. Med. Bull.* **1976**, *32*, 195–208.
(72) Brault, D.; Rougée, M. *Biochemistry* **1974**, *13*, 4591–4597.
(73) Collman, J. P.; Reed, C. A. *J. Am. Chem. Soc.* **1973**, *95*, 2048–2049.
(74) Spartalian, K.; Lang, G.; Collman, J. P.; Gagne, R. R.; Reed, C. A. *J. Chem. Phys.* **1975**, *63*, 5375–5382.
(75) Jameson, G. B.; Molinaro, F.; Ibers, J. A.; Collman, J. P.; Brauman, J. I.; Rose, E.; Suslick, K. S. *J. Am. Chem. Soc.* **1980**, *102*, 3224–3237.
(76) Brault, D.; Rougée, M. *Biochem. Biophys. Res. Commun.* **1974**, *57*, 654–659.
(77) Brault, D. Thesis, Université de Paris XI Orsay, 1976.
(78) Hoard, J. L. In *Porphyrins and Metalloporphyrins*; Smith, K. M., Ed.; Elsevier: Amsterdam, 1985; pp 317–380.
(79) Takano, T. *J. Mol. Biol.* **1977**, *110*, 569–584.
(80) Fermi, G.; Perutz, M. F.; Shaanan, B.; Fourme, R. *J. Mol. Biol.* **1984**, *175*, 159.
(81) Momenteau, M.; Scheidt, W. R.; Eigenbrot, C. W.; Reed, C. A. *J. Am. Chem. Soc.* **1988**, *110*, 1207–1215.
(82) Tuppy, M.; Bodo, G. *Monatsh. Chem.* **1954**, *85*, 1024–1045.
(83) Tuppy, M.; Paleus, S. *Acta Chem. Scand.* **1955**, *9*, 353–364.
(84) Sano, S.; Nanzyo, N.; Rimington, C. *Biochem. J.* **1964**, *93*, 270–280.
(85) Sano, S.; Ikeda, K.; Sakakibara, S. *Biochem. Biophys. Res. Commun.* **1964**, *15*, 284–289.
(86) Theodoropoulos, D.; Souchleris, I. *J. Org. Chem.* **1966**, *31*, 4009–4013.
(87) Momenteau, M.; Loock, B. *Biochim. Biophys. Acta* **1974**, *343*, 535–545.
(88) Chang, C. K.; Traylor, T. G. *Proc. Natl. Acad. Sci. U.S.A.* **1973**, *70*, 2647–2650.
(89) Van der Heijden, A.; Peer, H. G.; Van den Oord, A. H. A. *J. Chem. Soc., Chem. Commun.* **1971**, 369–371.
(90) Warme, P. K.; Hager, L. P. *Biochemistry* **1970**, *9*, 1599–1605.
(91) Warme, P. K.; Hager, L. P. *Biochemistry* **1970**, *9*, 1606–1614.
(92) Momenteau, M.; Rougée, M.; Loock, B. *Eur. J. Biochem.* **1976**, *71*, 63–76.
(93) Momenteau, M.; Loock, B.; Bisagni, E.; Rougée, M. *Can. J. Chem.* **1979**, *57*, 1804–1813.
(94) Momenteau, M.; Loock, B. *J. Mol. Catal.* **1980**, *7*, 315–320.
(95) Collman, J. P.; Brauman, J. I.; Doxsee, K. M.; Halbert, T. R.; Bunnenberg, E.; Linder, R. E.; La Mar, G. N.; Del Gaudio, J.; Lang, G.; Spartalian, K. *J. Am. Chem. Soc.* **1980**, *102*, 4182–4192.
(96) Mashiko, T.; Reed, C. A.; Haller, K. J.; Kastner, M. E.; Scheidt, W. R. *J. Am. Chem. Soc.* **1981**, *103*, 5758–5767.
(97) Walker, F. A. *J. Am. Chem. Soc.* **1980**, *102*, 3254–3256.
(98) Molinaro, F. S.; Little, R. G.; Ibers, J. A. *J. Am. Chem. Soc.* **1977**, *99*, 5628–5632.
(99) Young, R.; Chang, C. K. *J. Am. Chem. Soc.* **1985**, *107*, 898–909.
(100) Traylor, T. G.; Koga, N.; Deardurff, L. A. *J. Am. Chem. Soc.* **1985**, *107*, 6504–6510.
(101) Collman, J. P.; Brauman, J. I.; Doxsee, K. M.; Halbert, T. R.; Suslick, K. S. *Proc. Natl. Acad. Sci. U.S.A.* **1978**, *75*, 564–568.
(102) Geibel, J.; Cannon, J.; Campbell, D. H.; Traylor, T. G. *J. Am. Chem. Soc.* **1978**, *100*, 3575–3585.
(103) Collman, J. P.; Gagne, R. R.; Reed, C. A.; Halbert, T. R.; Lang, G.; Robinson, W. T. *J. Am. Chem. Soc.* **1975**, *97*, 1427–1439.
(104) Imai, H.; Sekizawa, S.; Kyuno, E. *Inorg. Chim. Acta* **1986**, *125*, 151–158.
(105) Imai, H.; Nakagawa, S.; Kyuno, E. *Inorg. Chim. Acta* **1992**, *193*, 105–109.
(106) Wuenschell, G. E.; Tétreau, C.; Lavalette, D.; Reed, C. A. *J. Am. Chem. Soc.* **1992**, *114*, 3346–3355.
(107) Collman, J. P.; Brauman, J. I.; Collins, T. J.; Iverson, B. L.; Lang, G.; Pettman, R. B.; Sessler, J.-L.; Walters, M. A. *J. Am. Chem. Soc.* **1983**, *105*, 3038–3052.
(108) Diekmann, H.; Chang, C. K.; Traylor, T. G. *J. Am. Chem. Soc.* **1971**, *93*, 4068–4070.
(109) Traylor, T. G.; Campbell, D.; Tsuchiya, S. *J. Am. Chem. Soc.* **1979**, *101*, 4748–4749.
(110) Ogoshi, H.; Sugimoto, H.; Yoshida, Z. *Tetrahedron Lett.* **1976**, *49*, 4477–4480.
(111) Traylor, T. G.; Koga, N.; Deardurff, L. A.; Swepston, P. N.; Ibers, J. A. *J. Am. Chem. Soc.* **1984**, *106*, 5132–5143.
(112) Collman, J. P.; Elliot, C. M.; Halbert, T. R.; Tovrog, B. S. *Proc. Natl. Acad. Sci. U.S.A.* **1977**, *74*, 18–22.
(113) Ward, B.; Wang, C.; Chang, C. K. *J. Am. Chem. Soc.* **1981**, *103*, 5236–5238.
(114) Battersby, A. R.; Buckley, D. G.; Hartley, S. G.; Turnbull, M. D. *J. Chem. Soc., Chem. Commun.* **1976**, 879–881.
(115) Chang, C. K. *J. Am. Chem. Soc.* **1977**, *99*, 2819–2822.
(116) Almog, J.; Baldwin, J. E.; Dyer, R. L.; Peters, M. *J. Am. Chem. Soc.* **1975**, *97*, 226–227.
(117) Almog, J.; Baldwin, J. E.; Huff, J. R. *J. Am. Chem. Soc.* **1975**, *97*, 227–228.
(118) Almog, J.; Baldwin, J. E.; Crossley, M. J.; Debernardis, J. F.; Dyer, R. L.; Huff, J. R.; Peters, M. K. *Tetrahedron* **1981**, *37*, 3589–3602.
(119) Ogoshi, H.; Sugimoto, M.; Yoshida, Z. *Tetrahedron Lett.* **1976**, *49*, 4481–4484.
(120) Ogoshi, H.; Sugimoto, M.; Miyake, M.; Yoshida, Z. *Tetrahedron* **1984**, *40*, 579–592.
(121) Baldwin, J. E.; Klose, T.; Peters, M. *J. Chem. Soc., Chem. Commun.* **1976**, 881–883.
(122) Baldwin, J. E.; Crossley, M. J.; Klose, T.; O'Rear, E. A.; Peters, K. M. *Tetrahedron* **1982**, *38*, 27–39.
(123) Baldwin, J. E.; Crossley, M. J.; Debernardis, J. *Tetrahedron* **1982**, *38*, 685–692.
(124) Wijesekera, T. P.; Paine, J. B., III; Dolphin, D. *J. Org. Chem.* **1988**, *53*, 1345–1352.
(125) El-Kasmi, D.; Tétreau, C.; Lavalette, D.; Momenteau, M. *J. Chem. Soc., Perkin Trans. 2* **1993**, 1799–1803.
(126) Uemori, Y.; Kyuno, E. *Inorg. Chim. Acta* **1987**, *138*, 9–10.
(127) Momenteau, M.; Loock, B.; Tétreau, C.; Lavalette, D.; Croisy, A.; Schaeffer, C.; Huel, C.; Lhoste, J.-M. *J. Chem. Soc., Perkin Trans. 2* **1987**, 249–257.
(128) Collman, J. P.; Brauman, J. I.; Fitzgerald, J. P.; Hampton, P. D.; Naruta, Y.; Sparapany, J. W.; Ibers, J. A. *J. Am. Chem. Soc.* **1988**, *110*, 3477–3486.
(129) Uemori, Y.; Kyuno, E. *Inorg. Chim. Acta* **1986**, *125*, L45–L46.
(130) Uemori, Y.; Miyakawa, H.; Kyuno, E. *Inorg. Chem.* **1988**, *27*, 377–382.
(131) Tétreau, C.; Léondiadis, L.; Lavalette, D.; Momenteau, M. *J. Chem. Soc., Perkin Trans. 2* **1992**, 73–77.
(132) Ellis, P. E.; Linard, J. E.; Szymanski, T.; Jones, R. D.; Budge, J. R.; Basolo, F. *J. Am. Chem. Soc.* **1980**, *102*, 1889–1896.
(133) Shriver, D. F.; Atkins, P. W.; Langford, C. H. *Inorganic Chemistry*; Freeman: New York, 1990; p 613.
(134) Jameson, G. B.; Ibers, J. A. *J. Am. Chem. Soc.* **1980**, *102*, 2823–2831.
(135) Sabat, M.; Ibers, J. A. *J. Am. Chem. Soc.* **1982**, *104*, 3715–3721.
(136) Spiro, T. G.; Burke, J. M. *J. Am. Chem. Soc.* **1976**, *98*, 5482–5489.

(137) Desbois, A.; Momenteau, M.; Lutz, M. *Inorg. Chem.* **1989**, *28*, 825–834.
(138) Perutz, M. F. *Ann. Rev. Biochem.* **1979**, *48*, 327–386.
(139) Perutz, M. F.; Hasnain, S. S.; Duke, P. J.; Sessler, J. L.; Hahn, J. E. *Nature (London)* **1982**, *295*, 535–538.
(140) Battersby, A. R.; Hartley, S. G.; Turnbull, M. D. *Tetrahedron Lett.* **1978**, 3169–3172.
(141) Battersby, A. R.; Hamilton, A. D. *J. Chem. Soc., Chem. Commun.* **1980**, 117–119.
(142) Battersby, A. R.; Bartholomew, S. A. J.; Nitta, J. *J. Chem. Soc., Chem. Commun.* **1983**, 1291–1293.
(143) Momenteau, M.; Loock, B.; Lavalette, D.; Tétreau, C.; Mispelter, J. *J. Chem. Soc., Chem. Commun.* **1983**, 962–964.
(144) Momenteau, M.; Mispelter, J.; Loock, B.; Lhoste, J.-M. *J. Chem. Soc., Perkin Trans. 1* **1985**, 61–70.
(145) Momenteau, M.; Mispelter, J.; Loock, B.; Lhoste, J.-M. *J. Chem. Soc., Perkin Trans. 1* **1985**, 221–231.
(146) Maillard, P.; Schaeffer, C.; Huel, C.; Lhoste, J.-M.; Momenteau, M. *J. Chem. Soc., Perkin Trans. 1* **1988**, 3285–3296.
(147) Meunier, B.; De Carvalho, M. E.; Bartolini, O.; Momenteau, M. *Inorg. Chem.* **1988**, *27*, 161–164.
(148) Orth, U.; Pfeiffer, H. P.; Breitmaier, E. *Chem. Ber.* **1986**, *119*, 3507–3514.
(149) Baldwin, J. E.; Cameron, J. H.; Crossley, M. J.; Dagley, E. J. *J. Chem. Soc., Dalton Trans.* **1984**, 1739–1746.
(150) Boitrel, B.; Lecas, A.; Rose, E. *Tetrahedron Lett.* **1988**, *29*, 5653–5656.
(151) Boitrel, B.; Lecas, A.; Renko, Z.; Rose, E. *New J. Chem.* **1989**, *13*, 73–99.
(152) Mispelter, J.; Momenteau, M.; Lhoste, J.-M. *Biochimie* **1981**, *63*, 911–914.
(153) Alben, J. O.; Fuchsman, W. H.; Beaudreau, C. A.; Caughey, W. S. *Biochemistry* **1968**, *7*, 624–635.
(154) Cohen, I. A.; Caughey, W. S. *Biochemistry* **1968**, *7*, 636–641.
(155) Sadasivan, N.; Eberspaecher, H. I.; Fuchsman, W. H.; Caughey, W. S. *Biochemistry* **1969**, *8*, 534–541.
(156) Cohen, I. A.; Caughey, W. S. In *Hemes and Hemoproteins*; Chance, B., Estabrook, R. W., Yonetani, T., Eds.; Academic Press: New York, 1966; pp 577–592.
(157) Weschler, C. J.; Anderson, D. L.; Basolo, F. *J. Am. Chem. Soc.* **1975**, *97*, 6707–6713.
(158) Hammond, G. S.; Wu, C. S. *Adv. Chem. Ser.* **1968**, *77*, 186–191.
(159) Mincey, T.; Traylor, T. G. *J. Am. Chem. Soc.* **1979**, *101*, 765–766.
(160) Balch, A. L.; Chan, Y. W.; Cheng, R. J.; La Mar, G. N.; Latos-Grazynski, L.; Renner, M. W. *J. Am. Chem. Soc.* **1984**, *106*, 7779–7785.
(161) Wallace, W. J.; Houtchens, R. A.; Maxwell, J. C.; Caughey, W. S. *J. Biol. Chem.* **1982**, *257*, 4966–4977.
(162) Misra, H. P.; Fridovich, I. *J. Biol. Chem.* **1972**, *247*, 6960–6962.
(163) Brantley, R. E.; Smerdon, S. J.; Wilkinson, A. J.; Singleton, E. W.; Olson, J. S. *J. Biol. Chem.* **1993**, *268*, 6995–7010.
(164) Dickerson, R. E.; Geis, I. In *Hemoglobin: Structure, Function, Evolution and Pathology*; Benjamin/Cummings: Menlo Park, 1983.
(165) Stanbury, D. M.; Haas, O.; Taube, H. *Inorg. Chem.* **1980**, *19*, 518–524.
(166) Dickerson, L. D.; Sauer-Masarwa, A.; Herron, N.; Fendrick, C. M.; Busch, D. H. *J. Am. Chem. Soc.* **1993**, *115*, 3623–3626.
(167) Sauer-Masarwa, A.; Herron, N.; Fendrick, C. M.; Busch, D. H. *Inorg. Chem.* **1993**, *32*, 1086–1094.
(168) Chu, M. M. L.; Castro, C. E.; Hathaway, G. M. *Biochemistry* **1978**, *17*, 481–486.
(169) Lavalette, D.; Tétreau, C.; Mispelter, M.; Momenteau, M.; Lhoste, J.-M. *Eur. J. Biochem.* **1984**, *145*, 555–565.
(170) Momenteau, M.; Loock, B.; Mispelter, J.; Bisagni, E. *Nouv. J. Chim.* **1979**, *3*, 77–79.
(171) Lexa, D.; Momenteau, M.; Savéant, J. M.; Xu, F. *Inorg. Chem.* **1985**, *24*, 122–127.
(172) Gerothanassis, I. P.; Momenteau, M.; Loock, B. *J. Am. Chem. Soc.* **1989**, *111*, 7006–7012.
(173) Mizutani, Y.; Hashimoto, S.; Tatsumo, Y.; Kitagawa, T. *J. Am. Chem. Soc.* **1990**, *112*, 6809–6814.
(174) Wang, J. H. *J. Am. Chem. Soc.* **1958**, *80*, 3168–3169.
(175) Chang, C. K.; Traylor, T. G. *J. Am. Chem. Soc.* **1973**, *95*, 8477–8479.
(176) Burwell, R. L.; Leal, O. *J. Chem. Soc., Chem. Commun.* **1974**, 342–343.
(177) Leal, O.; Anderson, D. L.; Bowman, R. G.; Basolo, F.; Burwell, R. L. *J. Am. Chem. Soc.* **1975**, *97*, 5125–5129.
(178) Tsuchida, E.; Honda, K.; Sata, H. *Inorg. Chem.* **1976**, *15*, 352–357.
(179) Fuhrhop, J. H.; Besecke, S.; Vogt, W.; Ernst, J.; Subramanian, J. *Makromol. Chem.* **1977**, *178*, 1621–1631.
(180) Tsuchida, E.; Honda, K.; Hasegawa, E. *Biochem. Biophys. Acta* **1975**, *393*, 483–495.
(181) Tsuchida, E.; Hasegawa, E.; Honda, K. *Biochem. Biophys. Acta* **1976**, *427*, 520–529.
(182) Tsuchida, E.; Hasegawa, E.; Kanayama, T. *Macromolecules* **1978**, *11*, 947–955.
(183) Bayer, E.; Holzbach, G. *Angew. Chem., Int. Ed. Engl.* **1977**, *16*, 117–118.
(184) Tsuchida, E. *Ann. N. Y. Acad. Sci.* **1985**, *446*, 429–442.
(185) Chang, C. K.; Traylor, T. G. *J. Am. Chem. Soc.* **1973**, *95*, 5810–5811.
(186) Mispelter, J.; Momenteau, M.; Lavalette, D.; Lhoste, J.-M. *J. Am. Chem. Soc.* **1983**, *105*, 5165–5166.
(187) Anderson, D. L.; Werchler, D. J.; Basolo, F. *J. Am. Chem. Soc.* **1974**, *96*, 5599–5600.
(188) Wagner, G. C.; Kassner, R. J. *J. Am. Chem. Soc.* **1974**, *96*, 5593–5595.
(189) Brinigar, W. S.; Chang, C. K. *J. Am. Chem. Soc.* **1974**, *96*, 5595–5597.
(190) Brinigar, W. S.; Chang, C. K.; Geibel, J.; Traylor, T. G. *J. Am. Chem. Soc.* **1974**, *96*, 5597–5599.
(191) Almog, J.; Baldwin, J. E.; Dyer, R. L.; Huff, J.; Wilkerson, C. J. *J. Am. Chem. Soc.* **1974**, *96*, 5600–5601.
(192) Collman, J. P.; Gagne, R. R.; Halbert, T. R.; Marchon, J. C.; Reed, C. A. *J. Am. Chem. Soc.* **1973**, *95*, 7868–7870.
(193) Collman, J. P.; Brauman, J. I.; Doxsee, K. M.; Sessler, J. L.; Morris, R. M.; Gibson, O. H. *Inorg. Chem.* **1983**, *22*, 1427–1432.
(194) Traylor, T. G.; Koga, N.; Dearduff, L. A.; Swepston, P. N.; Ibers, J. A. *J. Am. Chem. Soc.* **1984**, *106*, 5132–5143.
(195) Collman, J. P.; Brauman, J. I.; Collins, T. J.; Iverson, B.; Sessler, J. L. *J. Am. Chem. Soc.* **1981**, *103*, 2450–2452.
(196) Dolphin, D.; Hiom, J.; Paine, J. B. *Heterocycles* **1981**, *16*, 417–447.
(197) Uemori, Y.; Nakatsubo, A.; Imai, H.; Nakagawa, S.; Kyuno, E. *Inorg. Chim. Acta* **1986**, *125*, 153–160.
(198) Amundsen, A. R.; Vaska, L. *Inorg. Chim. Acta* **1975**, *14*, 249–256.
(199) Cense, J. M.; Le Quan, R. M. *Tetrahedron Lett.* **1979**, 3725–3728.
(200) Suslick, K. S.; Fox, M. M. *J. Am. Chem. Soc.* **1983**, *105*, 3507–3510.
(201) Komatsu, T.; Hasegawa, E.; Kumamoto, S.; Nishide, H.; Tsuchida, E. *J. Chem. Soc., Dalton Trans.* **1991**, 3281–3284.
(202) Komatsu, T.; Arai, K.; Nishide, H.; Tsuchida, E. *Chem. Lett.* **1992**, 799–802.
(203) Momenteau, M.; Loock, B.; Mispelter, J.; Bisagni, E. *J. Chem. Soc., Perkin Trans. 1* **1983**, 189–196.
(204) Lecas, A.; Boitrel, B.; Rose, E. *Bull. Soc. Chim. Fr.* **1991**, *128*, 407–413.
(205) Simonis, U.; Walker, F. A.; Lee, P. L.; Hanquet, B. J.; Meyerhoff, D. J.; Scheidt, W. R. *J. Am. Chem. Soc.* **1987**, *109*, 2659–2668.
(206) Mansuy, D.; Battioni, P.; Renaud, J.-P.; Guerin, P. *J. Chem. Soc., Chem. Commun.* **1985**, 155–156.
(207) Reddy, D.; Chandrashekar, T. K. *J. Chem. Soc., Dalton Trans.* **1992**, 619–625.
(208) Maillard, P.; Schaeffer, C.; Tétreau, C.; Lavalette, D.; Lhoste, J.-M.; Momenteau, M. *J. Chem. Soc., Perkin Trans. 2* **1989**, 1437–1442.
(209) Wittenberg, J. B.; Appleby, C. A.; Wittenberg, B. A. *J. Biol. Chem.* **1972**, *247*, 527–531.
(210) Antonini, E.; Brunori, M. In *Hemoglobin and Myoglobin and their reactions with ligands*; Elsevier: New York, 1971.
(211) Noble, R. W.; Gibson, Q. H.; Brunori, M.; Antonini, E.; Wyman, J. *J. Biol. Chem.* **1969**, *244*, 3905–3908.
(212) Gibson, R. H. *J. Physiol.* **1956**, *134*, 123–129.
(213) Chang, C. K.; Traylor, T. G. *Proc. Natl. Acad. Sci. U.S.A.* **1975**, *72*, 1166–1170.
(214) White, D. K.; Cannon, J. B.; Traylor, T. G. *J. Am. Chem. Soc.* **1979**, *101*, 2443–2454.
(215) Lavalette, D.; Tétreau, C.; Momenteau, M. *J. Am. Chem. Soc.* **1979**, *101*, 5395–5401.
(216) Momenteau, M.; Lavalette, D. *J. Am. Chem. Soc.* **1978**, *100*, 4322–4324.
(217) Lavalette, D.; Momenteau, M. *J. Chem. Soc., Perkin Trans. 2* **1982**, 385–388.
(218) Lavalette, D.; Tétreau, C.; Momenteau, M.; Mispelter, J.; Lhoste, J.-M.; Wuenschell, G. E.; Reed, C. *Laser Chem.* **1990**, *10*, 297–318.
(219) Tétreau, C.; Boitrel, B.; Rose, E.; Lavalette, D. *J. Chem. Soc., Chem. Commun.* **1989**, 1805–1806.
(220) Linke, W.; Seidell, A. In *Solubilities of Inorganic and Metallorganic Compounds*; Van Nostrand: Princeton, 1958; p 1236.
(221) Collman, J.-P.; Brauman, J. I.; Iverson, B. L.; Sessler, J.-L.; Morris, R. M.; Gibson, Q. M. *J. Am. Chem. Soc.* **1983**, *105*, 3052–3064.
(222) Traylor, T. G.; Traylor, P. S. *Ann. Rev. Biophys. Bioeng.* **1982**, *1*, 105–127.
(223) Brinigar, W. S.; Chang, C. K.; Geibel, J.; Traylor, T. G. *J. Am. Chem. Soc.* **1974**, *96*, 5597–5599.
(224) Traylor, T. G. *Acc. Chem. Res.* **1981**, *14*, 102–109.
(225) Sharma, V. S.; Geibel, J. F.; Ranney, H. M. *Proc. Natl. Acad. Sci. U.S.A.* **1978**, *75*, 3747–3750.
(226) Walker, F. A.; Lo, M. W.; Ree, M. T. *J. Am. Chem. Soc.* **1976**, *98*, 5552–5560.
(227) Doeff, M. M.; Sweigert, D. A. *Inorg. Chem.* **1982**, *21*, 3699–3705.
(228) Doeff, M. M.; Sweigart, D. A.; O'Brien, P. *Inorg. Chem.* **1983**, *22*, 851–852.
(229) Tondreau, G. A.; Sweigart, D. A. *Inorg. Chem.* **1984**, *23*, 1060–1065.
(230) Perutz, M. F.; Ladner, J. E.; Simon, S. R.; Ho, C. *Biochemistry* **1974**, *13*, 2163–2173.
(231) Perutz, M. F.; Fersht, A. R.; Simon, S. R.; Roberts, G. C. K. *Biochemistry* **1974**, *13*, 2174–2186.
(232) Traylor, T. D.; Popovitz-Biro, R. *J. Am. Chem. Soc.* **1988**, *110*, 239–243.
(233) Landrum, J. T.; Grimmett, D.; Haller, K. J.; Scheidt, W. R.; Reed, C. A. *J. Am. Chem. Soc.* **1981**, *103*, 2640–2650.

(234) Baldwin, J. M. *J. Mol. Biol.* **1980**, *136*, 103–128.
(235) Hanson, J. C.; Schoenborn, B. P. *J. Mol. Biol.* **1981**, *153*, 117–146.
(236) Peng, S. M.; Ibers, J. A. *J. Am. Chem. Soc.* **1976**, *98*, 8032–8036.
(237) Ricard, L.; Weiss, R.; Momenteau, M. *J. Chem. Soc., Chem. Commun.* **1986**, 818–820.
(238) Ascone, I.; Bianconi, A.; Dartyge, E.; Della Longa, S.; Fontaine, A.; Momenteau, M. *Biochem. Biophys. Acta* **1987**, *915*, 168–171.
(239) Collman, J. P.; Brauman, J. I.; Halbert, T. R.; Suslick, K. S. *Proc. Natl. Acad. Sci. U.S.A.* **1976**, *73*, 3333–3337.
(240) Tucker, P. W.; Philipps, S. E. V.; Perutz, M. F.; Houtchens, R.; Caughey, W. S. *Proc. Natl. Acad. Sci. U.S.A.* **1978**, *75*, 1076–1080.
(241) Hashimoto, T.; Dyer, R. L.; Crossley, M. L.; Baldwin, J. E.; Basolo, F. *J. Am. Chem. Soc.* **1982**, *104*, 2101–2109.
(242) Johnson, M. R.; Seok, W. K.; Ibers, J. A. *J. Am. Chem. Soc.* **1991**, *113*, 3998–4000.
(243) Collman, J. P.; Brauman, J. I.; Doxsee, K. M. *Proc. Natl. Acad. Sci. U.S.A.* **1979**, *76*, 6035–6039.
(244) Budge, J. R.; Ellis, P. E.; Jones, R. D.; Linard, J. E.; Basolo, F. *J. Am. Chem. Soc.* **1979**, *101*, 4760–4762.
(245) Budge, J. R.; Ellis, P. E.; Jones, R. D.; Linard, J. E.; Szymanski, T.; Basolo, F. *J. Am. Chem. Soc.* **1979**, *101*, 4762–4763.
(246) Linard, J. E.; Ellis, P. E.; Budge, J. R.; Jones, R. D.; Basolo, F. *J. Am. Chem. Soc.* **1980**, *102*, 1896–1904.
(247) Traylor, T. G.; Campbell, D.; Tsuchiya, S.; Mitchell, M.; Stynes, D. V. *J. Am. Chem. Soc.* **1980**, *102*, 5939–5941.
(248) Traylor, T. G.; Mitchell, M.; Tsuchiya, S.; Campbell, D. H.; Stynes, D. V.; Koga, N. *J. Am. Chem. Soc.* **1981**, *103*, 5234–5236.
(249) Ricard, L.; Fischer, J.; Weiss, R.; Momenteau, M. *Nouv. J. Chim.* **1984**, *8*, 639–642.
(250) Uemori, Y.; Kyuno, E. *Inorg. Chem. Acta* **1989**, *165*, 115–122.
(251) Moffat, K.; Deatherage, J. F.; Seybert, D. W. *Science (Washington DC)* **1979**, *206*, 1035–1042.
(252) Stynes, H. C.; Ibers, J. A. *J. Am. Chem. Soc.* **1972**, *94*, 5125–5127.
(253) Traylor, T. G.; Berzinis, A. *Proc. Natl. Acad. Sci. U.S.A.* **1980**, *77*, 3171–3175.
(254) Sharma, V. S.; Ranney, H. M.; Geibel, J. F.; Traylor, T. G. *Biochem. Biophys. Res. Commun.* **1975**, *66*, 1301–1306.
(255) Traylor, T. G.; Tsuchiya, S.; Campbell, D. H.; Mitchell, M.; Stynes, D. V.; Koga, N. *J. Am. Chem. Soc.* **1985**, *107*, 604–614.
(256) Jameson, G. B.; Rodley, G. A.; Robinson, W. T.; Gagne, R. R.; Reed, C. A.; Collman, J. P. *Inorg. Chem.* **1978**, *17*, 850–857.
(257) Jameson, G. B.; Drago, R. S. *J. Am. Chem. Soc.* **1985**, *107*, 3017–3020.
(258) Yonetani, T.; Yamamoto, H.; Itizuka, T. *J. Biol. Chem.* **1974**, *249*, 2168–2174.
(259) Momenteau, M.; Lavalette, D. *J. Chem. Soc., Chem. Commun.* **1982**, 341–343.
(260) Ho, C. *Advances in Protein Chemistry*; Academic Press: New York, 1992; Vol. 43, pp 153–311.
(261) Wüthrich, K. *NMR of Proteins and Nucleic Acids*; Wiley Intersciences: John Wiley and Sons: New York, 1986.
(262) Mabbutt, B. C.; Wright, P. E. *Biochim. Biophys. Acta* **1983**, *744*, 281–290.
(263) Schaeffer, C.; Craescu, C. T.; Mispelter, J.; Garel, M. C.; Rosa, J.; Lhoste, J. M. *Eur. J. Biochem.* **1988**, *173*, 317–325.
(264) Chang, C. K.; Ward, B.; Young, R.; Kondylis, M. P. *J. Macromol. Sci. Chem.* **1988**, *A25*, 1307–1326.
(265) Collman, J. P. Personal communication; Collman, J. P.; Zhang, X.; Wong, K.; Brauman, J. I. *J. Am. Chem. Soc.*, in press.
(266) Springer, B. A.; Egeberg, K.; Sligar, S. C.; Rohlfs, R. J.; Mathews, A. J.; Olson, J. S. *J. Biol. Chem.* **1989**, *264*, 3057–3060.
(267) Nagai, K.; Luisi, B.; Shih, D.; Niyazaki, G.; Imai, K.; Poyart, C.; De Young, A.; Kwiatkowsky, L.; Noble, R.; Lin, S. M.; Yu, N. T. *Nature (London)* **1987**, *329*, 858–860.
(268) Olson, J. S.; Mathews, A. J.; Rohlfs, R. J.; Springer, B. A.; Egeberg, K. D.; Sligar, S. G.; Tame, J.; Renaud, J.-P.; Nagai, K. *Nature (London)* **1988**, *336*, 265–266.
(269) Appleby, C. E.; Blumberg, W. E.; Bradbury, J. H.; Fuchsman, W. H.; Peisach, J.; Wittenberg, B. A.; Wittenberg, J. B.; Wright, P. E. In *Hemoglobin and Oxygen Binding*; Ho, C., Ed.; Elsevier North Holland: Amsterdam, 1982; pp 435–441.
(270) Appleby, C. E. Personal communication; *Science Progress*, in press.
(271) Carver, T. E.; Brantley, R. E.; Singleton, E. W.; Arduini, R. M.; Quillin, M. L.; Phillips, G. N.; Olson, J. S. *J. Biol. Chem.* **1992**, *267*, 14443–14450.
(272) Szabo, A. *Proc. Natl. Acad. Sci. U.S.A.* **1978**, *75*, 2108–2111.
(273) Moffat, K.; Korszun, Z. R. In *Hemoglobin and Oxygen Binding*; Chien, H., Ed.; Elsevier North Holland: Amsterdam, 1982; pp 137–140.
(274) Traylor, T. G.; Campbell, D. M.; Tsuchiya, S.; Stynes, D. V.; Mitchell, M. J. In *Hemoglobin and Oxygen Binding*; Chien, H., Ed.; Elsevier North Holland: Amsterdam, 1982; pp 425–433.
(275) Austin, R. H.; Beeson, K. W.; Eisenstein, L.; Frauenfelder, M.; Gunsalus, I. C. *Biochemistry* **1975**, *14*, 5355–5373.
(276) Alberding, N.; Austin, R. H.; Chan, S. S.; Eisenstein, L.; Frauenfelder, M.; Gunsalus, I. C.; Nordland, T. M. *J. Chem. Phys.* **1976**, 4701–4711.
(277) Alberding, N.; Chan, S. S.; Eiseinstein, L.; Frauenfelder, M.; Good, D.; Gunsalus, I. C.; Nordlund, T. M.; Perutz, M. F.; Reynolds, A. H.; Sorensen, L. B. *Biochemistry* **1978**, *17*, 43–51.
(278) Beece, D.; Eiseinstein, L.; Frauenfelder, M.; Good, D.; Morden, M. C.; Reinish, L.; Reynolds, A. H.; Sorensen, L. B.; Yue, K. T. *Biochemistry* **1980**, *23*, 5147–5157.
(279) Doster, W.; Beece, D.; Boisne, S. F.; Di Iorio, E. E.; Eisenstein, L.; Frauenfelder, H.; Reinish, L.; Shyamsunder, E.; Winterhalter, K. H.; Yue, K. T. *Biochemistry* **1982**, *21*, 4831–4839.
(280) Hasinoff, B. B.; Bano Chishti, S. *Biochemistry* **1982**, *21*, 4275–4278.
(281) Hasinoff, B. B.; Bano Chishti, S. *Biochemistry* **1983**, *22*, 58–61.
(282) Morris, R. J.; Gibson, Q. H. *J. Biol. Chem.* **1980**, *17*, 8050–8053.
(283) Tétreau, C.; Lavalette, D.; Momenteau, M.; Lhoste, J.-M. *Proc. Natl. Acad. Sci. U.S.A.* **1987**, *84*, 2267–2271.
(284) Tétreau, C.; Momenteau, M.; Lavalette, D. *Inorg. Chem.* **1990**, *29*, 1727–1731.
(285) Page, M. I.; Jencks, W. P. *Proc. Natl. Acad. Sci. U.S.A.* **1971**, *68*, 1678–1683.
(286) Frauenfelder, M.; Wolynes, P. G. *Science* **1985**, *229*, 337–345.
(287) Collman, J. P.; Brauman, J. I.; Rose, E.; Suslick, K. *Proc. Natl. Acad. Sci. U.S.A.* **1978**, *75*, 1052–1055.
(288) Tsuchida, E.; Honda, K. *Polym. J.* **1975**, *7*, 498–506.
(289) Tsuchida, E.; Hasegawa, E.; Honda, K. *Biochem. Biophys. Res. Commun.* **1975**, *67*, 864–869.
(290) Traylor, T. G.; Mitchell, M. J.; Ciccone, J. P.; Nelson, S. *J. Am. Chem. Soc.* **1982**, *104*, 4986–4989.
(291) Traylor, T. G.; Tatsumo, T.; Powell, D. W.; Cannon, J. B. *J. Chem. Soc., Chem. Commun.* **1977**, 732–734.
(292) Tabushi, I.; Sasaki, T. *J. Am. Chem. Soc.* **1983**, *105*, 2901–2902.
(293) Tabushi, I.; Kugimiya, S.; Kinnaird, M. G.; Sasaki, T. *J. Am. Chem. Soc.* **1985**, *107*, 4192–4199.
(294) Tabushi, I.; Kugimiya, S.; Sasaki, T. *J. Am. Chem. Soc.* **1985**, *107*, 5159–5163.
(295) Tabushi, I.; Sasaki, T. *Tetrahedron Lett.* **1982**, *23*, 1913–1916.
(296) Jameson, G. B.; Molinaro, F. S.; Ibers, J. A.; Collman, J. P.; Brauman, J. I.; Rose, E.; Suslick, K. S. *J. Am. Chem. Soc.* **1978**, *100*, 6769–6770.
(297) Weber, E.; Steigeman, W.; Jones, T. A.; Huber, R. *J. Mol. Biol.* **1978**, *120*, 327–336.
(298) Jameson, G. B.; Robinson, W. T.; Collman, J. P.; Sorrell, T. N. *Inorg. Chem.* **1978**, *17*, 858–864.
(299) Ricard, L.; Schappacher, M.; Weiss, R.; Montiel-Montoya, R.; Bill, E.; Gonser, U.; Trautwein, A. X. *Nouv. J. Chim.* **1983**, *7*, 405–408.
(300) Schappacher, M.; Ricard, L.; Fischer, J.; Weiss, R.; Bill, E.; Monteil-Montoya, R.; Winkler, H.; Trautwein, A. X. *Eur. J. Biochem.* **1987**, *168*, 419–429.
(301) Gouterman, M. In *The Porphyrins*; Dolphin, D., Ed.; Academic Press: New York, 1978; Vol. III, Part A, pp 1–165.
(302) Makinen, M. W.; Chung, A. K. In *Iron Porphyrins*; Lever, A. B. P., Gray, H. B., Eds.; Addison Wesley: Reading, MA, 1983; pp 141–235.
(303) Zerner, M.; Gouterman, M.; Kobayashi, H. *Theor. Chim. Acta* **1966**, *6*, 363–372.
(304) Perutz, M. F.; Ladner, J. E.; Simon, S. R.; Ho, C. *Biochemistry* **1974**, *13*, 2163–2171.
(305) Perutz, M. F.; Heidner, E. J.; Ladner, J. E.; Beetlestone, J. C.; Ho, C.; Slade, E. F. *Biochemistry* **1974**, *13*, 2187–2195.
(306) Cassoly, R. *Eur. J. Biochem.* **1976**, *65*, 461–464.
(307) Greene, B. I.; Hochstrasser, R. M.; Weisman, R. B.; Eaton, W. A. *Proc. Natl. Acad. Sci. U.S.A.* **1978**, *75*, 5255–5259.
(308) Eaton, W. A.; Hanson, L. K.; Stephens, P. J.; Sutherland, J. C.; Dunn, J. B. R. *J. Am. Chem. Soc.* **1978**, *100*, 4991–5003.
(309) Eaton, W. A.; Hofrichter, J.; Hanson, L. K.; Makinen, M. W. In *Metalloprotein Studies utilizing Paramagnetic Effect on the Metal Ions as Probes*; Kotani, M., Tasaki, A., Eds.; Osaka University: Osaka, Japan, 1975; pp 51–85.
(310) Makinen, M. W.; Eaton, W. A. *Ann. N.Y. Acad. Sci.* **1973**, *206*, 210–222.
(311) Churg, A. K.; Makinen, M. W. *J. Chem. Phys.* **1978**, *68*, 1913–1925.
(312) Makinen, M. W.; Churg, A. K.; Glick, H. A. *Proc. Natl. Acad. Sci. U.S.A.* **1978**, *75*, 2291–2295.
(313) Wang, C. M.; Brinigar, W. S. *Biochemistry* **1979**, *18*, 4960–4977.
(314) Sams, J. R.; Tsin, T. B. In *The Porphyrins*; Dolphin, D., Ed.; Academic Press: New York, 1978; Vol. 4, pp 425–478.
(315) English, D. R.; Hendrickson, D. N.; Suslick, K. S. *Inorg. Chem.* **1983**, *22*, 367–368.
(316) Lang, G.; Marshall, W. *Proc. Phys. Soc., London* **1966**, *87*, 3–34.
(317) Lang, G.; Marshall, W. *J. Mol. Biol.* **1966**, *18*, 385–404.
(318) Kirchner, R. F.; Loew, G. H. *J. Am. Chem. Soc.* **1977**, *99*, 4639–4647.
(319) Barlow, C. H.; Maxwell, J. E.; Wallace, W. J.; Caughey, W. S. *Biochem. Biophys. Res. Commun.* **1973**, *55*, 91–95.
(320) Maxwell, J. C.; Volpe, J. A.; Barlow, C. H.; Caughey, W. S. *Biochem. Biophys. Res. Commun.* **1974**, *58*, 166–171.
(321) Tsubaki, M.; Naigai, K.; Kitagawa, T. *Biochemistry* **1980**, *19*, 379–385.
(322) Desbois, A.; Lutz, M.; Banerjee, R. *Biochemistry* **1979**, *18*, 1510–1518.
(323) Irwin, M. J.; Armstrong, R. S.; Wright, P. E. *FEBS Lett.* **1981**, *133*, 239–242.
(324) Nagai, K.; Kitagawa, T.; Morinoto, H. *J. Mol. Biol.* **1980**, *136*, 271–289.
(325) Walters, M. A.; Spiro, T. G. *Biochemistry* **1982**, *21*, 6989–6995.

(326) Ogura, T.; Takahashi, S.; Shinzawa-Itoh, K.; Yoshihawa, S.; Kitagawa, T. *J. Am. Chem. Soc.* **1990**, *112*, 5630–5631.
(327) Burker, J. M.; Kincaid, J. R.; Peters, S.; Gagne, R. R.; Collman, J. P.; Spiro, T. G. *J. Am. Chem. Soc.* **1978**, *100*, 6083–6088.
(328) Walters, M. A.; Spiro, T. G.; Suslick, K. S.; Collman, J. P. *J. Am. Chem. Soc.* **1980**, *102*, 6857–6858.
(329) Oertling, W. A.; Kean, R. T.; Weaver, T.; Bathcock, C. T. *Inorg. Chem.* **1990**, *29*, 2633–2645.
(330) Wagner, W. D.; Paeng, I. R.; Nakamoto, K. *J. Am. Chem. Soc.* **1988**, *110*, 5565–5567.
(331) Nakamoto, K.; Paeng, I. R.; Kuroi, T.; Isobe, T.; Oshio, M. *J. Mol. Struct.* **1988**, *189*, 293–300.
(332) Yu, N. T.; Mackin-Thompson, H.; Chang, C. K. *Biophys. J.* **1987**, *51*, 283–287.
(333) Yuasa, M.; Yamamoto, K.; Nishide, H.; Tsuchida, E. *Bull. Chem. Soc. Jpn.* **1988**, *61*, 313–315.
(334) Watanabe, T.; Ama, T.; Nakamoto, K. *J. Phys. Chem.* **1984**, *88*, 440–445.
(335) Tsubaki, M.; Yu, N. T. *Proc. Natl. Acad. Sci. U.S.A.* **1981**, *78*, 3581–3585.
(336) Mackin, H. C.; Tsubaki, M.; Yu, N. T. *Biophys. J.* **1983**, *41*, 349–357.
(337) Brunner, H. *Naturwissenschaften* **1974**, *61*, 129–130.
(338) Strekas, T. C.; Spiro, T. G. *Biochem. Biophys. Acta* **1972**, *263*, 830–833.
(339) Benko, B.; Yu, N. T. *Proc. Natl. Acad. Sci. U.S.A.* **1983**, *80*, 7042–7046.
(340) Bajdor, K.; Oshio, H.; Nakamoto, K. *J. Am. Chem. Soc.* **1984**, *106*, 7273–7274.
(341) Spiro, T. G. *Iron Porphyrins*; Lever, A. B. P., Gray, H. B., Eds.; 1983; Part II, pp 89–159.
(342) Hori, H.; Kitagawa, T. *J. Am. Chem. Soc.* **1980**, *102*, 3608–3613.
(343) Koster, A. S. *J. Chem. Phys.* **1975**, *63*, 3284–3286.
(344) Ostrich, I. J.; Liu, G.; Dodgen, H. W.; Hunt, J. P. *Inorg. Chem.* **1980**, *19*, 619–621.
(345) Postel, M.; Brevard, C.; Arzoumanian, M.; Riess, J. G. *J. Am. Chem. Soc.* **1983**, *105*, 4922–4926.
(346) Lee, H. C.; Oldfield, E. *J. Magn. Reson.* **1986**, *69*, 367–370.
(347) Lee, H. C.; Oldfield, E. *J. Am. Chem. Soc.* **1989**, *111*, 1584–1590.
(348) Maricic, S.; Leigh, J. S.; Sunko, D. E. *Nature (London)* **1967**, *214*, 462–466.
(349) Pifat, G.; Maricic, S.; Petrinovic, M. *Croat. Chem. Acta* **1969**, *41*, 195–203.
(350) Irving, C. S.; Lapidot, A. *Nature (London) New Biol.* **1971**, *230*, 224.
(351) Gerothanassis, I. P.; Momenteau, M. *J. Am. Chem. Soc.* **1987**, *109*, 6944–6947.
(352) Gerothanassis, I. P.; Momenteau, M. In *Metal Ions in Biology and Medicine*; Anastassopoulou, J., Collery, Ph., Etienne, J. C., Theophanides, Th., Eds.; John Libbey Eurotext: Paris, 1992; Vol. 2, pp 14–19.
(353) Velenik, A.; Lynden-Bell, R. M. *Croat. Chem. Acta* **1969**, *41*, 205–211.
(354) Oldfield, E.; Lee, H. C.; Coretsopoulos, C.; Adebodun, F.; Park, K. D.; Yang, S.; Chung, J.; Philipps, B. *J. Am. Chem. Soc.* **1991**, *113*, 8680–8685.
(355) Gerothanassis, I. P.; Loock, B.; Momenteau, M. *J. Chem. Soc., Chem. Commun.* **1993**, 598–600.
(356) Kintzinger, J. P. In *NMR-Basic Principles and Progress*; Diehl, P., Fluck, E., Kosfeld, R., Eds.; Springer: Berlin, 1981; Vol. 17, pp 1–64.
(357) Boykin, D. W. In *^{17}O NMR Spectroscopy in Organic Chemistry*; CRC Press Inc.: Boston, 1991.
(358) Gerothanassis, I. P.; Loock, B.; Momenteau, M. Unpublished results.
(359) Ortiz de Montellano, P. R., Ed. In *Cytochrome P-450, Structure, Mechanism and Biochemistry*; Plenum Press: New York, 1986.
(360) Mansuy, D.; Battioni, P.; Battioni, J. P. *Eur. J. Biochem.* **1989**, *184*, 267–285.
(361) Poulos, T. L.; Finzel, B. C.; Gunsalus, I. C.; Wagner, G. C.; Kraut, J. *J. Biol. Chem.* **1985**, *260*, 16122–16130.
(362) Poulos, T. L.; Finzel, B. C.; Howard, A. *J. Biol. Chem.* **1986**, *25*, 5314–5322.
(363) Collman, J. P.; Sorrell, T. N.; Hoffman, B. M. *J. Am. Chem. Soc.* **1975**, *97*, 913–914.
(364) Ogoshi, H.; Sugimoto, H.; Yoshida, Z. *Tetrahedron Lett.* **1975**, 2289–2292.
(365) Tang, S. C.; Kock, S.; Papaefthymiou, G. C.; Foner, S.; Frankel, R. B.; Ibers, J. A.; Holm, R. H. *J. Am. Chem. Soc.* **1976**, *98*, 2414–2434.
(366) Chang, C. K.; Dolphin, D. *J. Am. Chem. Soc.* **1975**, *97*, 5948–5950.
(367) Bayer, E.; Hill, H. A. O.; Röder, A.; Williams, R. J. P. *J. Chem. Soc., Chem. Commun.* **1969**, 109–111.
(368) Kock, S.; Tang, S. C.; Holm, R. H.; Frankel, R. B.; Ibers, J. A. *J. Am. Chem. Soc.* **1975**, *97*, 916–918.
(369) Chang, C. K.; Dolphin, D. *J. Am. Chem. Soc.* **1976**, *98*, 1607–1609.
(370) Ruf, H. H.; Wende, P. *J. Am. Chem. Soc.* **1977**, *99*, 5499–5500.
(371) Traylor, T. G.; Mincey, T. C.; Berzinis, A. P. *J. Am. Chem. Soc.* **1981**, *103*, 7084–7089.
(372) Higuchi, T.; Uzu, S.; Hirobe, M. *J. Am. Chem. Soc.* **1990**, *112*, 7051–7053.
(373) Battersby, A. R.; Howson, W.; Hamilton, A. D. *J. Chem. Soc., Chem. Commun.* **1982**, 1266–1268.
(374) Collman, J. P.; Groh, S. E. *J. Am. Chem. Soc.* **1982**, *104*, 1391–1403.
(375) Staubli, B.; Fretz, H.; Piantini, U.; Woggon, W. D. *Helv. Chim. Acta* **1987**, *70*, 1173–1193.
(376) Woggon, W. D. *Nachr. Chem. Tech. Lab.* **1988**, *36*, 890–895.
(377) Patzelt, H.; Woggon, W. D. *Helv. Chim. Acta* **1992**, *75*, 523–530.
(378) Momenteau, M.; Loock, B.; Huel, C.; Lhoste, J. M. *J. Chem. Soc., Perkin Trans. 1* **1988**, 283–295.
(379) Schappaccher, M.; Ricard, L.; Weiss, R.; Montiel-Montoya, R.; Bill, E.; Gonser, U.; Trautwein, A. X. *J. Am. Chem. Soc.* **1981**, *103*, 7646–7648.
(380) Chottard, G.; Schappacher, M.; Ricard, L.; Weiss, R. *Inorg. Chem.* **1984**, *23*, 4557–4561.
(381) Montiel-Montoya, R.; Bill, E.; Trautwein, A. X.; Winkler, H.; Ricard, L.; Schappacher, M.; Weiss, R. *Hyperfine Interact.* **1986**, *29*, 1411–1414.
(382) Dawson, J. H.; Cramer, S. P. *FEBS Lett.* **1978**, *88*, 127–130.
(383) Ishimura, Y.; Ullrich, V.; Peterson, J. A. *Biochem. Biophys. Res. Commun.* **1971**, *42*, 140–146.
(384) Peterson, J. A.; Ishimura, Y.; Griffin, B. W. *Arch. Biochem. Biophys.* **1972**, *149*, 197–208.
(385) Bancharoenpaurpong, O.; Rizos, A. K.; Champion, P. M.; Jollie, D.; Sligar, S. G. *J. Biol. Chem.* **1986**, *261*, 8089–8092.
(386) Anzenbacher, P.; Dawson, J. H.; Kitagawa, T. *J. Mol. Struct.* **1989**, *214*, 149–158.
(387) Chottard, G.; Battioni, P.; Battioni, J. P.; Lange, M.; Mansuy, D. *Inorg. Chem.* **1981**, *20*, 1718–1722.
(388) Dawson, J. H.; Kan, L. S.; Penner-Hahn, J. E.; Sono, M.; Eble, K. S.; Bruce, G. S.; Hager, L. P.; Hodgson, K. O. *J. Am. Chem. Soc.* **1986**, *108*, 8114–8116.
(389) Sharrock, M.; Münck, E.; Debrunner, P. G.; Marshall, V.; Lipscomb, J. D.; Gunsalus, I. C. *Biochemistry* **1973**, *12*, 258–265.
(390) Champion, P. M.; Lipscomb, J. D.; Munck, E.; Debrunner, P.; Gunsalus, I. C. *Biochemistry* **1975**, *14*, 4151–4160.
(391) Sharrock, M.; Debrunner, P. G.; Schulz, C.; Lipscomb, J. D.; Marshall, V.; Gunsalus, I. C. *Biochim. Biophys. Acta* **1976**, *420*, 8–26.
(392) Schappacher, M.; Ricard, L.; Weiss, R.; Monteil-Montoya, R.; Gonser, U.; Bill, E.; Trautwein, A. X. *Inorg. Chim. Acta* **1983**, *78*, L9–L12.
(393) Debey, P.; Balny, C.; Douzou, P. *FEBS Lett.* **1976**, *69*, 231–235.
(394) Balny, C.; Debey, P.; Douzou, P. *FEBS Lett.* **1976**, *69*, 236–240.
(395) Guengerich, F. P.; Ballou, D. P.; Coon, M. J. *Biochem. Biophys. Res. Commun.* **1976**, *70*, 951–956.
(396) Rösen, P.; Stier, A. *Biochem. Biophys. Res. Commun.* **1973**, *51*, 603–611.
(397) Bonfils, C.; Debey, P.; Maurel, P. *Biochem. Biophys. Res. Commun.* **1979**, *88*, 1301–1307.
(398) Tuckey, E. C.; Kamin, H. *J. Biol. Chem.* **1982**, *257*, 9309–9314.
(399) Oprian, D. D.; Gorsky, L. D.; Coon, M. J. *J. Biol. Chem.* **1983**, *258*, 8684–8691.
(400) Tuckey, R. C.; Kamin, H. *J. Biol. Chem.* **1983**, *258*, 4232–4237.
(401) Gerber, N. C.; Sligar, S. G. *J. Am. Chem. Soc.* **1992**, *114*, 8742–8743.
(402) El-Kasmi, D.; Tétreau, C.; Lavalette, D.; Momenteau, M. To be published.
(403) Dawson, J. H.; Eble, K. S. In *Advances in Organic and Bioinorganic Mechanisms*; Academic Press Inc.: New York, 1986; Vol. 4, pp 1–64.
(404) Yonetani, T.; Yamamoto, H.; Woodrow, G. W. *J. Biol. Chem.* **1974**, *249*, 682–690.
(405) Keyes, M. H.; Falley, M.; Lumry, R. *J. Am. Chem. Soc.* **1971**, *93*, 2035–2039.
(406) Sharma, V. S.; Schmidt, M. R.; Ranney, H. M. *J. Biol. Chem.* **1976**, *251*, 4267–4272.
(407) Imai, K.; Yonetani, T.; Ikeda-Saito, M. *J. Mol. Biol.* **1977**, *109*, 83–97.
(408) Mac Quarrie, R.; Gibson, Q. H. *J. Biol. Chem.* **1971**, *246*, 5832–5835.
(409) Brunori, M.; Noble, R. W.; Antonini, E.; Wyman, J. *J. Biol. Chem.* **1966**, *241*, 5238–5243.
(410) Tyuma, I.; Shimizu, K.; Imai, K. *Biochem. Biophys. Res. Commun.* **1971**, *43*, 423–428.
(411) Imamura, T.; Riggs, A.; Gibson, Q. J. *J. Biol. Chem.* **1972**, *247*, 521–526.
(412) Chang, C. K.; Traylor, T. G. *Biochem. Biophys. Res. Commun.* **1975**, *62*, 729–735.
(413) Traylor, T. G.; Chang, C. K.; Geibel, J.; Berzini, A.; Minay, T.; Cannon *J. Am. Chem. Soc.* **1979**, *101*, 6716–6731.
(414) Traylor, T. G.; White, D. K.; Campbell, D. H.; Berzinis, A. P. *J. Am. Chem. Soc.* **1981**, *103*, 4932–4936.
(415) Traylor, T. G.; Campbell, D. H.; Sharma, V. S.; Geibel, J. F. *J. Am. Chem. Soc.* **1979**, *101*, 5376–5383.
(416) Lexa, D.; Momenteau, M.; Savéant, J.-M.; Xu, F. *Inorg. Chem.* **1986**, *25*, 4857–4865.